MARGINAL DETONATION IN TERNARY SYSTEMS OF HYDROCARBONS, OXYGEN AND NITROGEN

A Thesis submitted for the degree

of Doctor of Philosophy

of the University of London

by

Fariborz Rashidi

B.Sc., M.Sc.

Department of Chemical Engineering and Chemical Technology

Imperial College of Science and Technology

June 1981

ABSTRACT

Detonability regimes for ternary gaseous systems of ethane, n-propane and n-butane with oxygen and nitrogen have been established experimentally from measurements of detonation velocities in tubes of 2-inch internal diameter. The work has been carried out at ambient pressure and temperature and with initiating impact from a detonating stoichiometric mixture of hydrogen and oxygen. Comparable results for the system methane-oxygen-nitrogen collected from another source are included in further evaluations.

Introduction of normalization, based on homologous similarities of fuel molecules, leads to extensive correlation of ternary detonability limits of these systems, and opens the way to a single basis for prediction of hazards of detonation from any system of a saturated fuel with oxygen and nitrogen.

Chapman-Jouguet reaction temperatures and shock front temperatures were calculated under the assumptions of simplified reaction mechanisms and reaction products with the use of a computer program. From this, it appears that for such systems, detonation limit boundaries can equally be predicted with considerable accuracy on the basis of constant limiting temperature criteria associated with the simplified reaction products. However, it is concluded that, at this stage, no comment can be made on the relative merits of either C-J reaction-zone temperatures or shock temperatures as a critical parameter to detonation propagation.

ACKNOWLEDGEMENTS

I should like to express my deep gratitude to my supervisor, Dr. H.J. Michels, for his constant help and guidance during the course of the work, and the preparation of this thesis. I am also grateful to Dr. Michels for covering part of my financial difficulties with a personal grant, as well as to Professor F.J. Weinberg for arranging further financial aid in the last six months.

My thanks are also due to my co-worker, Mr. P. Lindstedt, for his assistance with some of the experimental work, and for his helpful discussions in developing the computer program. I would also like to thank Mr. R. Wood of the Electronics Laboratory for keeping all the systems going.

Finally, I wish to thank Miss M.J. McNeile for typing this thesis.

C O N T E N T S

		Page
CHAPTER 1	Stable Detonation	1
1.1	The Nature of detonation	1
1.2	Detonation Wave Velocity	2
1.3	The Chapman-Jouguet Plane	7
1.4	The Z-N-D Theory	7
1.5	Deficiencies of Chapman-Jouguet Theory	9
1.6	Marginal Detonation	10
1.6.1	Spinning and Pulsating Detonation	11
1.6.2	Detonability Limits	12
1.6.3	A Survey of Previous Studies	13
1.6.4	The Present Investigation	16
CHAPTER 2	Developments From Existing Detonation Theory	17
2.1	Introduction	17
2.2	Simplified Reaction Mechanisms for Marginal Detonations of Saturated Aliphatic Hydrocarbons With Oxygen and Nitrogen	19
2.3	Calculation of Reaction Zone Temperatures	19
2.4	Calculation of Shock Front Temperatures	21
2.5	Principles of Homology Correlation	22

		Page
CHAPTER 3	Review of Instrumentation	24
3.1	Apparatus	27
3.2	Experimental Method	36
3.3	Experimental Accuracy	37
3.3.1	Gas Purity	37
3.3.2	Test Mixture Composition	38
3.3.3	Accuracy of Velocity Measurement	39
3.4	Limit Determination	39
CHAPTER 4	Results	41
4.1	General	41
4.2	The System: Ethane-Oxygen-Nitrogen	41
4.3	The System: Propane-Oxygen-Nitrogen	42
4.4	The System: Butane-Oxygen-Nitrogen	42
4.5	The System: Ethylene-Oxygen-Nitrogen	42
CHAPTER 5	Evaluation of Results	75
5.1	Triangular Diagrams of Detonation Limits in Ternary Systems	75
5.2	Homologous Correlation of Composition Limits	75
5.3	Reaction Zone Temperatures and Shock Front Temperatures for Marginal Detonations of Fuel-Oxygen-Nitrogen Mixtures	85

Page

5.4 The Constant Temperature Criterion for Prediction of Detonation Limits in Ternary Systems 89

CHAPTER 6 Discussion 105

Conclusions and Suggestions for Further Investigation 114

REFERENCES 115

Appendix A1 The equations for calculation of reaction zone temperatures 118

Appendix A2 The equation for the calculation of detonation velocities 119

Appendix A3 Calculations of physical data 120

Appendix B1 The equations for the calculation of shock front temperatures for polytropic gases 122

Appendix B1.A The equations for the calculation of shock front temperatures for non-polytropic gases 123

Appendix B2 Calculations of physical data 125

Appendix C Listing of FORTRAN program for computation of reaction zone temperatures and shock front temperatures 126

Appendix D Temperature calculations using Taylor-Lewis's method 130

LIST OF FIGURES

		Page
1.1	Gas parameters associated with a detonation wave in two coordinate systems	2
1.2	Hugoniot curve illustrating the hypothetical C-J detonation state	5
1.3	Hugoniot curves illustrating variations in the state of a gas on passing through a detonation wave-front to reach the C-J state	8
3.1-3.2	Detonation tube	28-9
3.3	Stoichiometric H_2-O_2 mixing system	31
3.4	Gas mixing and vessel pressure measuring system	33
3.5a	Ionization probe assembly	35
3.5b	Probe circuit	35
3.5c	Counter system	35
4.2a-4.2g	Detonation velocity for the system: ethane-oxygen-nitrogen	66-8
4.3a-4.3h	Detonation velocity for the system: propane-oxygen-nitrogen	69-71
4.4a-4.4g	Detonation velocity for the system: butane-oxygen-nitrogen	72-4
5.1.1-5.1.4	Limits of detonability for the systems: CH_4-O_2-N_2, C_2H_6-O_2-N_2, C_3H_8-O_2-N_2 and C_4H_{10}-O_2-N_2.	77-80

		Page
5.2.1	Detonation regimes on homology basis for ternary systems of oxygen and nitrogen with methane, ethane, n-propane and n-butane	84
5.3.1	Block diagram for program DTEMP	86
5.4a-5.4d	Estimate of composition limits to detonation in ternary systems containing nitrogen based on critical temperature values for corresponding binary systems	93-100
5.4e-5.4h	Theoretical plots of constant reaction zone temperature and constant shock front temperature for the systems: CH_4-O_2-N_2, C_2H_6-O_2-N_2, C_3H_8-O_2-N_2 and C_4H_{10}-O_2-N_2.	101-104
6.1	Detonation regime boundary for the mixtures of C_2H_4-O_2-N_2 with higher nitrogen dilution than for the air line	112
D.1-D.2	Estimate of composition limits for fuel-rich side in ternary systems of CH_4-O_2-N_2 and C_3H_8-O_2-N_2 based on critical temperature values for corresponding binary systems "based on Taylor-Lewis method"	132-133
D.3-D.4	Theoretical plots of constant reaction zone temperature and constant shock front temperature for the fuel-rich side of the systems: CH_4-O_2-N_2 and C_3H_8-O_2-N_2 "based on Taylor-Lewis method"	134-135

LIST OF TABLES

		Page
3.1	Calibration of H_2-O_2 flow controllers	31
4.2a-4.2g	Detonation velocity for the systems: ethane-oxygen-nitrogen	43-49
4.3a-4.3h	Detonation velocity for the systems: propane-oxygen-nitrogen	50-57
4.4a-4.4g	Detonation velocity for the systems: butane-oxygen-nitrogen	58-64
4.5a	Some miscellaneous detonation velocities for the system: ethylene-oxygen-nitrogen	65
5.1.1	(Fuel-lean fuel-rich) detonation limit compositions for systems of oxygen and nitrogen with methane, ethane, n-propane and n-butane	76
5.2.1-5.2.2	Detonation limits and corresponding homology composition values	82-83
5.3a-5.3d	Reaction zone temperatures and shock front temperatures near detonation limits for the systems: CH_4-O_2-N_2, C_2H_6-O_2-N_2, C_3H_8-O_2-N_2 and C_4H_{10}-O_2-N_2	87-88
6.1	Comparison of calculated and experimental velocities in marginal detonable mixtures of saturated aliphatic hydrocarbons, oxygen and nitrogen	106
6.2	Reaction and shock temperatures near detonation limits for the system: C_2H_4-O_2-N_2	113

		Page
A.3.1	Coefficients for the equation of the heat capacity of the reaction products	120
B.2.1	Coefficients for the equation of the heat capacity of the reactants	125
D.1	Comparison of reaction and shock temperatures calculated in this work and by Taylor-Lewis (1977) for the system CH_4-O_2-N_2	130
D.2	Reaction temperatures and shock temperatures near detonation limits for the system C_3H_8-O_2-N_2 "based on Taylor-Lewis method"	131

CHAPTER 1

STABLE DETONATION

1.1 The Nature of Detonation

In unconfined explosive mixtures of gases an ordinary plane flame front usually propagates quite slowly, at a speed, known as the burning velocity, which is a characteristic of the mixture and its physical conditions. Maximum values for such burning velocities (mixtures with oxygen) are only a few metres/sec. When the explosive mixture is narrowly confined, such as in a long tube, the expansion of the heated gas behind the flame front causes gas movements which may greatly increase the speed of the front. The explosion may then change its character, and become extremely violent and destructive. This phenomenon is known as detonation. It is found that the detonation wave travels at very high speed, usually between 1500 and 3500 meters/sec. A detonation consists essentially of a strong shock front, very closely followed by a combustion zone; the shock front heats the gases to a high temperature, above the spontaneous thermal ignition temperature, and then the heat of the combustion process provides the energy to maintain the shock front.

There are thus some essential differences between an ordinary flame front and a detonation. The relatively low burning velocity of an ordinary flame depends mainly on chemical processes involving activation energies and the rate of radical diffusion and heat transfer. The detonation velocity depends almost entirely on the speed of sound in the burnt gases, and the heat available from the chemical reaction and is quite insensitive to the chemical processes by which the heat release occurs; the chemical processes do, however, determine the gas mixture limits over which detonation is possible, e.g. Lewis and von Elhe (1961), Fickett and Davis (1979).

1.2 Detonation Wave Velocity

The relationship between hydrodynamics and chemical energy release of a detonation wave was first identified by Chapman (1899) and developed into a mathematical treatment which was an extension of Hugoniot's analysis of shock waves.

A simplification of the mathematics is obtained if a coordinate system is used, based on a stationary wave. Figure 1.1 illustrates differences in flow in the regions of a detonation wave as a result of such changes in the coordinate system.

Fig. 1.1 - Gas parameters associated with a detonation wave in two coordinate systems



(a) Observer coordinates (b) Wave coordinates

U, W = velocity T = temperature M = molecular weight

P = pressure V = specific volume

The measured detonation velocity, W_d in (a) represents the speed of propagation into a gas mixture initially at rest. Particles behind the detonation wave have a velocity W_2.

If the detonation wave is considered to be at rest, in (b), unreacted gas from state 1 enters the wave with a velocity U_1, and reaction products leave the wave for state 2 with a velocity U_2. The two coordinate systems used are related by the following equations:

$$U_1 = W_d \tag{1.1}$$

$$U_2 = W_d - W_2 \tag{1.2}$$

The particle velocity behind the wave can now be expressed as

$$W_2 = U_1 - U_2 \tag{1.3}$$

To visualise the propagation of a steady-state detonation wave in a tube, it is useful to consider first a detonation in an ideal gas which has a specific heat independent of temperature. The general picture obtained will still be applicable to real gases. To find the velocity of propagation (W_d) and the velocity, W_2, of the gas behind the wave, often referred to as particle velocity, consider the passage of a unit mass of gas through a unit area (see Fig. 1.1b). Application of the usual conservation equations from fundamental equations of motion leads to the following expressions:

Conservation of mass

$$\frac{U_1}{V_1} = \frac{U_2}{V_2} \tag{1.4}$$

Conservation of momentum

$$P_1 + \frac{U_1^2}{V_1} = P_2 + \frac{U_2^2}{V_2} \tag{1.5}$$

Conservation of energy

$$H_1 + \tfrac{1}{2} U_1^2 + \Delta E_c = H_2 + \tfrac{1}{2} U_2^2 \tag{1.6}$$

$H_2 - H_1$ is the enthalpy rise in the gas and ΔE_c is the energy released in the combustion process. The above equations are similar to Hugoniot's analysis of shock waves except that the energy difference given by the Hugoniot equation for shock-waves represents only the change in enthalpy caused by compression, whereas now the enthalpy of the burnt gas has been increased due to the energy ΔE_c released in the chemical reaction. For a gas initially at rest in the tube, the detonation propagation speed W_d, and the particle velocity, W_2, are found from equations (1.3), (1.4) and (1.5) to be:

$$W_d = U_1 = V_1\sqrt{\frac{P_2-P_1}{V_1-V_2}} \tag{1.7}$$

$$W_2 = U_1 - U_2 = (V_1-V_2)\sqrt{\frac{P_2-P_1}{V_1-V_2}} \tag{1.8}$$

By using equations (1.7) and (1.8), together with the enthalpy equation for an ideal gas: $H = C_pT = C_vT + PV$; the equation for the conservation of energy (1.6) may be written in the form of energy balance equations:

$$\Delta E = C_v(T_2-T_1) - \Delta E_c \tag{1.9}$$

$$C_v(T_2-T_1) - \Delta E_c = \tfrac{1}{2}(P_2+P_1)(V_1-V_2) \tag{1.10}$$

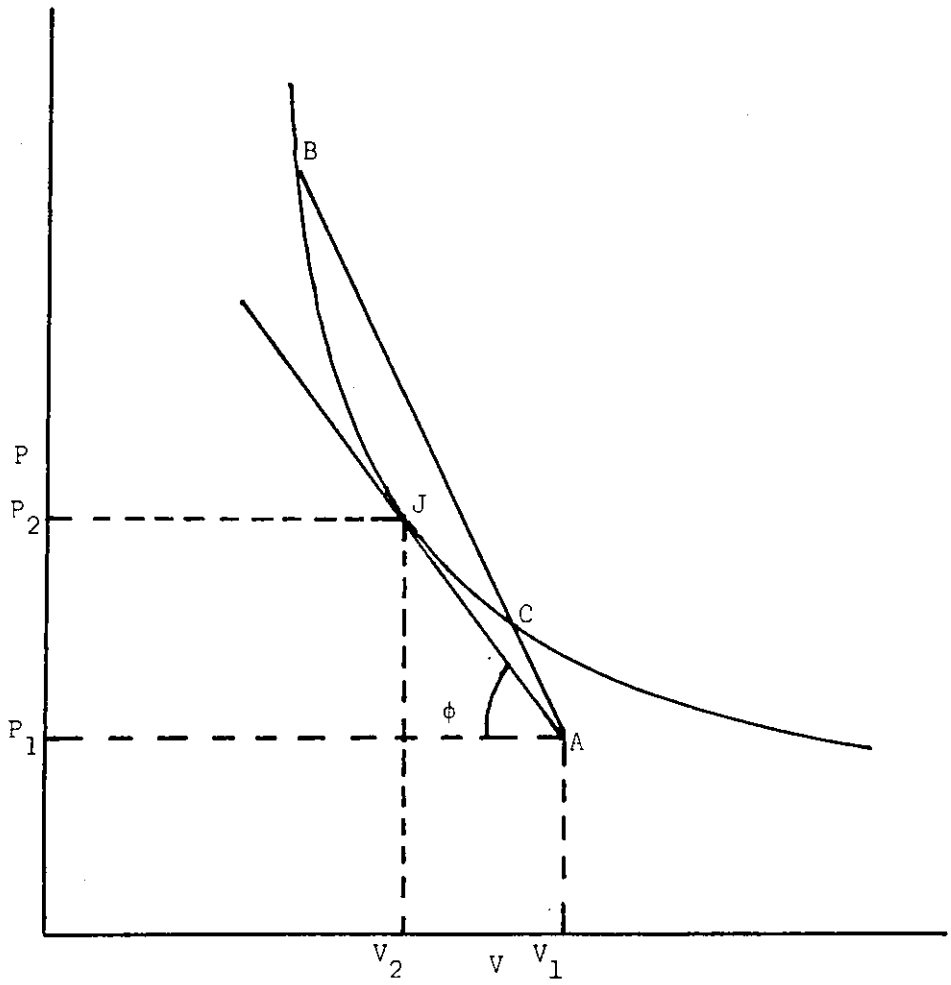
For the solution of the problem four equations are now available, namely (1.7), (1.8), (1.9) and (1.10); but they contain six unknowns, namely U_1, W_2, P_2, V_2, ΔE and T_2. One more equation can be obtained from the equation of the state of the gas as:

$$\frac{P_2}{P_1} = \frac{V_1}{V_2} \cdot \frac{T_2}{T_1} \cdot \frac{M_1}{M_2} \tag{1.11}$$

It has been found experimentally that the propagation velocity of detonation is a fixed value for a given mixture; consequently, an additional relationship is required to find fixed values for the six variables mentioned above. This final relationship would be revealed after a study of the behaviour of burnt products on a P-V diagram. It was mentioned earlier that equation (1.10) is, in fact, the Hugoniot equation with the extra terms of ΔE_c due to chemical reaction. Inserting in equation (1.10) the value of $\frac{T_2}{T_1}$, obtained from the equation (1.11), a P-V diagram may be obtained (see Fig. 1.2) in which, unlike a Hugoniot P-V diagram for shock conditions, the initial state of gas does not lie on the curve, in which all possible values of P_2, V_2 which arise

from a particular initial state P_1, V_1, are plotted.

Fig. 1.2 - Hugoniot curve illustrating the hypothetical C-J detonation state 'J'



The state corresponding to the actual value of P_2, V_2 in the detonation wave will lie somewhere on this curve. A study of this curve enables the other important relation to be found.

$$\tan.\phi = (P_2-P_1)/(V_1-V_2) \qquad (1.12)$$

From this, and equations (1.7) and (1.8)

$$W_d = V_1\sqrt{\tan.\phi} \tag{1.13}$$

$$W_2 = (V_1-V_2)\sqrt{\tan.\phi} \tag{1.14}$$

Since any straight line, commonly termed as Rayleigh lines, from A will intersect the curve at two points such as B and C, it would appear that, for a particular detonation speed in a given gas, two stable detonation states corresponding to the two points are possible; such a situation is not confirmed experimentally. However, the two points coalesce at the intersection of the tangent to the curve at J, and this point meets all requirements to qualify as the true point corresponding to the state of the detonation.

In view of this, Chapman (1899) made the now historic hypothesis that this point represents the actual value of P_2 and V_2 in the detonation. It was argued later, by Jouguet (1905) and Becker (1922) that the true final state is indeed the point of tangency, J, as was already suggested by Chapman. At the point J, the slope of the curve is given by relation

$$\frac{d\,P_2}{d\,V_2} = -\frac{(P_2-P_1)}{(V_1-V_2)} \tag{1.15}$$

From the definition of the speed of sound in a gas, equation (1.15) may be written as,

$$C_2^2 = \frac{d\,P_2}{d\,\rho_2} = V_2^2\,\frac{P_2-P_1}{V_1-V_2} \tag{1.16}$$

C_2 is the speed of sound in the burnt gas. From equations (1.7), (1.8) and (1.16) it is easy to show that $U_2 = C_2$, which indicates that burnt gas moves relative to the front at the local speed of sound. From equation (1.2) it is apparent that

$$W_d = C_2 + W_2 \tag{1.17}$$

which shows that a detonation wave travels at a speed equal to the sum of the particle speed (W_2) behind the front and the local sound speed in the burnt gas (C_2).

1.3 The Chapman-Jouguet Plane

The classical hydrodynamic theory of detonations treats the phenomenon as a one-dimensional process, in which the detonation front moves with uniform velocity into a gas initially at rest. To determine the velocity of a detonation wave we have the initial state of the gas and the Hugoniot curve of the burnt gas. From all possible values of (W_d) the velocity of the stable detonation is singled out by applying the Chapman-Jouguet condition: for a stable detonation the Rayleigh line is tangential to the Hugoniot curve of the final products.

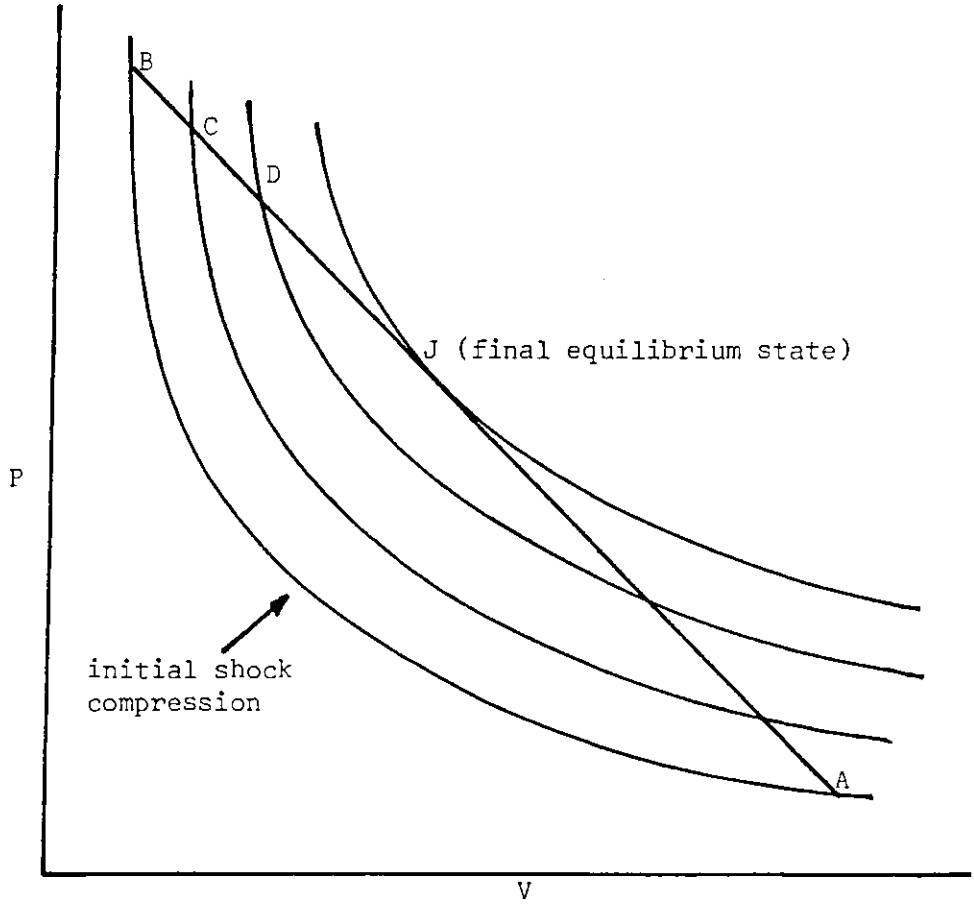
In a real gas, the chemical reaction which is initiated by the rapid shock wave heating of the gas at the detonation front, will take a finite time to reach equilibrium, and the reaction or combustion zone will therefore extend over some distance to the position of equilibrium occurring some plane behind the front. The condition of the gas at this plane will correspond to the Chapman-Jouguet state, and this plane is thus referred to as the Chapman-Jouguet plane.

1.4 The Z-N-D Theory

The changes induced in a real gas by the passage of a detonation wave can be followed by referring to Fig. 1.3. The series of curves in this figure represent Hugoniot curves which correspond to various stages in the passage of the gas through the reaction zone. The lower curve is the Hugoniot for the normal shock-wave compression from state A to B with $\Delta E_c = 0$. With initiation of combustion, the temperature begins to increase, and the gas expands from state B to lower values of density and pressure at points such as C and D; these are on other Hugoniot curves which relate the planes in the reaction zone corresponding to values of ΔE_c appropriate to the fraction of gas reacted at these stages. The uppermost curve is the Hugoniot corresponding

essentially to completion of reaction; and the equilibrium state of gas will be on this curve at J, where the line BCDJA is a tangent.

Fig. 1.3 - Hugoniot curves illustrating variation in the state of a gas on passing through a detonation wave-front to reach the C-J state



The speed of detonation is given by the slope of this line. It will be noted that the line intersects the other Hugoniots at two points, and these would appear to be two paths by which the gas initially at state A can reach state J. However, the direct path AJ is inadmissible, since it implies a spontaneous ignition in the initial gas, whilst along the upper path the gas is first raised to a temperature and pressure at which chemical reaction can occur.

On the basis of this analysis of a detonation, which was developed independently by Zeldovich (1940), Von Neuman (1942) and Döring (1943), and is commonly known as Z-N-D theory, the front region of

the wave is characterised by an initial sharp rise in temperature, pressure and density, and then by a fall in pressure and density and a further rise in temperature through the reaction zone. This narrow region of high pressure and high gas density at the front of the detonation wave, is usually referred to as the Von-Neuman 'spike'.

This is a more detailed theory of stable detonation than the original C-J theory. It presents more realistically the sequence of events in a detonation wave. However, its ability to predict accurately detonation velocity is as before, not dependent in any recognisable way on all the steps in the sequence of reactions that take place between the detonation front and the Chapman-Jouguet plane, but only on the overall energy release.

1.5 Deficiencies of Chapman-Jouguet Theory

None of the hydrodynamic theories predicts either the existence or the location of composition limits for propagation of detonation waves. In fact, according to C-J theory, there exists unique wave velocity for any detonable gas mixture throughout the whole concentration range of each component, but this is not so. Failure of detonation propagation in mixtures with composition outside a particular range, resulted in formal determination of detonation limits for many fuel-oxidant mixtures. Experimental work aimed at the determination of composition limits, brought out several aspects of detonation which are not within the validity range of the C-J theory, e.g. Bone *et al.* (1932, 1936). It was noted that near the limits, the propagation velocity of detonations first varies widely in a sinosoidal way and subsequently drops sharply. Experimental work also showed that the composition of gas mixtures at the limits (i.e. when propagation fails) depends on factors which do not appear to influence steady-state

propagation. The reproducibility of experimental work near limits has been shown to be possible only under certain experimental constraints.

1.6 Marginal Detonation

With progressive dilution of a detonable gas mixture by one of the components, a composition region develops at which the observed, linear velocity of detonation propagation is no longer uniform. The propagation adopts an increasingly fluctuating nature, until it fails at the limits. This is the composition region of marginal detonation. The velocity fluctuations of marginal detonations are initially due to a noticeable occurrence of spinning detonation and close to the limits to pulsating detonation arising from instabilities in the combustion of weak gas mixtures.

The C-J theories which consider a plane detonation wave moving in only one direction, in a laminar flow, are unable to describe adequately the nature and behaviour of marginal detonation of a gaseous mixture, where the flow is turbulent and the front itself is distorted. However, the detonation velocities predicted by the C-J theory often hold up well into the marginal region of detonability as they are usually quite close to velocities measured experimentally over sufficiently long distances or the mean velocity of sufficiently many short distances. Differences between calculated and measured velocities start to rise rapidly as the instabilities in weak detonations become more prominent towards detonation limits.

Since, in the present investigation, no attempt is made to resolve details of the three-dimensional nature of a real, limiting detonation, details of the nature of such phenomena, as detonation wave structure or transverse structure of an advancing detonation front, e.g.

Strehlow et al. (1965, 1967) will not be discussed here. In the following sections, only some main aspects of marginal detonations, i.e. spinning detonation, pulsating detonation and limits of detonability, will be considered.

1.6.1 Spinning and pulsating detonation

As the name suggests, the phenomena called spin are associated with non-one-directional combustions. However, it does not involve the rotation of the gas mass as a whole but only the 'head' of the detonation. There is always some transverse motion in the gas immediately behind the shock front due to accoustic vibrations - Manson (1947) and Fay (1952). The components of motion normal to the tube axis result in localized pressure 'heads' at the tube wall which rotate around the axis of the tube. For most stable detonations, such three-dimensional variations are very small and multiple across the detonation front. With short induction times, the detonation front may thus readily be represented as a planar wave. In weak detonations, however, the induction time is not very short. As a result, such localized pressures in the relatively wide induction zone increase in size, leading to larger and fewer rotating heads, which eventually are of the size of the tube cross-section. When the chemical reaction starts within these pressure heads, it can be noticed as the phenomenon called 'spin'.

Earlier in Section 1.4, it was mentioned that both the pressure and density begin to fall behind the shock front as soon as the temperature rises due to initiation of chemical reaction. This expansion process continues throughout the reaction zone, so that essentially a rarefaction wave is formed, and this follows the detonation wave along the tube. It has been argued (Brinkley and Richardson, 1953; Kirkwood and

Wood, 1954) that, in some cases, the chemical reaction is still proceeding in the rarefaction wave, i.e. mostly in very weak mixtures, where the completion of chemical reaction due to slow rates of chemical reactions takes place beyond what they call the sub-ideal C-J plane. As a result, the separation between the true equilibrium plane and shock front is very large. In such cases, at least a certain fraction of the energy released in the rarefaction wave will be delivered forward until it overtakes the sub-ideal C-J plane and increases the energy released there. This generates strong support for the detonation front, in the form of pressures pulses, which eventually overtake the front itself, increasing the strength and velocity of the shock front such that, in time, it becomes sufficiently strong to ignite the gas mixture and proceed as an overdriven detonation wave. In most cases, the latter wave cannot ultimately sustain itself and normally slows down. The reason for this slowing process lies in the fact that although the shock front has been strengthened by the pulses from rarefaction wave of the previous combustion zone section, the reaction zone immediately behind the new shock front is a continuously extending one due to weak combustible gas mixtures of near detonability limits. Eventually the separation between the shock front and the equilibrium plane increases itself again, and the process may repeat itself. This is noticed as 'pulsating detonation' near the detonability limits where complete combustion may not occur rapidly to contribute fully to propagation. See also 'Fluctuating Detonation in Gases', Munday et al., (1968).

1.6.2 Detonability limits

The most simple description of a detonation wave requires that the propagation of the shock front is supported by energy released during chemical reaction. For a readily combustible gas mixture, the one-

dimensional C-J theory predicts experimental detonation velocity very closely, by assuming that all the energy which has been released when the combustion products reach equilibrium, is used for propagation of the wave. If the composition is altered such that one component is in excess, the chemical combustion yields less energy due to decreased product formation. The C-J theory continues to give a good approximation to the experimental velocity until composition limits are approached. Thus it might be assumed that throughout most of the composition range in which detonation occurs, only a small amount of the total theoretical enthalpy is unavailable to forward propagation. As the composition limit is approached, it is believed that somehow the total theoretical enthalpy is not thoroughly spent on forwarding the propagation, and this can be seen in the difference between calculated and experimental velocity at and near the detonation limits. As the rate of enthalpy loss reaches some critical value, the detonation wave (due to insufficient energy support) fails to propagate. The corresponding mixture composition is referred to as detonability limit. The enthalpy loss may occur in several alternative ways, but studies of marginal detonations inevitably aim to establish methods by which a comparison can be made between different reacting systems in an attempt to identify any common factor in limiting processes which is described by a critical parameter.

1.6.3 A survey of previous studies

For detonation to occur, a gaseous system should contain at least:

- fuel(s), and
- oxidant(s), while further mixture components may be
- inerts

such as N_2, which is of practical relevance, because of industrial use of air.

Vast research has been done on detonation phenomena concerning combustion and kinetics and wave structure of detonations, as well as hydrodynamical studies of detonation velocities and detonation limits. One of the main objectives of a practically-based study of gaseous detonation is to construct a regime of detonability by which one can safely predict the hazards of detonation without specifying the components of each individual system. In practice, this would mean representing a system (for instance, in a triangular diagram) in which all fuels could be represented by one corner, and oxygen and inerts each by another corner, and in which a unique regime of detonability applies for all detonating fuels. For this purpose, it is absolutely necessary to study the detonations, both stable and marginal, of many comparable systems and especially to examine the behaviour of individual systems near the limits. With proper selection and care, one may find systematic similarities in individual detonating systems which may be used to evaluate a single master regime of detonability.

With this in mind, the project was started by H. Michels (1967) with work on a series of single fuel and oxygen systems. He studied the detonations of several binary mixtures of aliphatic hydrocarbons with oxygen. Using experimentally evaluated Mach-product (γM^2) values as an indication of energy release in detonations, he constructed a master curve by using a homology-based correlation for predicting the detonation boundary regime for simple fuel/oxygen systems. This will be explained in more detail in Section 2.5. The general uniformity of results, normalized on the basis of homology, suggested that molecular structure of the fuel molecule plays only a secondary role in the steady-state and marginal detonations of binary systems studied in that work.

The temperatures involved in a detonation wave propagation, namely shock front temperature and reaction zone temperature, are factors which

through their behaviour (especially near detonation limits) might reveal some information on the interpretation of detonation propagation failure at the limits.

It has been found that for limit compositions, the shock temperatures are substantially the same - around 1100 ^{o}K for all 'hydrogen-oxygen-diluent' systems. This temperature evidently represents the initiating temperature which the mixture must attain in order to react at sufficiently high rate. Michels calculated shock temperatures through measured velocities at detonation limits. Because of their similarities and behaviour at fuel lean sides, he suggested that marginal detonations at fuel lean side can be interpreted in terms of a critical temperature rise which may be related to a critical rate of an initial cracking mechanism.

R. Way (1971) studied the detonation of mixed fuels (CH_4, C_2H_4) with oxygen. He put the results on a ternary diagram and found that the regime of detonation for (CH_4, C_2H_4)/O_2 systems is bound between two straight lines. Although he did not conduct his study on the basis of straight boundaries for detonation regimes in ternary composition diagrams, it is believed that conversion of mixture compositions in mole percentage to composition in homology percentage will lead to alignment of the two detonation regime boundaries parallel to the fuel side of the diagram. This implies that homology correlations might also work for mixtures of fuels with oxygen.

Taylor Lewis (1977) studied a ternary system of methane, oxygen and nitrogen. He aimed at calculating reaction and shock temperatures at and near detonability limits, but not by using the measured values of velocity; instead reaction and shock temperatures were calculated based on the nominal energy release from a simple reaction mechanism

and with simple reaction products. The study then suggested that a constant 'shock temperature' criterion provides a reliable basis for prediction of detonation limit boundaries for the system: methane, oxygen and nitrogen.

1.6.4 The present investigation

This work started with studying the steady-state and marginal detonations of some ternary systems of homologous hydrocarbons, oxygen and inert (in this case N_2). The investigation then aimed to:

(a) Examine the possibility of correlating the different experimentally obtained detonation regimes into one master detonability regime of fuel, oxygen and nitrogen, as a direct contribution of the works mentioned earlier.

(b) Examine the suggestion of Lewis's work on the usefulness of 'shock temperature' as a meaningful criterion to predict the detonation limits of $CH_4/O_2/N_2$ system, for its validity for other ternary systems as studied in this work.

In trying to repeat Lewis's calculations, it was concluded that the theoretical part of his work contains some errors. Despite this, it seemed very practical to investigate further the idea that detonation limit boundaries could be predicted with reasonable accuracy in a simple way for a number of detonable mixture systems of fuel, oxidant and inert, by the use of a single critical parameter, such as temperature, without having to consider the actual detailed equilibrium state at C-J plane.

CHAPTER 2

DEVELOPMENTS FROM EXISTING DETONATION THEORY

2.1 Introduction

Experimentally-observed detonation limits naturally give rise to speculation as to what factors determine both the existence and the mixture composition of detonation limits. One common assumption to explain the properties of marginal detonation and of the ultimate failure of detonation propagation is that combustion instability is the prime cause of these phenomena. The essentially one-dimensional theory based on the concept of a planar shock front and combustion zone has been superseded by the more complex model of localized combustion, initiated by transverse waves, which arise from shock interaction behind a multi-headed front (e.g. White, 1961; Strehlow et al., 1965 and 1967).

The present investigation was not aimed at utilising the three-dimensional nature of a real detonation to resolve its near-limit behaviour. As it was more concerned with the physico-chemical properties of the reactants, it was necessary to decide which of the characteristic properties of a detonation can be used to define a limiting condition. One of these is the principle of homology of the fuel molecules in different systems (H. Michels, 1967), and aspects of such methods relevant to this work will be discussed at a later stage.

Detonation propagation and detonation limits depend, at least in part, on the extent of energy release in the reaction zone, and on energy feed-back to the shock front of the wave. This energy factor is taken into account in the equation for the conservation of energy, which is

used to derive the Hugoniot relation. The success of Hugoniot equation in the evaluation of detonation velocities, justifies the energy assumption. Calculation of the energy release in detonation is the key to evaluation of two other crucial parameters already mentioned in Chapter 1, namely reaction zone temperature and shock front temperature.

The major theoretical contribution of this work is related to aspects of the calculation of reaction zone temperature and shock temperature in marginal detonations. In this study, these temperatures were not calculated through the usual procedures, which take into consideration the actual, detailed equilibrium conditions at the C-J plane for calculation of reaction zone temperatures (e.g. Way, 1971). From these, or from experimentally-obtained detonation velocities (e.g. Michels, 1967), shock temperatures can then be evaluated. However, such methods are respectively tedious and uncertain due to vast velocity fluctuations near detonation limits. Instead, the energy released in the process was calculated on the basis of a simplified reaction mechanism with simple reaction products and from this, by a short iteration process, reaction temperatures were obtained. Detonation velocities were evaluated, using these reaction temperature values and from these, ultimately, shock front temperatures were calculated.

This is, therefore, a simplified evaluation of critical parameters of detonation for the further investigation of their behaviour under marginal conditions. In doing this, it was considered that if temperature was a decisive factor in the prediction of detonation limits, the values obtained - even if not calculated with great accuracy - should reveal this when the method was applied to comparable systems, such as saturated gaseous mixtures prepared from a sequence of hydrocarbons.

2.2 Simplified Reaction Mechanisms for Marginal Detonations of Saturated Aliphatic Hydrocarbons With Oxygen and Nitrogen

It is proposed to use two simple reaction mechanisms for marginal detonations of systems of saturated aliphatic hydrocarbons, oxygen and nitrogen as a basis for calculations of reaction and shock temperatures near detonation limits. The mechanisms refer respectively to the fuel-lean and the fuel-rich end of the composition range for which detonation was experimentally observed. In both cases, the following assumptions are made:

(1) Heat losses are negligible.

(2) The reaction proceeds to completion, forming only undissociated products.

(3) Specific heat values at temperatures chosen above the maximum for which products can exist in the undissociated form, are fixed at the value for that maximum temperature.

The mechanisms chosen are those simple chemical reaction equations which most closely agree with the compositions for which the limits were experimentally recorded. For the fuel-lean side the reaction products are assumed to be carbon dioxide and water vapour, the excess oxygen remaining in its undissociated form. For the fuel-rich side, it is assumed that carbon monoxide is the major product. If additional oxygen is available, water vapour will also be formed. In cases where there is too little oxygen for complete conversion of carbon to carbon monoxide, graphite carbon will also be formed.

2.3 Calculation of Reaction Zone Temperatures

Once the energy release in the assumed, simple reaction mechanism has been established, a related reaction zone (C-J)-temperature and shock front temperature can be duly evaluated for the assumptions stated in

the previous section. Any combination of equations, properly derived from the three fundamental equations for the conservation of mass, momentum and energy, may be used. For the present purpose, following the procedures used by Taylor-Lewis (1977), reaction temperatures could be calculated using two equations, as given by Lewis and Von Elhe (1961). The two equations are

$$\text{I} \qquad \frac{V_1^2}{V_2^2} - \frac{\gamma_2+1}{\gamma 2} \cdot \frac{V_1}{V_2} + \frac{n_1}{n_2} \cdot \frac{T_1}{T_2\gamma_2} = 0$$

$$\text{II} \qquad \overline{C}_V(T_2-T_1) - \Delta E_c - \frac{R}{2}\left(\frac{V_1}{V_2} - 1\right)\left(n_2T_2 + n_1T_1\frac{V_2}{V_1}\right) = 0$$

V = specific volume

T = absolute temperature (degrees Kelvin, K)

γ = specific heat ratio

R = gas constant (calories/deg.mole)

n = number of moles per gram of mixture

ΔE_c = effective energy release of reaction (calories/gram of mixture)

$\overline{C}_V$ = average specific heat at constant volume over the range T_1-T_2 (calories/ K.gram)

The subscripts 1 and 2 refer to conditions before and after the passage of the detonation front respectively.

The calculation proceeds as follows:

A value for T_2 is chosen. ΔE_c, $\overline{C}_V$ and γ_2 are calculated. Equation I is then solved for $\frac{V_1}{V_2}$, and this value is used in equation II to solve for a better value of T_2. The new value of T_2 is used to repeat the calculation until convergence. The detonation velocity, D, may now be calculated according to the equation $D = \frac{V_1}{V_2}\sqrt{n_2\ \gamma_2\ RT_2}$. The derivation of these equations is given in Appendix A.1 and A.2. Procedures for obtaining $\overline{C}_V$ values are recorded in Appendix A.3.

Although within the three assumptions mentioned earlier such procedures can be applied for any composition, they are, in the context of this thesis, only used near the composition limits of detonation.

2.4 Calculation of Shock Front Temperatures

Similarly, shock temperatures are calculated using detonation velocities derived theoretically, as explained in the previous section. Perfect gas behaviour and specific heat ratio values averaged over the initial and shocked condition are assumed. The equations are:

III $$\frac{T_1}{T_0} = y \frac{1 + \mu y}{\mu + y}$$

where $$y = M^2(1+\mu) - \mu$$

$$\mu = \frac{\bar{\gamma} - 1}{\bar{\gamma} + 1}$$

$$M = \frac{D}{C_o}$$

In these equations

T_1 = shock temperature (degrees Kelvin, K)

T_0 = initial temperature (298 K)

$\bar{\gamma}$ = average specific heat ratio over the range T_0-T_1

M = Mach number

C_o = sonic velocity in unburnt gas (metres/sec)

D = detonation velocity (metres/sec)

Derivation of these equations are given in Appendix B.1. Procedures for obtaining $\bar{\gamma}$ values are recorded in Appendix B1.A. The shock temperature calculation proceeds similar to reaction temperature calculations. A value for T_1 is chosen. $\bar{\gamma}$, μ, M and y are calculated. A better value for T_1 is calculated through equation III. The new value for T_1 is used to repeat the procedure until the two values for T_1 converge.

2.5 Principles of Homology Correlation

As pointed out in the introduction, another way to utilise the chemical nature of the reactants in studies of detonation, is based on the similarity analysis of reactants of different systems and on comparison of their near-limit behaviour.

In his work Michels (1967) first constructed the velocity vs. composition curves from experimentally-observed velocities. To expand the investigation in direct relation with the amount of energy released per mole of mixture, he usefully converted the velocities into Mach products, (γM^2), where $\gamma M^2 = \frac{D^2.m_1}{RT_o}$; m_1 is the mean molecular weight of reactants. Since physico-chemical properties of reaction products at the C-J plane depend, in a very complicated way, on the mixture of all the atoms, radicals and molecules present, he examined the simplifying assumption that bond rupture and bond rearrangements occur freely in the reaction zone, so that binary mixtures of homologous hydrocarbons with oxygen give similar product concentration at the C-J plane, for a similar initial ratio of C:H:O, regardless of the initial bond structure of the fuel molecules used. On this 'homology' basis, the fuel molecules were represented as the appropriate number of CH_2 groups and one hydrogen molecule; the sum of all the fuel elements ($n\ CH_2 + H_2$) in each mixture was then expressed as a percentage of the sum of all fuel elements and oxygen molecules in that mixture. Normalisation on the basis of explained homologous similarity of the fuel molecules, led to extensive correlation of the results obtained for the different systems. Comparison of results calculated for homologous-related unburnt mixtures revealed a close correspondence in the state parameters and composition of the C-J conditions. The similarity also extended to the actual limit composition for the various systems.

The excellent correlation of results for steady-state detonations, and approximate correlation of detonation limits for binary systems of hydrocarbons and oxygen on the basis of 'homologous' similarity of the fuel molecules, lead to the expectation that the ternary systems investigated in this work may also be normalised by the use of appropriate techniques. This should result in only minor changes, like a gradual shift, in the composition ratios of fuel, oxygen and inert of different ternary systems at the boundaries of the detonability regimes, because of small but systematic differences in structural and physico-chemical properties of the comparable fuel molecules.

CHAPTER 3

REVIEW OF INSTRUMENTATION

Experimental investigation of detonation propagation in gaseous mixtures involves the following operations:

(a) Detonations are to be initiated and stabilised;

(b) The propagation is to be studied.

(c) Gas mixtures of selected compositions must be prepared.

(a) As with shock waves, detonations are normally studied during their propagation in long tubes because, after initiation, the detonation wave requires distance to reach more or less stable conditions. In many cases, (i.e. generally for stable detonations) the use of long tubes permits a description of a detonation wave as a planar and one-dimensional process.

Initiation of detonation is concerned with all developments in the tube from the initial conditions to the first occurrence of detonation. This can be realised in a number of ways. In many cases, it is possible to achieve detonation propagation by a spark or by hot wire ignition of the test mixture. As the flame spreads out, it sends compression waves ahead into the unburnt gas, preheating it and causing, in turn, gradual acceleration of the flame, until shock waves are formed, leading to detonation ahead of the still subsonic flame (Bone et al., 1936).

Under marginal conditions, however, energy libration caused by spark ignition is relatively slow and the essential shock waves will consequently require a long time and a very long tube length to be formed. As it is often accepted that the determination of detonation limits should not depend significantly on the initiation method, but rather on

the readiness of a test mixture to continue propagation of existing detonation, and because of the requirement for tubes with extremely long initiation section, spark, or hot wire ignition is less suitable for investigation of marginal detonation. An alternative for detonation initiation is the impact method, which can be applied by detonating a strong solid explosive in the test mixture or bursting a diaphragm, which separates the test mixture from a reservoir with "driver gas" at higher pressure.

A most satisfactory impact, also used in this work, can be obtained from hot-wire ignited detonation of a highly explosive standard mixture As the initial pressure of this "primer" can be the same as the pressure in the test mixture, the diaphragm can be replaced by a valve, which is to be opened prior to ignition. After initiation has been achieved, detonation in the stabilisation section can either settle down to a stable velocity or propagate in a pulsating manner, characteristic for the marginal detonation.

(b) For velocity studies the most common methods are the optical recording of detonation wave propagation on a rotating film or the measurement of time intervals between the passage of the detonation wave over consecutive timing stations in the tube wall. The former technique provides a continuous speed record but requires very careful adjustments. The measurement of time intervals allows only calculation of mean velocities, but the method is very simple and reliable. Probes, to be used as timing stations in detonation tubes, are usually situated in one line along the tube wall and should be sensitive to one of the rapid physical changes that are caused in their environment by the passing detonation front. There are a number of designs for these probes, the most common being pressure-transducers,

temperature-dependent resistance elements, light probes, such as photodiodes, and ionisation gauges. These detectors are part of an electronic circuit, which produces an output signal in response to changes at the sensing element of the probe.

Evaluation of detonation velocities requires determination of the distance between the probes and of the time intervals between their consecutive signals. Time intervals are, for instance, measured by means of electronic counters or by photographic recordings of oscilloscope traces.

(c) Preparation of gas mixtures

The two systems most commonly applied for the preparation of gaseous mixtures, are the flow method, by which gas can be mixed and supplied to the detonation tube in one single operation, and the static method, which initially requires successive introduction of measured amounts of gas into a storage system, followed by a mixing phase before the mixture can be transferred to the tube and the detonation experiments carried out. The first technique is based on adjusting two or many separate flows of component gases in such a way that their combined supply delivers a mixture of constant selected composition. However, the initial flow adjustment could be tedious and might result in considerable loss of expensive gases. In the second method, gas quantities can be determined either by partial volume or by partial pressure. The latter method is very attractive and technically it is most simple to mix the components by their successive admission to a vessel. As the non-additivity of partial pressures in mixtures of dissimilar molecules is generally not larger than 0.1% for mixtures containing equal amounts of gaseous component and oxygen or nitrogen (Michels and Boerboom, 1953, etc.) it is wise to ignore this factor, especially for steady-state conditions.

3.1 Apparatus

The main items of equipment used in this study are the

(a) Detonation tube;

(b) Stoichiometric hydrogen-oxygen mixing system;

(c) Test mixture preparation system;

(d) Velocity measuring system;

(e) Miscellaneous equipment.

Equipment used in this work is more or less the same as that used by R. Way (1971) and Taylor Lewis (1977) with a number of alterations and modifications. The various parts of the apparatus in their present state are as follows:

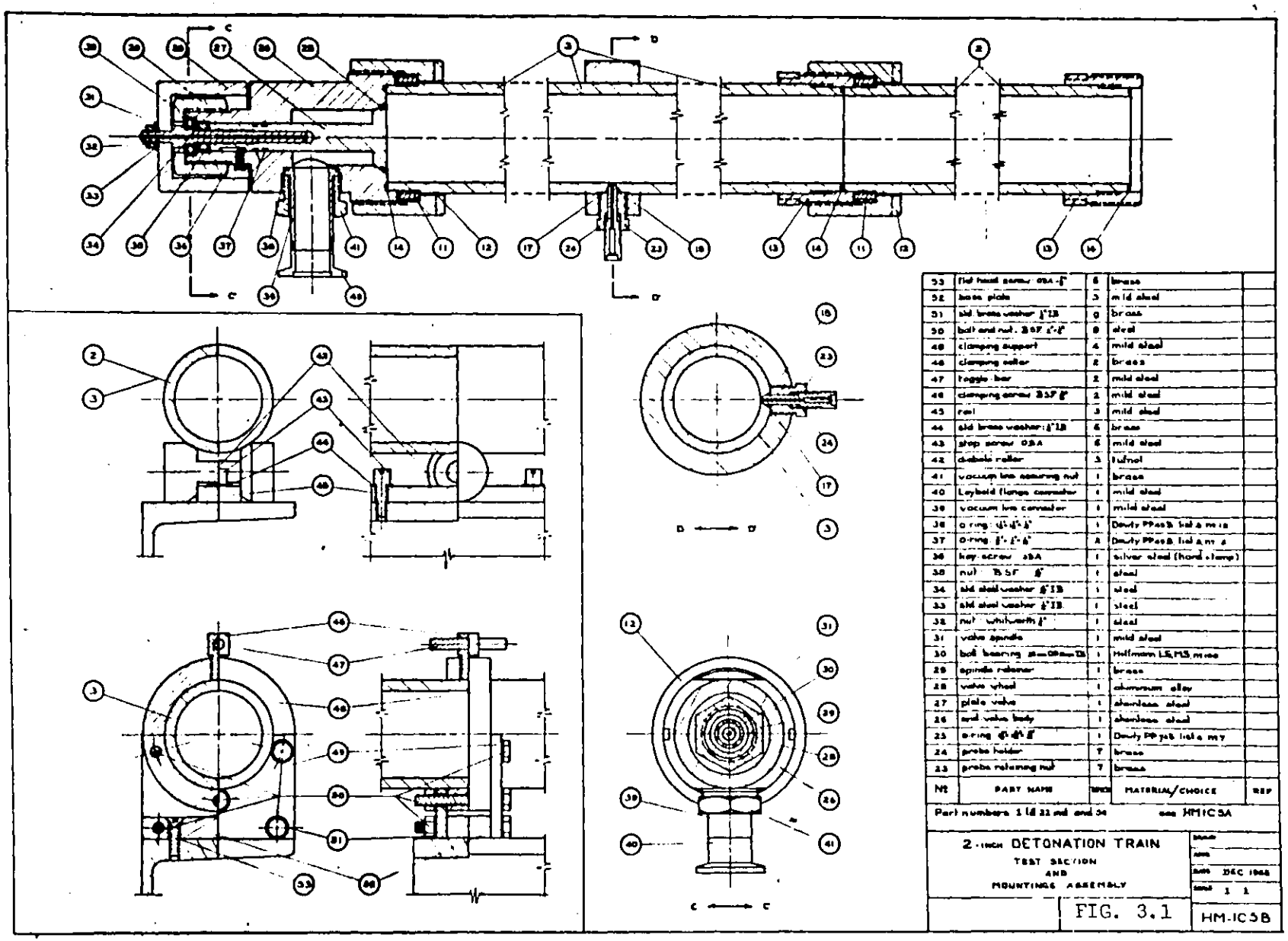
(a) Detonation tube

A 5.08 cm bore stainless steel detonation tube was used for all experiments in this work. The tube is made in three sections with brass couplings, and a pressure/vacuum seal is achieved by using rubber "O" rings fitted into grooves in the tube wall:

(i) The priming section 2.05 metres long. The initiating coil is described in section (e).

(ii) Test section of 4.35 metres long which is divided into a stabilisation section 2.2 metres long followed by a 2.15 metres long measuring section with measuring probes spaced at 0.305 metre intervals along the tube wall.

(iii) The ball valve, separating (i) and (ii), is of identical bore, and allows each section to be filled with their respective mixtures. In order to minimize disturbances generated at the mixture interface, the hollow ball is always filled with priming mixture. General engineering details of the detonation tube are given in Figs. 3.1 and 3.2, taken from H. Michels (1967).



No	PART NAME	QTY	MATERIAL/CHOICE	REF
53	flat head screw 0BA-½"	6	brass	
52	base plate	3	mild steel	
51	std brass washer ½"ID	9	brass	
50	bolt and nut - BSF ½"-½"	9	steel	
49	clamping support	4	mild steel	
48	clamping collar	2	brass	
47	toggle bar	2	mild steel	
46	clamping screw BSF ½"	2	mild steel	
45	rail	3	mild steel	
44	std brass washer ½"ID	6	brass	
43	stop screw 0BA	6	mild steel	
42	dobeli roller	3	tufnol	
41	vacuum line retaining nut	1	brass	
40	Laybold flange connector	1	mild steel	
39	vacuum line connector	1	mild steel	
38	o-ring ½"-½"-⅛"	1	Dowty PP258 Std & mtrls	
37	o-ring ½"-½"-⅛"	8	Dowty PP258 Std & mtrls	
36	key screw 2BA	1	silver steel (hand clamp)	
35	nut BSF ½"	1	steel	
34	std steel washer ½"ID	1	steel	
33	std steel washer ½"ID	1	steel	
32	nut Whitworth ½"	1	steel	
31	valve spindle	1	mild steel	
30	ball bearing [illegible]	1	Hoffmann LS,MS,mtrls	
29	spindle retainer	1	brass	
28	valve wheel	1	aluminium alloy	
27	plate valve	1	stainless steel	
26	seat valve body	1	stainless steel	
25	o-ring ½"-½"-⅛"	1	Dowty PP258 Std & mtrls	
24	probe holder	7	brass	
23	probe retaining nut	7	brass	

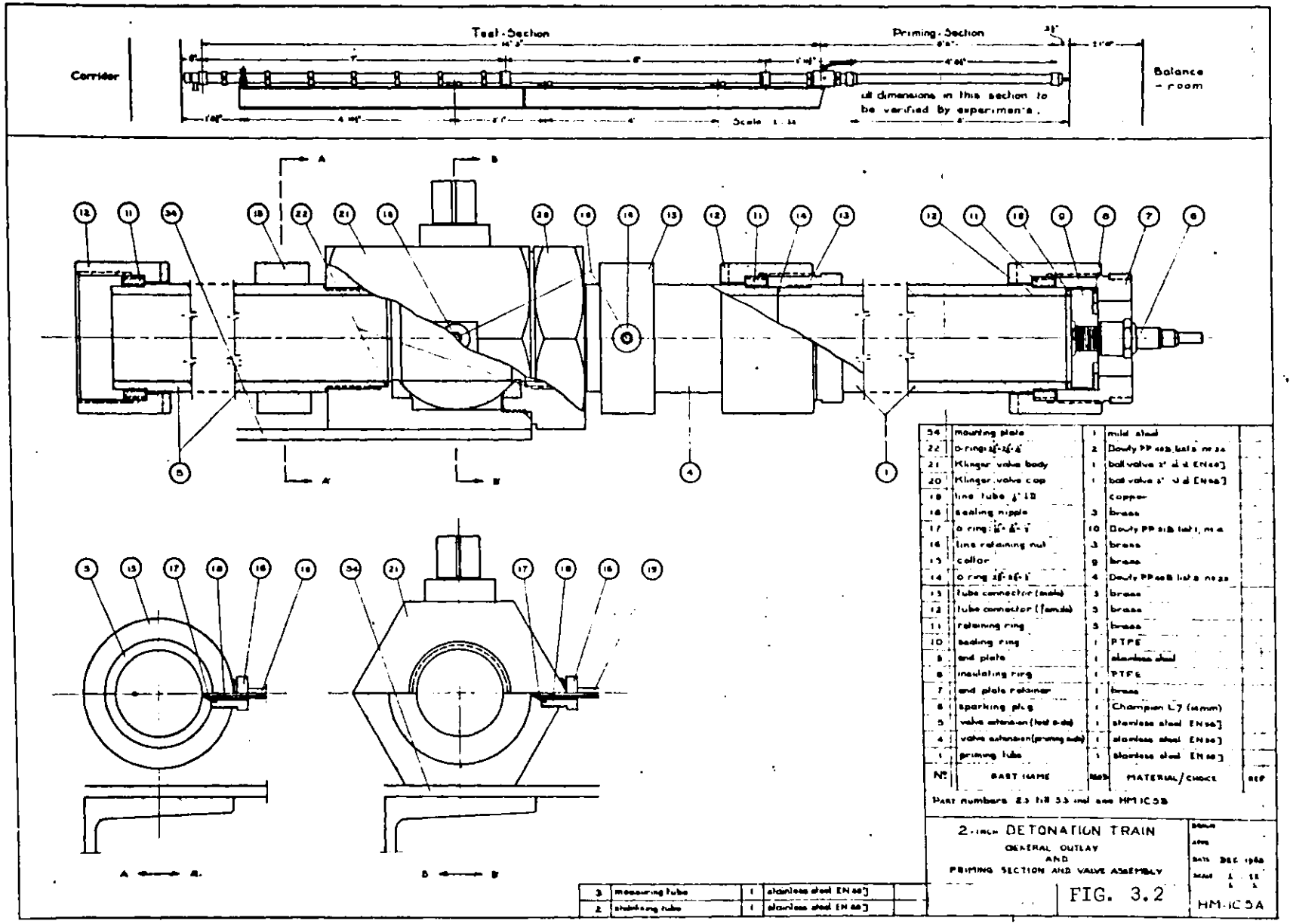
Part numbers 1 (d 22 and and 54 see HM1C5A

2-inch DETONATION TRAIN
TEST SECTION
AND
MOUNTINGS ASSEMBLY

DATE DEC 1968

FIG. 3.1

HM-1C5B



No	PART NAME	REQ	MATERIAL/CHOICE	REF
54	mounting plate	1	mild steel	
22	O-ring 2⅜"-2⅝"-¼"	2	Dowty PP 468 butyl no 22	
21	Klinger valve body	1	ball valve 2" std EN 58J	
20	Klinger valve cap	1	ball valve 2" std EN 58J	
19	line tube ⅜" ID		copper	
18	sealing nipple	3	brass	
17	O ring ⅜"-½"-⅛"	10	Dowty PP 418 butyl no 6	
16	line retaining nut	3	brass	
15	collar	9	brass	
14	O ring 2⅜"-2⅝"-¼"	4	Dowty PP 468 butyl no 22	
13	tube connector (male)	3	brass	
12	tube connector (female)	3	brass	
11	retaining ring	5	brass	
10	sealing ring	1	PTFE	
9	end plate	1	stainless steel	
8	insulating ring	1	PTFE	
7	end plate retainer	1	brass	
6	sparking plug	1	Champion L7 (14mm)	
5	valve extension (test end)	1	stainless steel EN 58J	
4	valve extension (priming end)	1	stainless steel EN 58J	
1	priming tube	1	stainless steel EN 58J	
3	measuring tube	1	stainless steel EN 58J	
2	shattering tube	1	stainless steel EN 58J	

Part numbers 23 118 53 and see HM1C5B

2-inch DETONATION TRAIN
GENERAL OUTLAY AND PRIMING SECTION AND VALVE ASSEMBLY

FIG. 3.2

DRAWN
APPD
DATE DEC 1960
SCALE ¼ ½ 1

HM-1C5A

(b) Stoichiometric hydrogen-oxgyen mixing system

A constant supply of priming mixture is made available to remove the need for batch preparations otherwise required. Fig. 3.3 illustrates the system used.

Two vessels with a 2:1 volume ratio, are filled with hydrogen and oxygen at 22 psi and connected to outlet lines containing a check valve and a diaphragm flow controller. These two lines merge to form a common filling line to the evacuated priming section. Through a T-junction this line is also connected, via a needle valve, to a specially made mercury manometer, (see Fig. 3.4), marked to allow reading of the pressure of mixture at the priming section. During the tube-filling operation, a second set of vessels are automatically filled from high pressure cylinders.

A hydrogen to oxygen flowrate of 2:1 throughout the tube-filling operation is obtained by setting the pressure differential across both flow controllers to specific levels. Since the downstream pressure was common to both, this requirement was satisfied by the vessels being filled to the same starting pressure, and the calibration of the flow controllers was achieved by measuring the detonation velocity in mixtures prepared at various settings and comparing them with the standard velocity of stoichiometric hydrogen-oxygen. Table 3.1 shows the various positions of control valves in order to obtain a 2:1 ratio of H_2/O_2.

(c) Test mixture preparation

Test mixtures are prepared by static method using partial pressures of component gases as described earlier (the total pressure in the vessel is obtained by adding up the individual pressures of component gases) in a 20 litre cylindrical glass vessel, which was used with a

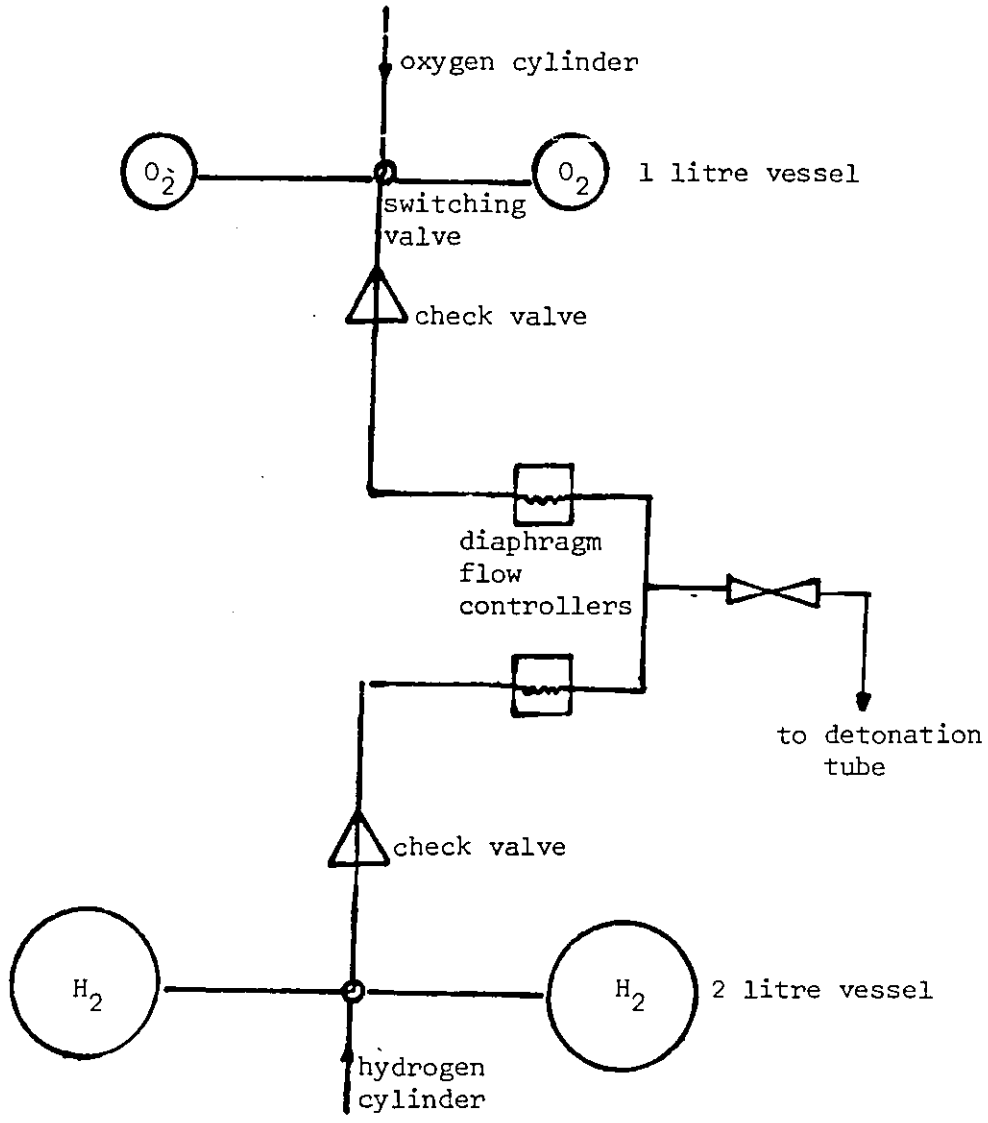


Fig. 3.3 - Stoichiometric H_2-O_2 mixing systems

No. of times oxygen control valve closed	2	3	4	5	6	7	8
No. of times hydrogen control valve should be closed	2	3.2	4.3	5.8	7.8	8.5	10

Table 3.1 - Calibration of H_2-O_2 flow controllers

system, illustrated in Fig. 3.4. Gas flow was controlled by needle valves, diaphragm valves and a specially constructed, spring-loaded, vessel-isolation valve, which prevented back-mixing into the manifold, while also allowing evacuation of the vessel and manifold when required. Pressure measurements, needed to determine the composition, were made using a differential pressure transducer which has a diaphragm as the sensing element and a coil with moving core as output generator in conjunction with a compensating system.

The diaphragm used in this work is made of beryllium-bronze and its operating range is 0-50 millibar. On reaching a pre-determined level the transducer output signal operates a solenoid valve which ensures that the pressure difference across the diaphragm never exceeds the operating range. Increase of pressure in the vessel, as it is filled, causes the output signal to rise until the solenoid valve opens to admit nitrogen to the other side of the diaphragm and thus reduces the pressure difference. When the vessel is to be emptied, or the mixture is bled into the detonation tube, the nitrogen balance is replaced by a vacuum by means of a switching valve in the common line to the solenoid valve, to compensate for decreasing pressure.

The true pressure reading thus consists of the height of mercury in the vessel manometer connected to the compensating line (see Fig. 3.4) plus or minus (depending on direction of deflection) the pressure difference across the diaphragm, which is registered in mm of mercury on a digital voltmeter. Several inaccuracies and hazards associated with direct pressure measurement by a mercury manometer are avoided in this way. For instance, (i) the vessel volume in this system is effectively constant, unlike the changing volume resulting from a moving mercury column directly connected to the mixing vessel; (ii) explosive and

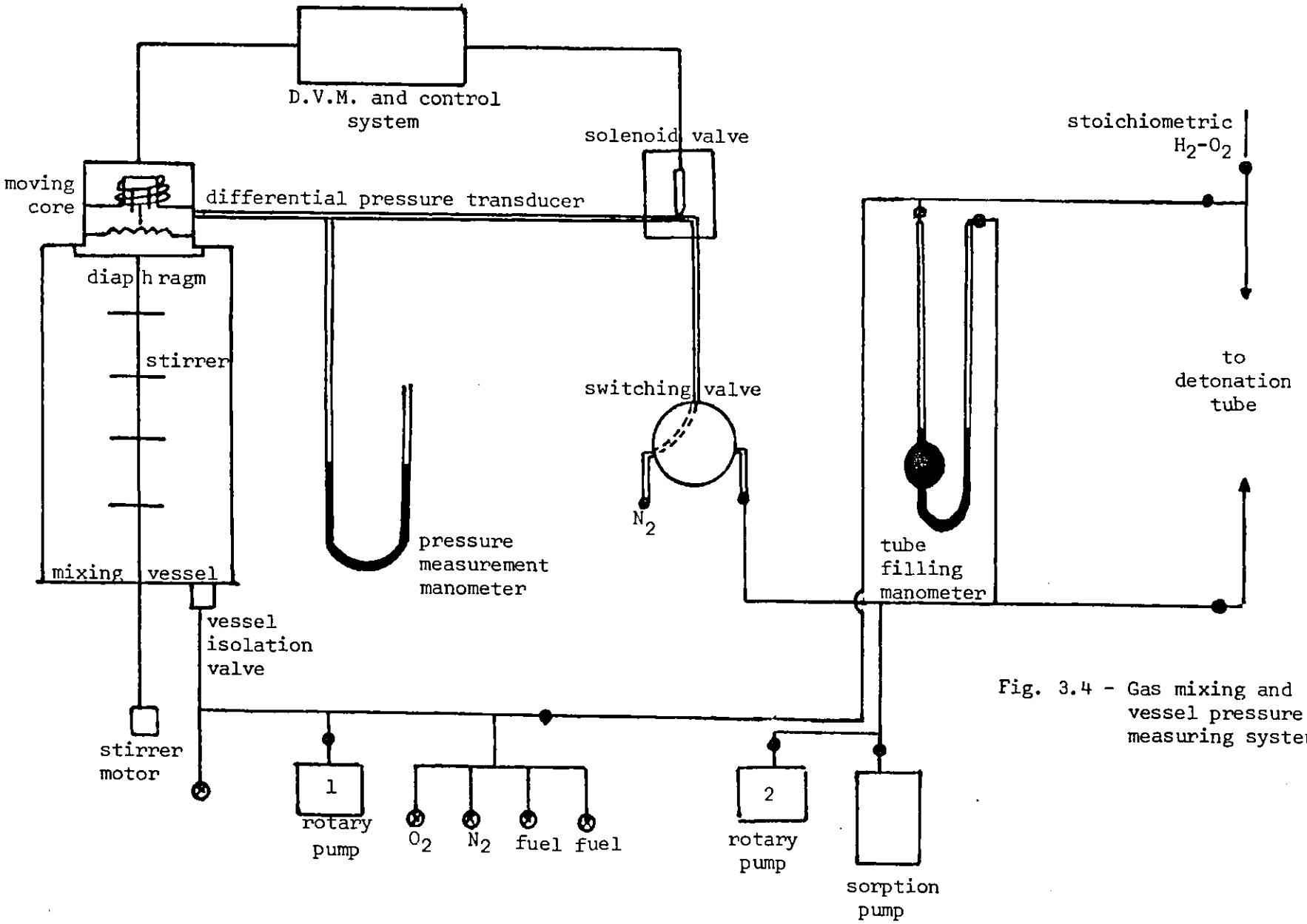


Fig. 3.4 - Gas mixing and vessel pressure measuring system

corrosive (if any) gases do not make contact with mercury; (iii) there can be no condensation in narrow tubes.

(d) Velocity measuring system

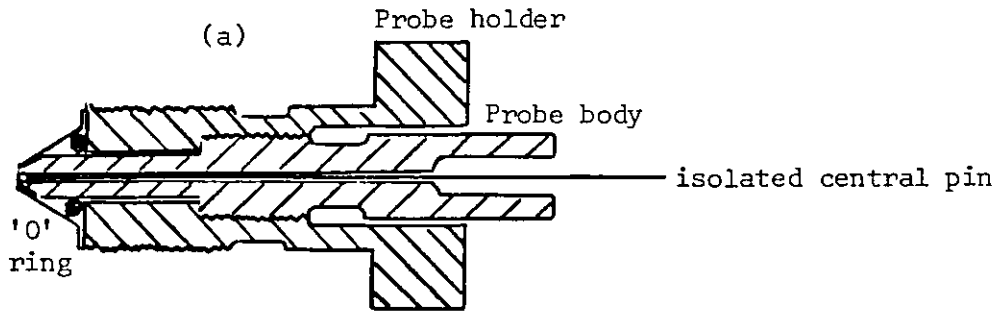
Ionization probes located in the wall of the test section of the detonation tube at 1 ft. (.305 metre) intervals were used to record the passage of the detonation wave along the tube. These probes consisted of a cylindrical brass body with an insulated central pin. Previously the insulation was achieved by sealing the central pin with araldite into a brass body. In the present work this sealing has been found to be unsatisfactory. The insulation was achieved surrounding the central pin with a glass sleeve, for which a Linderman X-ray sample tube was used. Picene wax was used to fill the two gaps between the probe body, and between the glass sheath and the central rod. The central pin can thus be changed easily or resealed whenever the probe loses sensitivity or insulation is lost. These probes can readily be cleaned, which is particularly useful when condensation products from the detonation are formed.

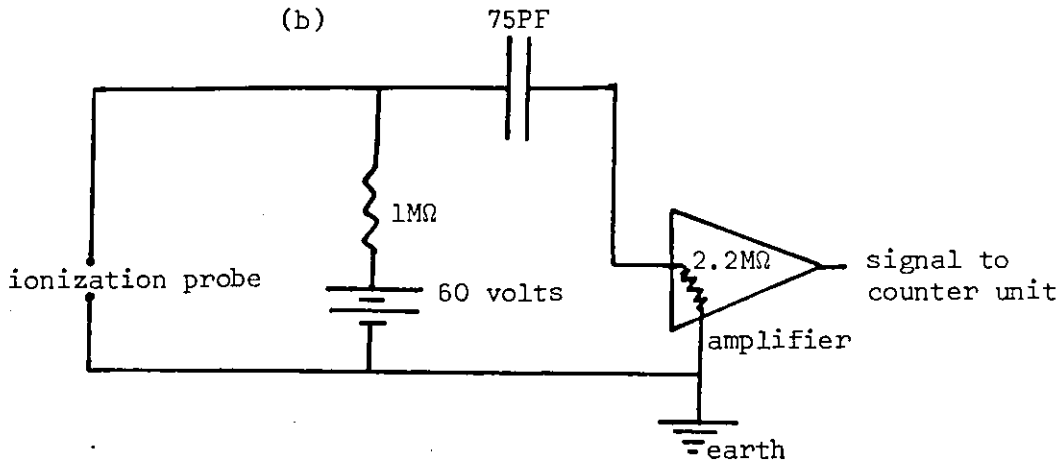
Ionization probes are basically a simple break in an electric circuit, which is momentarily closed by the small extent of conductivity that can still be found in the detonation front under marginal conditions. Figs. 3.5a and 3.5b show the assembly of a probe and the probe circuit. As a probe becomes conductive a current is drawn through the 1 MΩ resistor causing the voltage across the probe to drop. This voltage drop (change) is coupled through the isolation capacitor in the circuit to the probe amplifier. This amplifier is a high input resistance amplifier which will retard recharging of the capacitor from the supply sufficiently to prevent repetitive discharge by the same detonation wave. The output voltage pulse from the amplifier goes through a coupling cable to a 4-decade counter in a 4-channel timing system. The counter system consists of 5 threshold detectors and 4 counters (Fig. 3.5c). Each counter

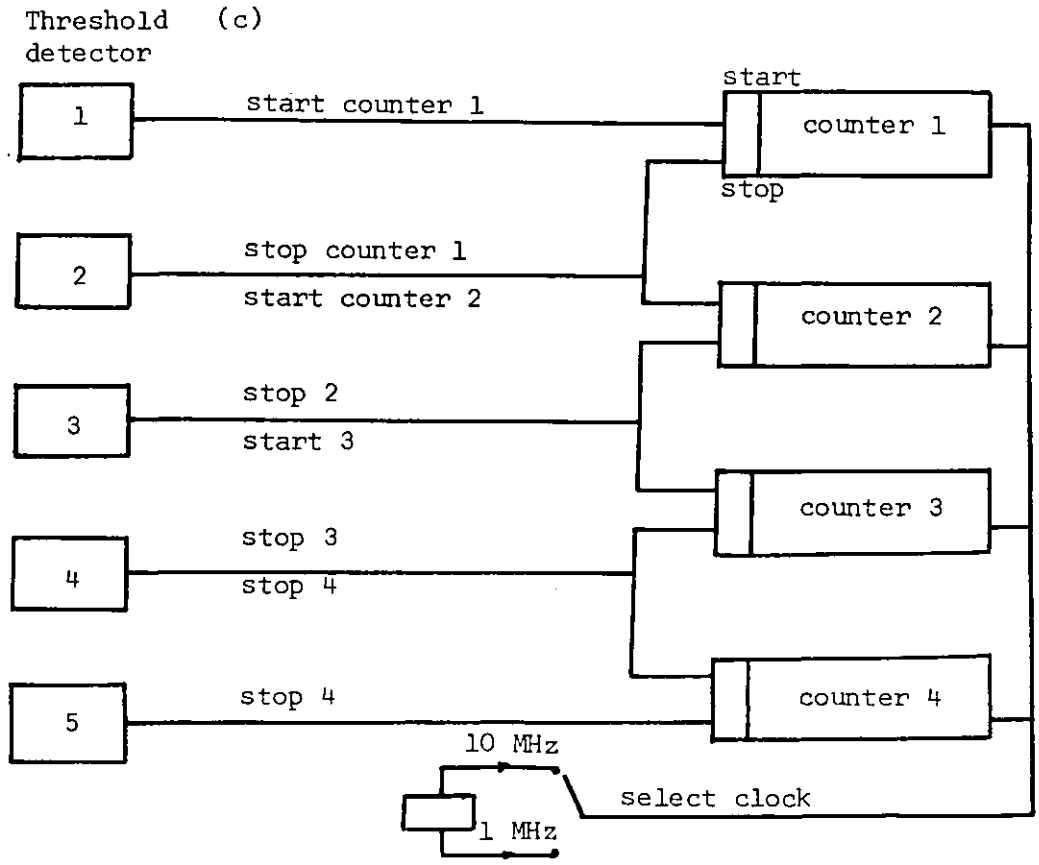
Fig. 3.5a - Ionization probe assembly

Fig. 3.5b - Probe circuit

Fig. 3.5c - Counter system







is started by a signal from one probe and stopped by the signal from the secondary probe as the detonation wave propagates along the tube. Thus each counter displays the time interval for the detonation front to propagate between two consecutive probes. The counter system has a resolution of either 1 μ sec or 100 n sec (selected by choosing a 1 M Hz or 10 M Hz count rate), and displays a maximum value of 1999 counts.

(e) Miscellaneous equipment

In all experiments a detonation wave was propagated into the gaseous test mixture by initiation with a fully established detonation in the priming mixture of stoichiometric hydrogen-oxygen. The ignition of the priming mixture was achieved with a 6 cm heated wire with a resistance of 3.8 ohms/metre in conjunction with a transformer of 6 volts and 5 amps. The wire was mounted in the end plate of the detonation tube.

To obtain a high vacuum in relatively short time, a system consisting of two pumps in series were used. A rotary pump was connected to the detonation tube until a vacuum of up to .15 torr was achieved. The rotary pump was then sealed off and an absorption pump was opened to the system to acquire a vacuum of up to 10^{-2} torr.

3.2 Experimental Method

A test mixture was prepared by admitting gases to the evacuated mixing vessel and measuring the total pressure after the addition of each component. The vessel isolation valve enables the manifold to be evacuated before admission of a different gas (see Fig. 3.4) which could enter the vessel only when its pressure is sufficient to open the valve.

Filling the vessel to an absolute pressure of 1560 mm mercury provides enough test mixture for two identical runs in the detonation tube. Each mixture was stirred for at least 40 minutes before use. The two sections

of detonation tube were respectively filled with priming mixture and test mixture to an initial pressure of 760 mm. mercury, after which all feed lines were evacuated and isolated. The recording equipment was then switched on. Immediately after opening the ball valve, the supply to the transformer was switched on, and the current through the ignition wire initiated the detonation of the priming mixture.

After each run, results were recorded. Any solid products were collected by a high power industrial vacuum cleaner, and then burnt product gases were evacuated from the tube. The probe tips required cleaning after a couple of experiments to maintain their sensitivity. The ball valve had to be disconnected from the system regularly to be thoroughly cleaned, especially after a series of experiments with condensating products, to avoid leakage from priming section to test section of the detonation tube.

3.3 Experimental Accuracy

3.3.1 Gas purity

Commercially supplied gases were used without further treatment in all the experiments.

Gas	% purity	Main impurities
Hydrogen	99.9	Nitrogen
Oxygen	99.5	"
Nitrogen	99.9	Argon
Ethylene	99.85	Other hydrocarbons
Ethane	99.0	"
Propane	99.0	"
Butane	99.0	"

3.3.2 Test mixture composition

Systematic and experimental errors in mixture preparation affect the accuracy with which mixtures can be prepared and reproduced. For limit specification it is ideally desirable to prepare detonating and non-detonating mixtures with a composition difference of not more than the uncertainty error.

Inaccuracies arising from the non-additivity of partial pressures, as mentioned earlier, have been shown by Michels (1967) to be less than .06% of the total composition for these hydrocarbon-oxygen/nitrogen mixtures. This is well within the required accuracy but will not affect the reproducibility anyway, if the gases are always added in the same order. Volume changes arising from expansion cooling and compression heating are avoided by allowing sufficient time for the temperature to attain ambiance before further component additions are made. The laboratory temperature can be assumed to have been sufficiently constant for the duration of the mixing operations.

For pressure/manometer readings, all diaphragm readings are subject to an error of ±0.2 mm.Hg. for diaphragm displacement as well as ±.05 mm.Hg. for the output stability of the digital voltmeter (R. Way, 1971). The major factor controlling the reproducibility of mixture composition is the accuracy with which the actual pressure in the mixing vessel could be measured. In this work, the pressures are read directly off a millimetric scale mounted behind the mercury manometer (Fig. 3.4). We must allow for a reading error of ±0.5 mm.Hg. in every column reading, which introduces a maximum error of ±1 mm.Hg. in each pressure measurement. Combined with the other errors mentioned, an absolute error of ±1.25 mm.Hg. is attached to every pressure measurement. The pressure of each component has been evaluated by subtraction or addition of two

differences in mercury levels of the manometer and are therefore accurate to ±2.5 mm.Hg. The maximum absolute error for a total pressure of 1560 mm.Hg. in any component is therefore $\pm.16 \times 10^{-2}$ or ±.16% of mixture composition. Although the maximum absolute error for both fuel-rich and fuel-lean side is the same, the uncertainty effect on small components is relatively more prominent. The greater spread of results towards fuel-lean side might suggest this as well.

3.3.3 Accuracy of velocity measurements

In the timing system used in this work to detect the time intervals for the passage of detonation front between successive probes for evaluation of detonation velocities, each counter is subjected to a maximum error of ±1 count. Since the timing throughout the whole experiments was done by μ sec, this means a maximum uncertainty of ±1 μ sec for each time interval. From this, the uncertainty in the tabulated velocities can be quickly estimated. For example, for a typical wave velocity of 2000 metre/sec, this would result in a maximum error of ∿±10 m/sec or an accuracy of ∿0.5%.

3.4 Limit Determination

The accuracy with which a limit composition can be determined depends not only on accuracy of the mixture composition, but also upon the way in which the velocity decays as the limit is approached. Extrapolation of the velocity curves is not a reliable method, since the actual point of failure may occur abruptly. In ternary systems studied in this work, the two diluent compositions furthest apart, for which detonation passage could be recorded by at least two counters of the timing system, were chosen as the detonation limit compositions for that particular system.

It should be mentioned that in some cases an apparent increase of the average detonation velocity towards the limits has been observed, This is not uncommon, as there are many other examples of this phenomena, e.g. in

detonation velocity of NH_3-O_2 (Breton, 1936) or of C_2H_6-O_2 mixtures (Schüller *et al.*, 1954). It is generally assumed that these detonations are not stable, and after 15 to 25 metres, the velocities reach a stable value.

CHAPTER 4

RESULTS

4.1 General

Results from the investigation of detonation in ternary mixtures of oxygen and nitrogen with, respectively, ethane, propane, butane and ethylene, are given in this chapter. Velocities are expressed as the means of values calculated from the recorded time intervals between consecutive probes. Fluctuations are given as maximum deviations from mean values of detonation velocities, and become significant in approaching the composition region of marginal detonation.

Within each system of hydrocarbon, oxygen and nitrogen, the data with the corresponding velocity-composition curves are given in consecutive sections as below. Recorded velocities are grouped according to the amount of nitrogen contained in each mixture with varying volume (mole) ratios of hydrocarbon to oxygen. The experimental relation between detonation velocity and mixture composition is also shown for each system by a curve. Generally two runs were attempted from each mixture prepared, especially for mixture compositions in marginal regions of detonation. In the following tables the letter 'F' denotes an unsuccessful run, due to either equipment failure or failure to detonate the mixture. As limiting compositions were approached, some systems gave widely differing results for consecutive runs.

4.2 The System: Ethane-Oxygen-Nitrogen

Tables 4.2a to 4.2g with corresponding Figures 4.2a to 4.2g present the detonation velocities in mixtures of ethane, oxygen and nitrogen.

4.3 The System: Propane-Oxygen-Nitrogen

Tables 4.3a to 4.3h with corresponding Figures 4.3a to 4.3h present the detonation velocities in mixtures of propane, oxygen and nitrogen.

4.4 The System: Butane-Oxygen-Nitrogen

Tables 4.4a to 4.4g with corresponding Figures 4.4a to 4.4g present the detonation velocities in mixtures of butane, oxygen and nitrogen.

4.5 The System: Ethylene-Oxygen-Nitrogen

Table 4.5a presents some detonation velocities in mixtures of ethylene, oxygen and nitrogen towards nitrogen reach side. The inclusion of this set of detonation velocities will be discussed at some later stage.

TABLE 4.2a

Detonation Velocity for the System $\frac{\text{Ethane-Oxygen-Nitrogen}}{\text{0\% Nitrogen}}$

Run no.	% Ethane (mole)	Mean Detonation Velocity (metre/sec)	Fluctuations in Detonation Velocity (metre/sec)
1	3.4	F	-
2	3.4	F	-
1	3.53	2890	+108, -160
2	3.53	F	-
1	3.92	1567	+8, -8
1	4	1544	+6, -6
1	5	1652	+25, -17
2	5	1650	+31, -18
1	6.75	1794	+4, -3
1	12.8	2073	+5, -3
2	12.8	2071	+4, -3
1	19.4	2302	+16, -10
2	19.4	2310	+15, -9
1	30	2575	+13, -7
2	30	2582	+10, -6
1	40	2575	+22, -12
2	40	2575	+22, -12
1	43.17	2489	+35, -21
1	44.6	2400	+13, -12
2	44.6	2393	+13, -11
1	46.82	2276	+8, -17
2	46.82	2270	+13, -15
1	47.15	2260	+21, -12
1	47.5	2234	+19, -28
2	47.5	2243	+21, -20
1	48.65	2157	+28, -26
1	49.3	2117	+62, -62
1	49.4	2099	+46, -39
2	49.4	2090	+64, -73
1	50.7	2016	+37, -37
1	51.5	2031	+45, -30
1	52	1955	+145, -130
2	52	2000	+45, -73
1	52.40	1950	+175, -185
2	52.40	1978	+182, -198
1	53	F	F
2	53	F	F

TABLE 4.2b

Detonation Velocity for the System $\frac{\text{Ethane-Oxygen Nitrogen}}{\text{10\% Nitrogen}}$

Run No.	% Ethane (mole)	Mean Detonation Velocity (metre/sec)	Fluctuations in Detonation Velocity (metre/sec)
1	3	F	-
2	3	2661	+201, -105
1	3.5	1571	+30, -32
2	3.5	2445	+972, -504
1	3.75	1592	+13, -10
2	3.75	1580	+25, -18
1	6.3	1786	+7, -5
1	8.6	1912	+3, -3
2	8.6	1917	+3, -2
1	10.8	2011	+4, -3
1	18.25	2288	+5, -3
2	18.25	2284	+4, -2
1	22.58	2421	+12, -10
2	22.58	2418	+10, -7
1	27.5	2497	+7, -4
1	33.9	2538	+13, -15
1	37.1	2469	+18, -16
2	37.1	2460	+25, -27
1	39.6	2370	+26, -39
2	39.6	2368	+13, -16
1	42.25	2192	+12, -10
2	42.55	2210	+15, -10
1	44	2070	+58, -66
2	44	2050	+69, -73
1	44.75	2031	+70, -38
2	44.75	2009	+12, -9
1	45.1	1986	+107, -123
2	45.1	1981	+125, -132
1	45.3	1980	+198, -198
2	45.3	F	-
1	45.5	F	-
1	45.8	F	-

TABLE 4.2c

Detonation Velocity for the System $\frac{\text{Ethane-Oxygen-Nitrogen}}{\text{20\% Nitrogen}}$

Run No.	% Ethane (mole)	Mean Detonation Velocity (metre/sec)	Fluctuations in Detonation Velocity (metre/sec)
1	2.85	F	-
2	2.85	F	-
1	3.01	2655	+30, -33
1	3.25	2474	+202, -209
1	3.95	2445	+972, -504
1	4.1	1600	+14, -14
2	4.1	1611	+21, -17
1	8.74	1916	+3, -3
1	10.15	2041	+40, -46
2	10.15	2032	+32, -22
1	11.72	2053	+18, -17
2	11.72	2067	+12, -10
1	17.3	2285	+0, -0
1	23.19	2471	+58, -116
1	27.4	2455	+15, -10
2	27.4	2464	+12, -23
1	29.1	2425	+70, -38
2	29.1	2400	+65, -41
1	32.55	2389	+4, -5
1	36.45	2162	+15, -12
2	36.45	2185	+21, -13
1	38.5	2042	+53, -38
2	38.5	2055	+94, -67
1	38.7	2005	+74, -60
1	39	1981	+112, -199
2	39	2100	+195, -195
1	39.2	2195	+200, -200
2	39.2	F	-
1	40	F	-
1	40.4	F	-
2	40.4	F	-

TABLE 4.2d

Detonation Velocity for the System $\frac{\text{Ethane-Oxygen-Nitrogen}}{\text{40\% Nitrogen}}$

Run. No.	% Ethane (mole)	Mean Detonation Velocity (metre/sec)	Fluctuations in Detonation Velocity (metre/sec)
1	2.5	F	-
2	2.5	F	-
1	3	2258	+627, -318
1	3.94	1814	+138, -339
1	4.43	1631	+9, -16
2	4.43	1671	+22, -15
1	6.54	1825	+7, -8
2	6.54	1800	+10, -7
1	10.84	2039	+1, -1
1	15.57	2209	+3, -3
1	19.33	2290	+3, -6
1	25	2103	+9, -8
1	27.85	1790	+228, -129
1	28	1730	+125, -109
2	28	1745	+143, -121
1	28.3	1713	+138, -108
2	28.3	1941	+259, -258
1	28.6	F	-
2	28.6	F	-
1	29	F	-

TABLE 4.2e

Detonation Velocity for the System $\frac{\text{Ethane-Oxygen-Nitrogen}}{\text{50\% Nitrogen}}$

Run No.	% Ethane (mole)	Mean Detonation Velocity (metre/sec)	Fluctuations in Detonation Velocity (metre/sec)
1	2.5	F	-
2	2.5	F	-
1	2.95	2330	+185, -234
2	2.95	2285	+623, -472
1	4.1	1622	+18, -20
2	4.1	1619	+12, -15
1	5.6	1760	+8, -7
2	5.6	1758	+11, -8
1	7	1825	+2, -3
1	9.9	2013	+5, -4
2	9.9	2001	+6, -3
1	12.56	2097	+0, -0
1	17.92	2132	+12, -10
1	20.8	2018	+69, -73
2	20.8	2012	+118, -124
1	21.75	1880	+85, -72
2	21.75	1851	+35, -52
1	21.9	1862	+132, -114
1	22.2	1840	+152, -152
2	22.2	F	-
1	22.5	F	-
2	22.5	F	-

TABLE 4.2f

Detonation Velocity for the System $\frac{\text{Ethane-Oxygen-Nitrogen}}{\text{60\% Nitrogen}}$

Run No.	% Ethane (mole)	Mean Detonation Velocity (metre/sec)	Fluctuations in Detonation Velocity (metre/sec)
1	2.5	F	-
2	2.5	F	-
1	2.98	2336	+266, -434
2	2.98	2572	+152, -214
1	3.23	2341	+778, -550
1	3.98	1622	+21, -30
2	3.98	1600	+18, -24
1	5.45	1777	+13, -8
1	6.88	1836	+77, -53
1	8.47	2118	+69, -69
1	10.03	2077	+77, -144
1	11.55	2114	+492, -659
1	14.82	1928	+50, -36
2	14.82	1900	+32, -30
1	15.4	1987	+17, -17
1	15.83	1760	+190, -124
1	16.16	1789	+40, -52
2	16.16	1798	+35, -48
1	16.7	1746	+52, -48
2	16.7	1751	+112, -144
1	17.1	1792	+152, -227
2	17.1	1700	+170, -214
1	17.4	F	-
1	17.7	F	-

TABLE 4.2g

Detonation Velocity for the System $\frac{\text{Ethane-Oxygen-Nitrogen}}{\text{75\% Nitrogen}}$

Run No.	% Ethane (mole)	Mean Detonation Velocity (metre/sec)	Fluctuations in Detonation Velocity (metre/sec)
1	2.5	F	-
1	3	F	-
1	3.5	2377	+845, -649
1	4.02	1647	+11, -11
2	4.02	1609	+21, -14
1	6	1863	+75, -121
1	8.05	1662	+52, -70
1	8.42	1691	+110, -48
1	9	1756	+222, -210
2	9	1783	+301, -290
1	9.4	F	-
2	9.4	F	-
1	10	F	-

Ethane-Oxygen-80% Nitrogen: no detonation.

TABLE 4.3a

Detonation Velocity for the System $\frac{\text{Propane-Oxygen-Nitrogen}}{\text{0\% Nitrogen}}$

Run. No.	% Propane (mole)	Mean Detonation Velocity (metre/sec)	Fluctuations in Detonation Velocity (metre/sec)
1	1.8	F	-
2	1.8	F	-
1	2.2	2651	+600, -725
1	2.45	2565	+150, -381
1	2.75	1564	+60, -42
2	2.75	1558	+54, -38
1	2.98	1607	+12, -9
2	2.98	1601	+3, -2
1	4.95	1819	+2, -2
1	9.9	2110	+1, -1
1	14.8	2330	+2, -3
2	14.8	2333	+3, -3
1	19.75	2485	+2, -3
2	19.75	2485	+2, -3
1	24.8	2581	+0, -0
1	28.75	2602	+7, -10
2	28.75	2600	+3, -5
1	30.85	2591	+1, -1
2	30.85	2590	+4, -6
1	33.7	2536	+10, -5
1	34.8	2474	+9, -13
2	34.8	2484	+12, -12
1	37.43	2292	+3, -5
2	37.43	2290	+6, -4
1	39.82	2111	+33, -48
2	39.82	2100	+65, -77
1	41.8	1981	+88, -88
1	42.55	1900	+111, -134
2	42.55	1990	+190, -190
1	42.7	1882	+77, -93
2	42.7	1875	+92, -113
1	43.07	1855	+212, -194
2	43.07	F	-
1	43.45	F	-
2	43.45	F	-

TABLE 4.3b

Detonation Velocity for the System $\frac{\text{Propane-Oxygen-Nitrogen}}{\text{15\% Nitrogen}}$

Run. No.	% Propane (mole)	Mean Detonation Velocity (metre/sec)	Fluctuations in Detonation Velocity (metre/sec)
1	1.8	F	-
1	2.1	F	-
2	2.1	2410	+997, -637
1	2.55	2207	+874, -489
2	2.55	2185	+652, -776
1	3.3	1626	+79, -48
2	3.3	1772	+151, -381
1	3.44	1649	+3, -3
1	4.86	1806	+4, -5
1	5.65	1870	+6, -8
2	5.65	1871	+2, -2
1	7.75	1980	+1, -2
1	9.34	2085	+0, -0
1	10.77	2181	+0, -0
2	10.77	2186	+3, -4
1	13.75	2296	+2, -3
2	13.75	2296	+2, -3
1	16.9	2397	+3, -2
1	18.7	2428	+7, -10
2	18.7	2426	+5, -4
1	22.74	2503	+9, -5
1	28.32	2399	+9, -10
2	28.32	2403	+7, -10
1	32.02	2132	+28, -38
2	32.02	2131	+25, -30
1	34.16	1989	+228, -147
1	35	1900	+111, -135
2	35	1892	+113, -144
1	35.44	1871	+49, -94
2	35.44	2194	+529, -723
1	36.4	2020	+190, -190
2	36.4	F	-
1	37	F	-
1	37.65	F	-
2	37.65	F	-

TABLE 4.3c

Detonation Velocity for the System $\frac{\text{Propane-Oxygen-Nitrogen}}{25\% \text{ Nitrogen}}$

Run No.	% Propane (mole)	Mean Detonation Velocity (metre/sec)	Fluctuations in Detonation Velocity (metre/sec)
1	2	F	-
1	2.3	2526	+986, -467
2	2.3	2611	+815, -352
1	2.46	2796	+201, -125
1	2.9	1549	+12, -15
2	2.9	1550	+13, -15
1	3.24	1631	+7, -6
2	3.24	1633	+5, -7
1	4.4	1765	+2, -3
1	7.35	1995	+1, -1
1	11	2178	0, 0
2	11	2178	0, 0
1	16.8	2380	+4, -2
2	16.8	2385	+5, -2
1	18.78	2428	+0, -0
1	19.79	2426	+2, -1
2	19.79	2428	+4, -3
1	24	2364	+4, -4
2	24	2365	+4, -4
1	26.39	2237	+7, -6
2	26.39	2235	+6, -4
1	28.25	2101	+6, -5
1	30	1930	+68, -42
2	30	1938	+72, -58
1	30.25	1919	+100, -86
1	30.44	1877	+73, -111
2	30.44	1875	+58, -100
1	30.75	1870	+158, -192
2	30.75	1877	+143, -143
1	31.1	F	-
1	31.4	1947	+365, -617
2	31.4	1963	+221, -221
1	32.3	2016	+414, -301
2	32.3	F	-
1	32.95	F	-
2	32.95	F	-

TABLE 4.3d

Detonation Velocity for the System $\frac{\text{Propane-Oxygen-Nitrogen}}{\text{40\% Nitrogen}}$

Run No.	% Propane (mole)	Mean Detonation Velocity (metre/sec)	Fluctuations in Detonation Velocity (metre/sec)
1	1.8	F	-
2	1.8	F	-
1	2	2796	+148, -120
2	2	F	-
1	2.7	1554	+16, -18
2	2.7	1560	+18, -17
1	3.25	1650	+12, -12
1	3.66	1707	+19, -29
2	3.66	1703	+15, -11
1	5	1830	+7, -5
2	5	1831	+9, -6
1	7.5	2002	+4, -6
2	7.5	2000	+4, -7
1	10.01	2131	-
1	10.73	2172	+16, -21
2	10.73	2173	+16, -21
1	13.2	2241	+9, -8
2	13.2	2236	+10, -10
1	15.2	2285	+9, -8
1	15.88	2298	+14, -14
2	15.88	2295	+12, -10
1	17.6	2287	+12, -9
1	20.9	2139	+30, -21
2	20.9	2136	+25, -19
1	22	2000	+11, -19
1	22.42	1930	+6, -6
2	22.42	1930	+5, -5
1	23.04	2267	+316, -473
2	23.04	2037	+288, -267
1	23.5	F	-
2	23.5	F	-
1	24	F	-

TABLE 4.3e

Detonation Velocity for the System $\frac{\text{Propane-Oxygen-Nitrogen}}{\text{50\% Nitrogen}}$

Run No.	% Propane (mole)	Mean Detonation Velocity (metre/sec)	Fluctuations in Detonation Velocity (metre/sec)
1	2	F	-
2	2	F	-
1	2.16	2616	+312, -180
2	2.16	2647	+421, -203
1	2.47	2198	+658, -768
2	2.47	2195	+523, -690
1	2.9	1594	+46, -29
1	2.95	1630	+25, -37
1	4.1	1742	+16, -6
2	4.1	1745	+23, -21
1	5	1829	+11, -13
2	5	1827	+10, -13
1	7.5	2021	+4, -6
2	7.5	2018	+7, -7
1	10.18	2138	+4, -3
1	10.7	2159	+14, -21
2	10.7	2156	+12, -18
1	14.6	2122	+11, -13
2	14.6	2124	+5, -13
1	15.8	2000	+34, -28
2	15.8	2006	+34, -26
1	16.25	1845	+68, -89
1	16.5	1922	+201, -293
2	16.5	1840	+190, -150
1	17	F	-
2	17	F	-
1	17.5	F	-

TABLE 4.3f

Detonation Velocity for the System $\frac{\text{Propane-Oxygen-Nitrogen}}{\text{60\% Nitrogen}}$

Run No.	% Propane (mole)	Mean Detonation Velocity (metre/sec)	Fluctuations in Detonation Velocity (metre/sec)
1	2	F	-
2	2	F	-
1	2.3	F	-
2	2.3	2868	+63, -81
1	2.79	1602	+10, -13
2	2.79	1588	+14, -26
1	3.25	1681	+8, -5
2	3.25	1680	+8, -3
1	4.45	1830	+9, -7
2	4.45	1831	+8, -6
1	5.88	1940	+5, -9
1	7.5	2003	+3, -3
2	7.5	2000	+4, -3
1	10.75	1992	+5, -6
1	11.8	1937	+14, -22
2	11.8	1939	+14, -15
1	12.35	1860	+50, -68
2	12.35	1851	+68, -80
1	12.5	1821	+72, -93
2	12.5	1810	+46, -75
1	12.6	1786	+87, -87
2	12.6	F	-
1	12.75	F	-
2	12.75	F	-
1	13	F	-

TABLE 4.3g

Detonation Velocity for the System $\frac{\text{Propane-Oxygen-Nitrogen}}{\text{70\% Nitrogen}}$

Run No.	% Propane (mole)	Mean Detonation Velocity (metre/sec)	Fluctuations in Detonation Velocity (metre/sec)
1	2	F	-
2	2	F	-
1	2.35	F	-
2	2.35	1566	+18, -20
1	2.55	1719	+14, -16
1	2.7	1632	+51, -64
1	2.97	1634	+41, -44
2	2.97	1635	+96, -53
1	3.17	1688	+21, -13
2	3.17	1688	+19, -8
1	3.23	1677	+24, -18
1	4.5	1820	+65, -78
2	4.5	1821	+19, -31
1	5.72	1904	+8, -10
2	5.72	1900	+14, -20
1	7	1866	+21, -25
1	7.7	1826	+45, -58
2	7.7	1824	+47, -39
1	8.5	1782	+14, -19
2	8.5	1780	+16, -7
1	9	1690	+111, -111
1	9.2	1648	+112, -150
2	9.2	F	-
1	9.7	F	-
2	9.7	F	-

TABLE 4.3h

Detonation Velocity for the System $\frac{\text{Propane-Oxygen-Nitrogen}}{77\% \text{ Nitrogen}}$

Run No.	% Propane (mole)	Mean Detonation Velocity (metre/sec)	Fluctuations in Detonation Velocity (metre/sec)
1	2.5	F	-
2	2.5	F	-
1	2.8	F	-
2	2.8	2120	+397, -855
1	3	1700	+51, -56
2	3	1694	+22, -24
1	3.98	1758	+93, -45
2	3.98	1728	+51, -45
1	4.7	1782	+31, -21
2	4.7	1780	+14, -16
1	5.5	1772	+88, -94
2	5.5	1770	+92, -99
1	6.01	1751	+123, -134
2	6.01	1799	+185, -185
1	6.3	F	-
1	6.45	F	-
2	6.45	F	-

Propane-Oxygen-80% Nitrogen: no detonation.

TABLE 4.4a

Detonation Velocity for the System $\frac{\text{Butane-Oxygen-Nitrogen}}{\text{0\% Nitrogen}}$

Run No.	% Butane (mole)	Mean Detonation Velocity (metre/sec)	Fluctuations in Detonation Velocity (metre/sec)
1	1.8	F	-
1	2.15	2255	+744, -581
2	2.15	2149	+740, -600
1	2.2	2778	+70, -42
2	2.2	2798	+218, -155
1	2.4	2089	+17, -13
1	3.8	1617	+14, -25
2	3.8	1634	+12, -31
1	5.2	1912	+14, -22
1	8.6	2214	+8, -4
2	8.6	2189	+13, -12
1	15.9	2466	+10, -9
2	15.9	2460	+6, -7
1	22.9	2589	+25, -22
2	22.9	2587	+27, -17
1	29.9	2460	+22, -26
2	29.9	2452	+27, -17
1	34.7	2220	+34, -47
1	37.6	1960	+93, -85
2	37.6	1992	+124, -97
1	37.9	1936	+54, -36
2	37.9	1926	+73, -88
1	38.15	1905	+57, -66
2	38.15	1899	+77, -99
1	38.9	1890	+223, -223
2	38.9	F	-
1	39.2	F	-
2	39.2	F	-

TABLE 4.4b

Detonation Velocity for the System $\frac{\text{Butane-Oxygen-Nitrogen}}{10\% \text{ Nitrogen}}$

Run No.	% Butane (mole)	Mean Detonation Velocity (metre/sec)	Fluctuations in Detonation Velocity (metre/sec)
1	1.8	F	-
2	1.8	F	-
1	2	2745	+404, -300
1	2.2	2233	+545, -481
2	2.2	2301	+473, -581
1	2.7	1586	+12, -14
2	2.7	1598	+16, -24
1	4.2	1760	+7, -3
1	5.15	1918	+6, -4
2	5.15	1923	+3, -3
1	6.9	2058	+7, -5
1	9.55	2197	+2, -3
1	15.7	2420	+10, -8
1	22.33	2485	+14, -11
2	22.33	2472	+21, -17
1	25.73	2416	+15, -9
1	28.83	2200	+34, -22
2	28.83	2175	+42, -29
1	31.25	2026	+65, -78
1	31.70	1945	+88, -95
2	31.70	1973	+111, -101
1	32.2	1918	+73, -51
2	32.2	1945	+121, -132
1	32.75	1910	+93, -85
1	32.98	1900	+131, -143
2	32.98	1850	+144, -144
1	33.3	F	-
2	33.3	F	-

TABLE 4.4c

Detonation Velocity for the System $\frac{\text{Butane-Oxygen-Nitrogen}}{\text{25\% Nitrogen}}$

Run No.	% Butane (mole)	Mean Detonation Velocity (metre/sec)	Fluctuations in Detonation Velocity (metre/sec)
1	1.5	F	-
1	1.7	2673	+116, -92
1	1.8	1582	+19, -20
2	1.8	1600	+21, -17
1	2.4	1814	+20, -47
1	5.1	1934	+9, -4
2	5.1	1928	+7, -2
1	7.2	2086	+4, -3
2	7.2	2050	+2, -4
1	9.25	2197	+0, -0
1	12.50	2330	+2.3, -3
1	15.75	2428	+2, -2
2	15.75	2430	+3, -2
1	20.89	2334	+23, -16
2	20.89	2312	+10, -8
1	22.54	2227	+15, -11
2	22.54	2231	+16, -13
1	24.67	2001	+20, -20
1	25.24	1945	+75, -61
2	25.24	1940	+98, -105
1	25.75	1932	+78, -58
2	25.75	1932	+78, -58
1	26	1910	+46, -40
2	26	1870	+73, -52
1	26.3	F	-
1	26.85	F	-
2	26.85	F	-

TABLE 4.4d

Detonation Velocity for the System $\frac{\text{Butane-Oxygen-Nitrogen}}{\text{40\% Nitrogen}}$

Run No.	% Butane (mole)	Mean Detonation Velocity (metre/sec)	Fluctuations in Detonation Velocity (metre/sec)
1	1.8	F	-
1	1.94	2665	+672, -672
1	2.42	F	-
2	2.42	1653	+40, -67
1	2.6	1644	+46, -46
2	2.6	1635	+16, -23
1	3.8	1824	+12, -10
1	5.1	1943	+12, -9
2	5.1	1940	+9, -7
1	8.91	2158	+26, -17
2	8.91	2160	+14, -10
1	12.16	2291	+5, -4
1	12.72	2280	+3, -3
1	17.4	2092	+15, -30
2	17.4	2065	+45, -64
1	18.07	2038	+62, -77
2	18.07	2030	+72, -84
1	19	1918	+124, -75
1	19.87	1877	+147, -123
2	19.87	1860	+162, -162
1	20.5	1832	+150, -150
1	20.72	1790	+158, -127
2	20.72	1700	+173, -145
1	21	F	-
1	21.2	F	-
2	21.2	F	-

TABLE 4.4e

Detonation Velocity for the System $\frac{\text{Butane-Oxygen-Nitrogen}}{\text{50\% Nitrogen}}$

Run No.	% Butane (mole)	Mean Detonation Velocity (metre/sec)	Fluctuations in Detonation Velocity (metre/sec)
1	1.80	F	-
2	1.80	F	-
1	1.95	1790	-
2	1.95	1796	+15, -9
1	2.4	1829	+8, -5
2	2.4	1830	+9, -8
1	4.3	1957	+0, -0
2	4.3	1957	+3, -8
1	8	2092	+12, -16
1	10	2132	+7, -7
2	10	2130	+3, -3
1	11.90	2085	+0, -0
2	11.90	2095	+14, -19
1	13.87	2056	+23, -27
2	13.87	2048	+32, -21
1	14.56	1938	+39, -71
1	14.8	1940	+66, -87
1	15	1966	+29, -62
2	15	1960	+70, -94
1	15.2	1950	+111, -111
2	15.2	F	-
1	15.4	F	-
2	15.4	F	-

TABLE 4.4f

Detonation Velocity for the System $\frac{\text{Butane-Oxygen-Nitrogen}}{60\% \text{ Nitrogen}}$

Run No.	% Butane (mole)	Mean Detonation Velocity (metre/sec)	Fluctuations in Detonation Velocity (metre/sec)
1	1.8	F	-
1	2	2508	+221, -185
2	2	F	-
1	2.4	1760	+25, -18
2	2.4	1765	+14, -11
1	3	1840	+31, -21
2	3	1847	+12, -7
1	4.25	1900	+8, -6
1	8	2021	+7, -9
2	8	2028	+11, -8
1	10.2	1972	+5, -3
1	11.1	1896	+3, -3
2	11.1	1800	+37, -37
1	11.45	2010	+147, -130
2	11.45	F	-
1	12	2050	+267, -141
2	12	F	-
1	12.1	F	-
2	12.1	F	-
1	12.5	F	-

TABLE 4.4g

Detonation Velocity for the System $\frac{\text{Butane-Oxygen-Nitrogen}}{\text{70\% Nitrogen}}$

Run No.	% Butane (mole)	Mean Detonation Velocity (metre/sec)	Fluctuations in Detonation Velocity (metre/sec)
1	1.8	F	-
2	1.8	F	-
1	2.1	2525	+794, -510
2	2.1	F	-
1	2.65	1755	+18, -10
1	3.46	1849	+9, -4
2	3.46	1855	+3, -3
1	6.61	1761	+46, -92
1	7.53	1773	+47, -51
2	7.53	1760	+56, -50
1	8	1685	+93, -78
2	8	1705	+123, -111
1	8.3	1663	+121, -121
2	8.3	1700	+185, -134
1	8.5	F	-
2	8.5	F	-

Butane-Oxygen-78% Nitrogen: no detonation.

TABLE 4.5a

Some Detonation Velocity for the System C_2H_4-O_2-N_2 Towards Nitrogen Rich Side

Run No.	% Nitrogen (mole)	% Ethylene (mole)	Mean Detonation Velocity (metre/sec)	Fluctuations in Detonation Velocity (metre/sec)
1	86	3.5	F	-
2	86	3.5	F	-
1	84	4	1650	+115, -170
2	84	4	1590	+83, -72
1	80.5	4.9	1687	+11, -11
1	76	4	1627	+13, -13
2	76	4	1631	+27, -34
1	76	3.5	F	-
2	76	3.5	F	-
1	74	7	1832	+12, -11
1	74	12	1600	+83, -83
2	74	12	1583	+97, -68
1	74	12.5	F	-
1	70	11	1872	+1, -1
1	70	15.1	1603	+73, -62
2	70	15.1	1561	+112, -112
1	70	15.5	F	-
2	70	15.5	F	-
1	68	14	1846	+2, -1
2	68	14	1850	+3, -3
1	68	16.5	1575	+78, -69
2	68	16.5	1583	+55, -55
1	68	17.1	F	-
2	68	17.1	F	-
1	66.8	15.3	1711	+100, -99
1	65	18	1732	+104, -138
1	65	18.7	1581	+27, -27
2	65	18.7	1602	+93, -47
1	65	19.1	F	-
1	61	22	F	-
2	61	22	F	-

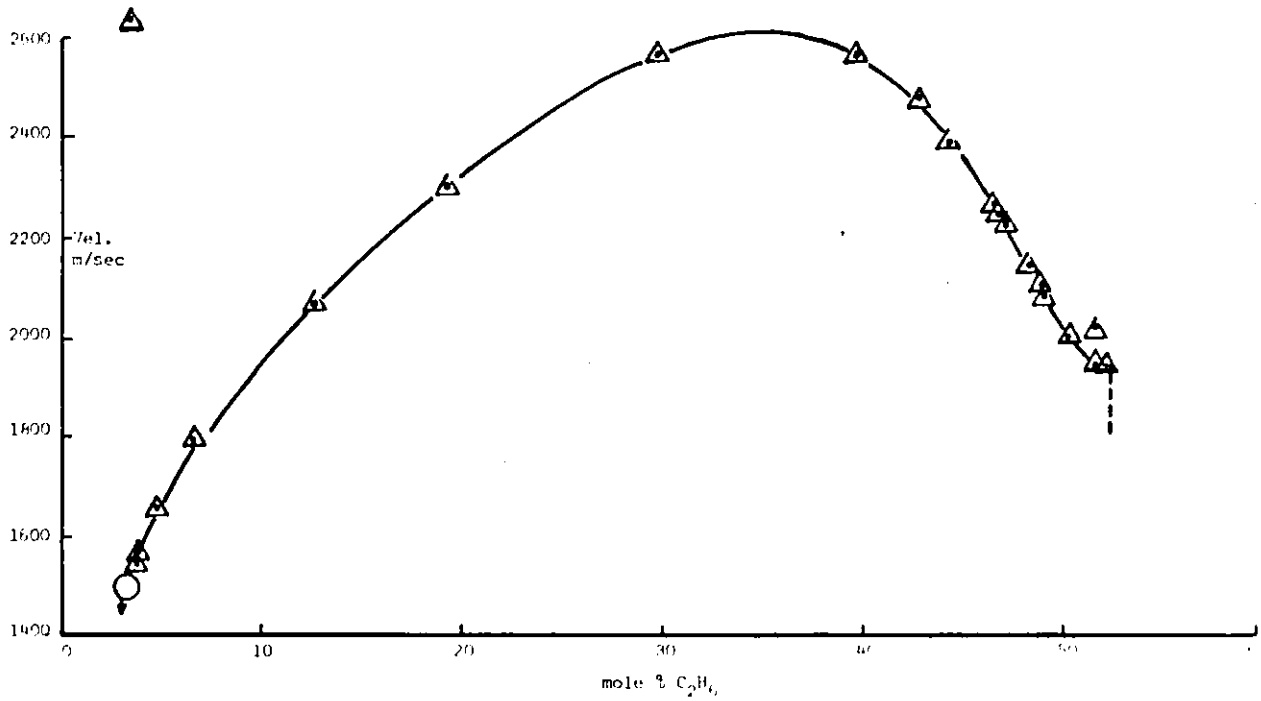
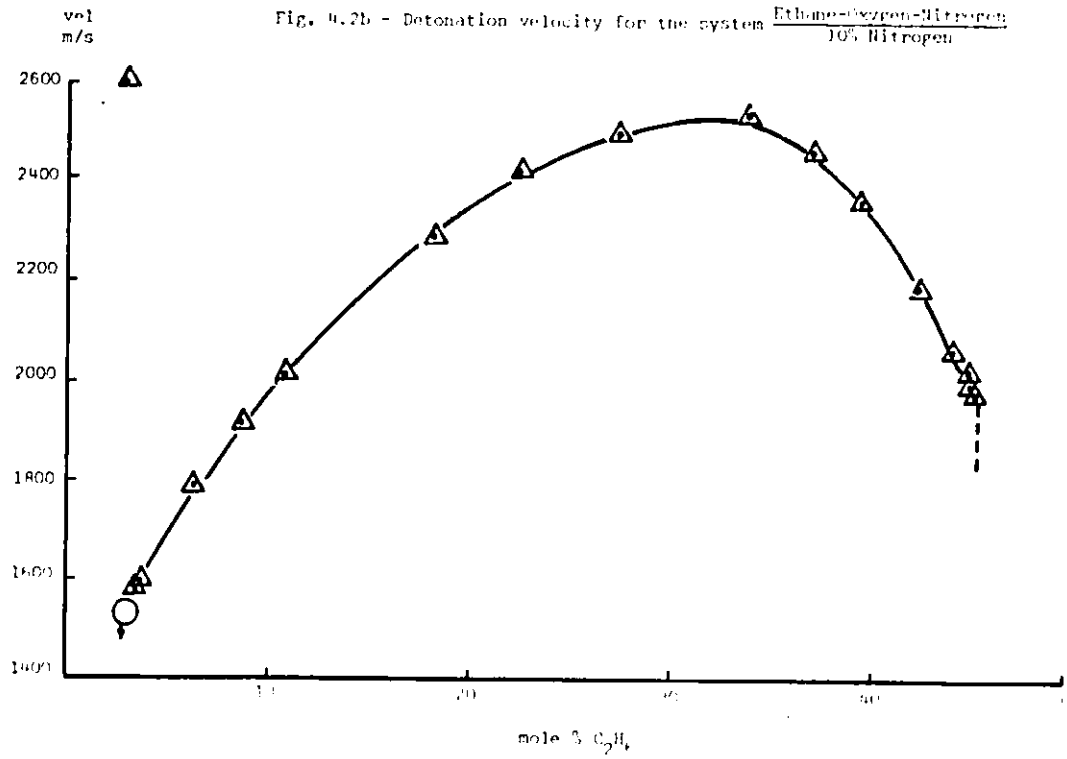


Fig. 4.2a - Detonation velocity for the system $\frac{\text{Ethane-Oxygen-Nitrogen}}{0\% \text{ Nitrogen}}$

Fig. 4.2b - Detonation velocity for the system $\frac{\text{Ethane-Oxygen-Nitrogen}}{10\% \text{ Nitrogen}}$



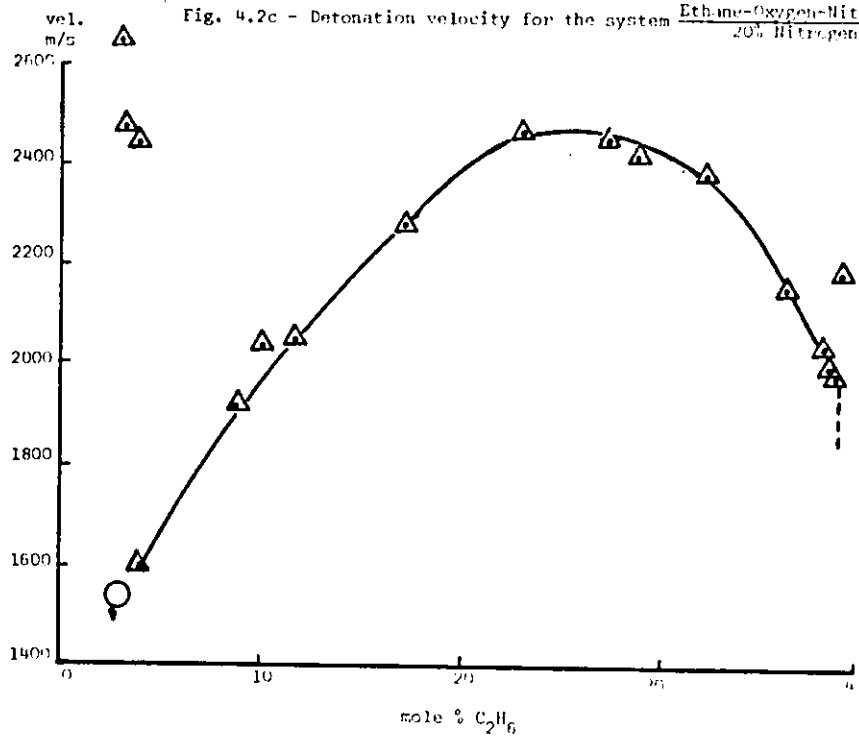


Fig. 4.2c - Detonation velocity for the system $\frac{\text{Ethane-Oxygen-Nitrogen}}{20\% \text{ Nitrogen}}$

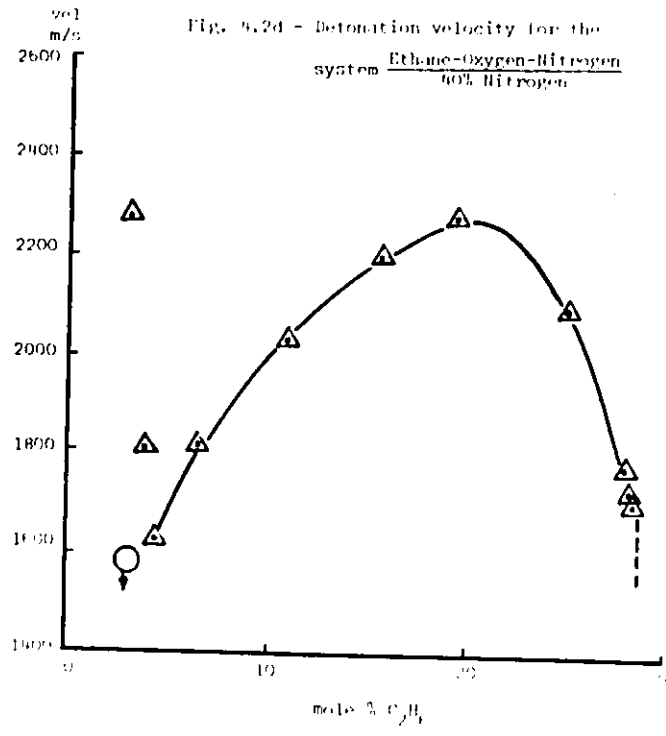


Fig. 4.2d - Detonation velocity for the system $\frac{\text{Ethane-Oxygen-Nitrogen}}{60\% \text{ Nitrogen}}$

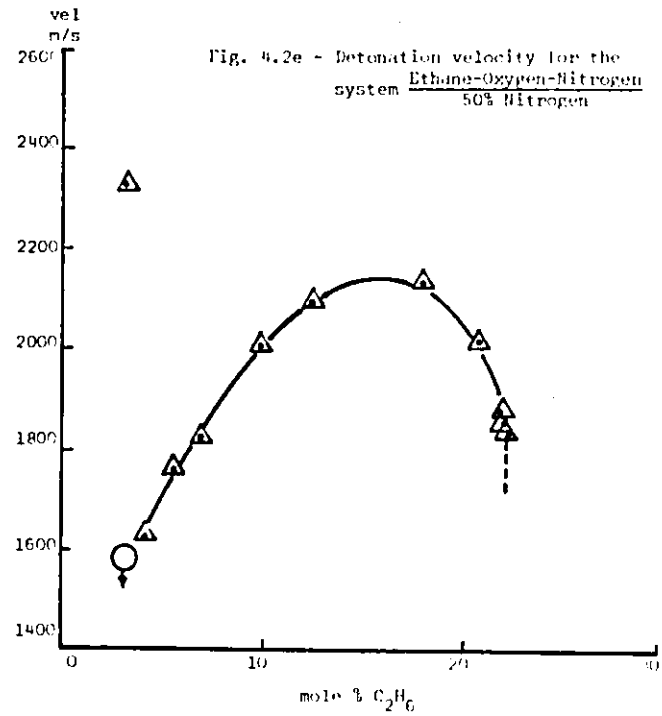


Fig. 4.2e - Detonation velocity for the system $\frac{\text{Ethane-Oxygen-Nitrogen}}{\text{50\% Nitrogen}}$

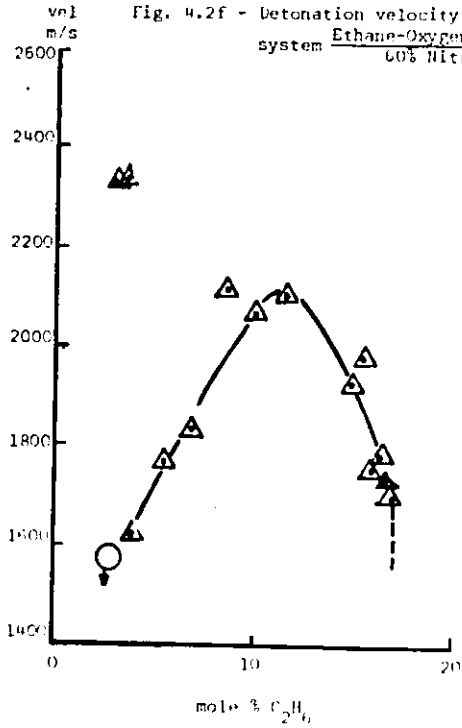


Fig. 4.2f - Detonation velocity for system $\frac{\text{Ethane-Oxygen-Nitrogen}}{\text{60\% Nitrogen}}$

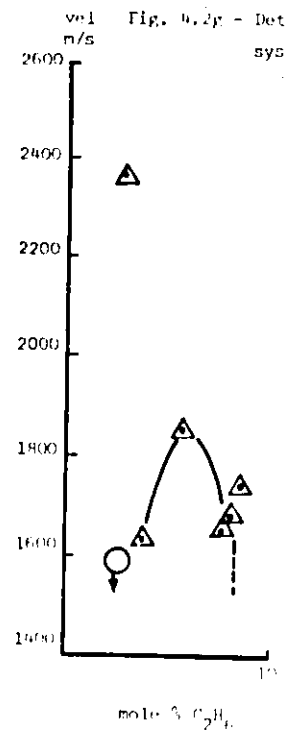


Fig. 4.2g - Detonation velocity for system $\frac{\text{Ethane-Oxygen-Nitrogen}}{\text{70\% Nitrogen}}$

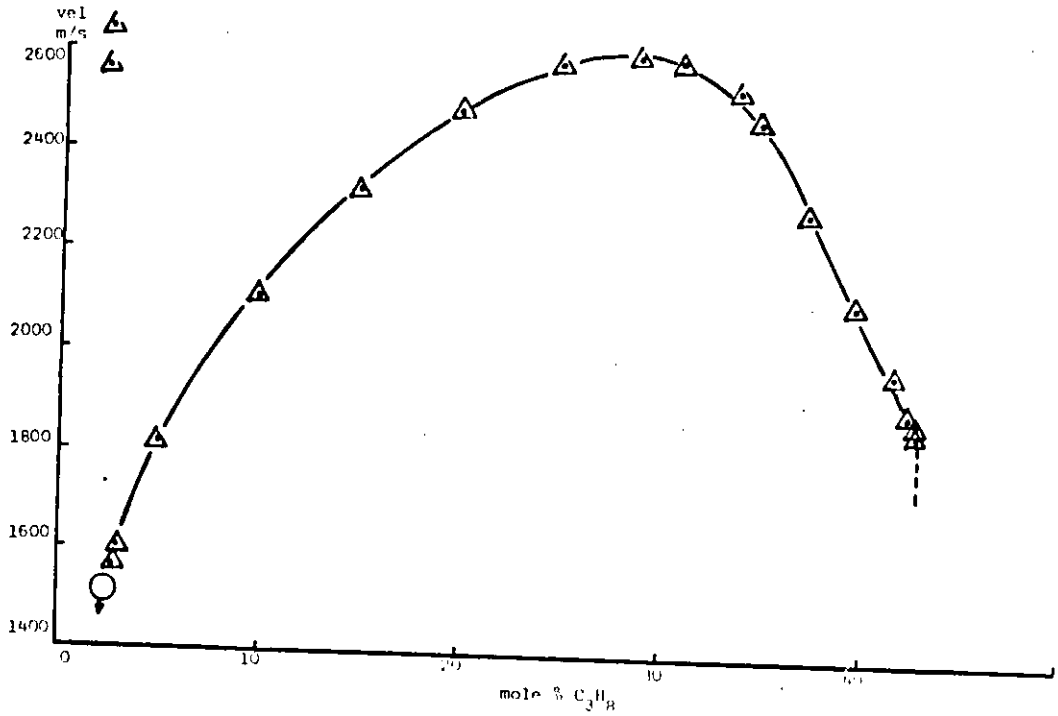
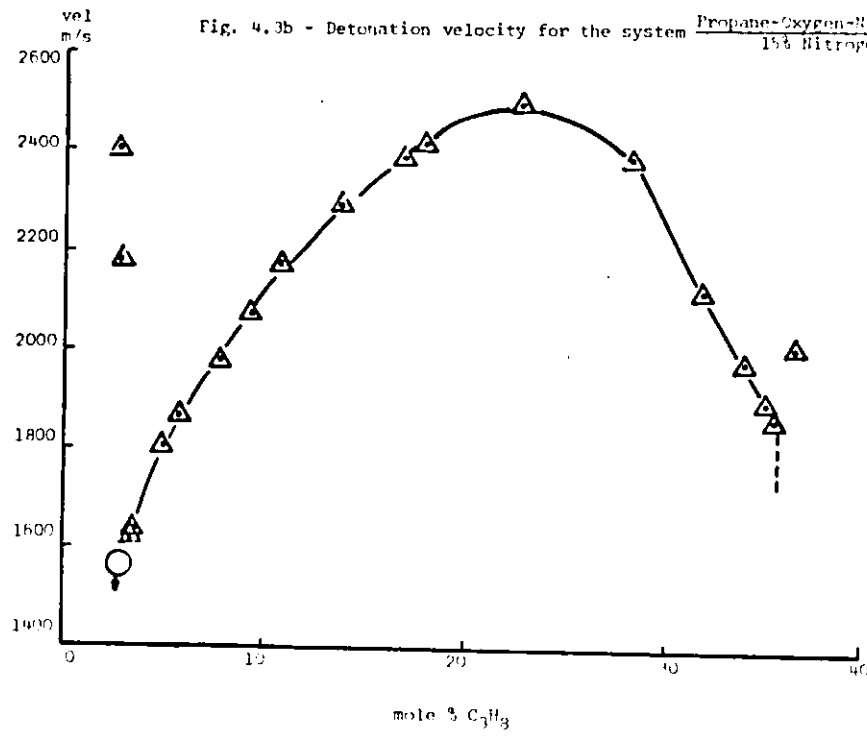


Fig. 4.3a - Detonation velocity for the system $\frac{\text{Propane-Oxygen-Nitrogen}}{0\% \text{ Nitrogen}}$

Fig. 4.3b - Detonation velocity for the system $\frac{\text{Propane-Oxygen-Nitrogen}}{15\% \text{ Nitrogen}}$



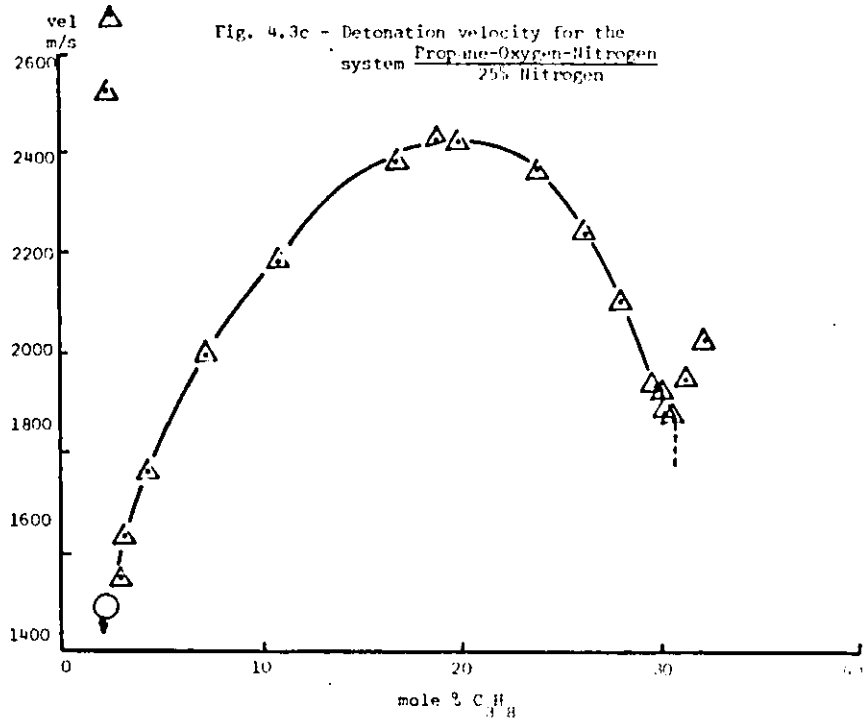


Fig. 4.3c - Detonation velocity for the system $\frac{\text{Propane-Oxygen-Nitrogen}}{25\% \text{ Nitrogen}}$

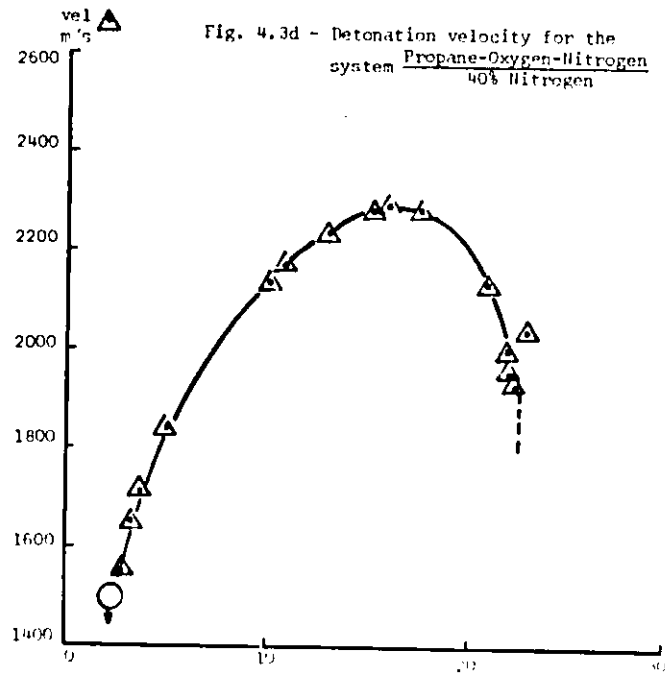


Fig. 4.3d - Detonation velocity for the system $\frac{\text{Propane-Oxygen-Nitrogen}}{40\% \text{ Nitrogen}}$

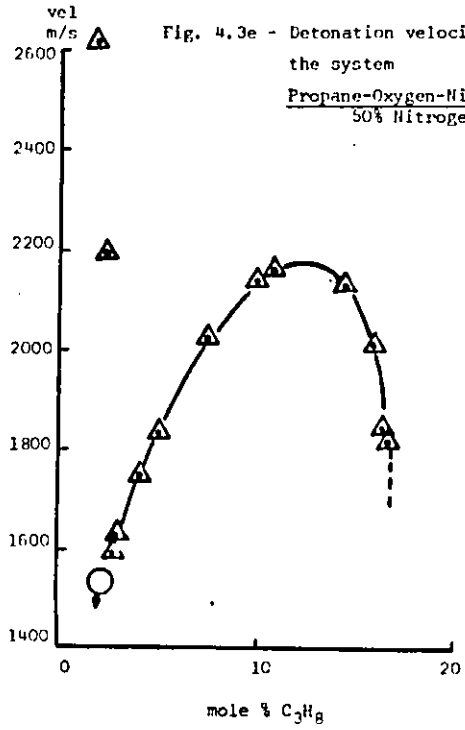


Fig. 4.3e - Detonation velocity in the system Propane-Oxygen-Nitrogen 50% Nitrogen

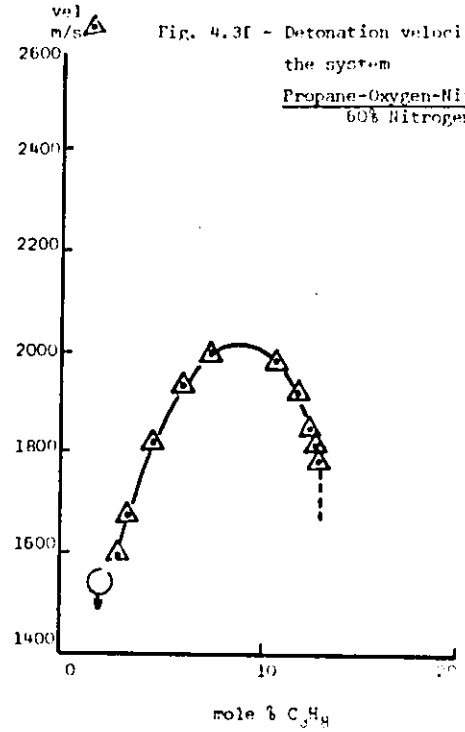


Fig. 4.3f - Detonation velocity in the system Propane-Oxygen-Nitrogen 60% Nitrogen

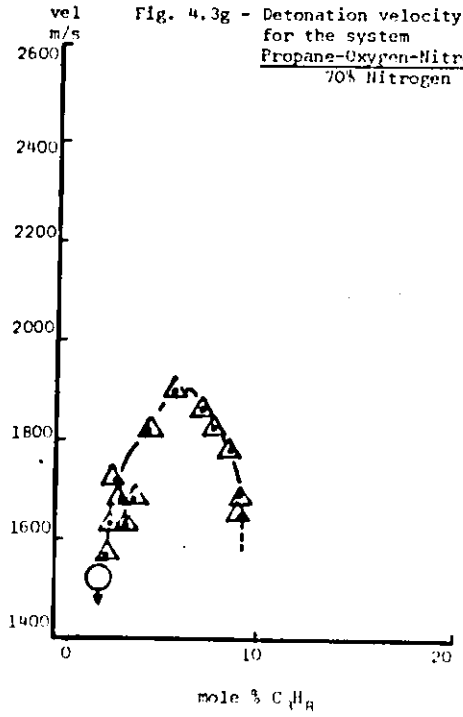


Fig. 4.3g - Detonation velocity for the system Propane-Oxygen-Nitrogen 70% Nitrogen

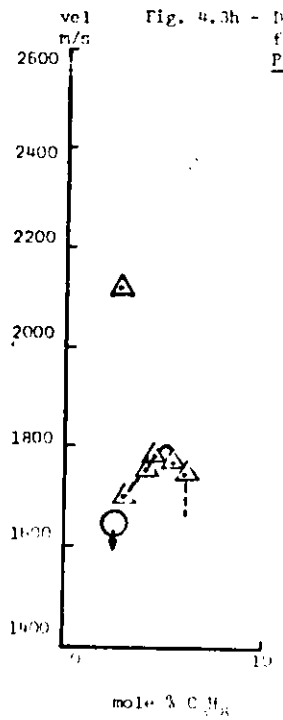


Fig. 4.3h - Detonation velocity for the system Propane-Oxygen-Nitrogen 75% Nitrogen

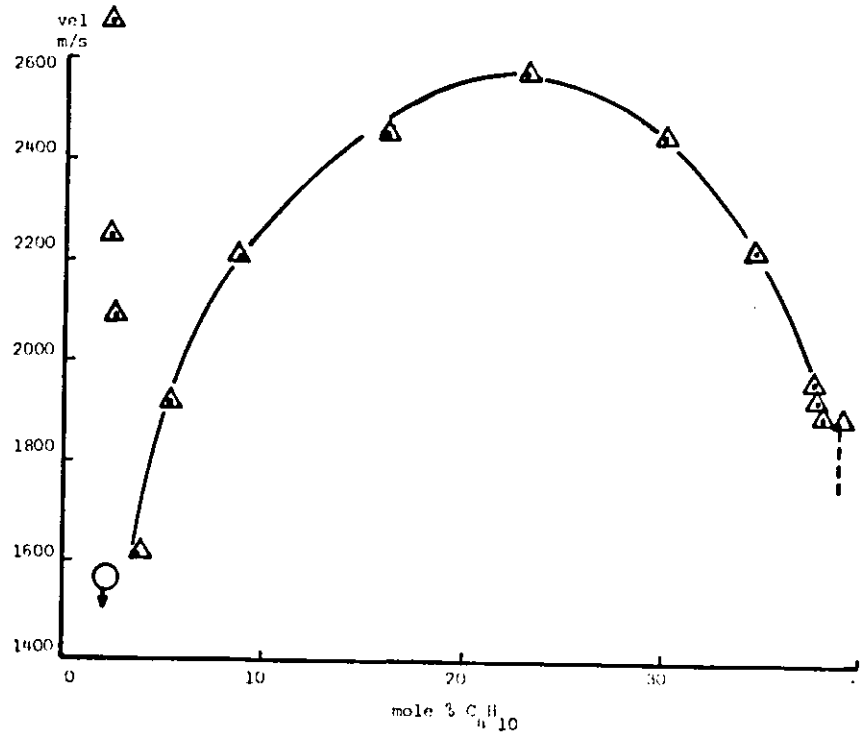


Fig. 4.4a - Detonation Velocity for the System $\frac{\text{Butane-Oxygen-Nitrogen}}{0\% \text{ Nitrogen}}$

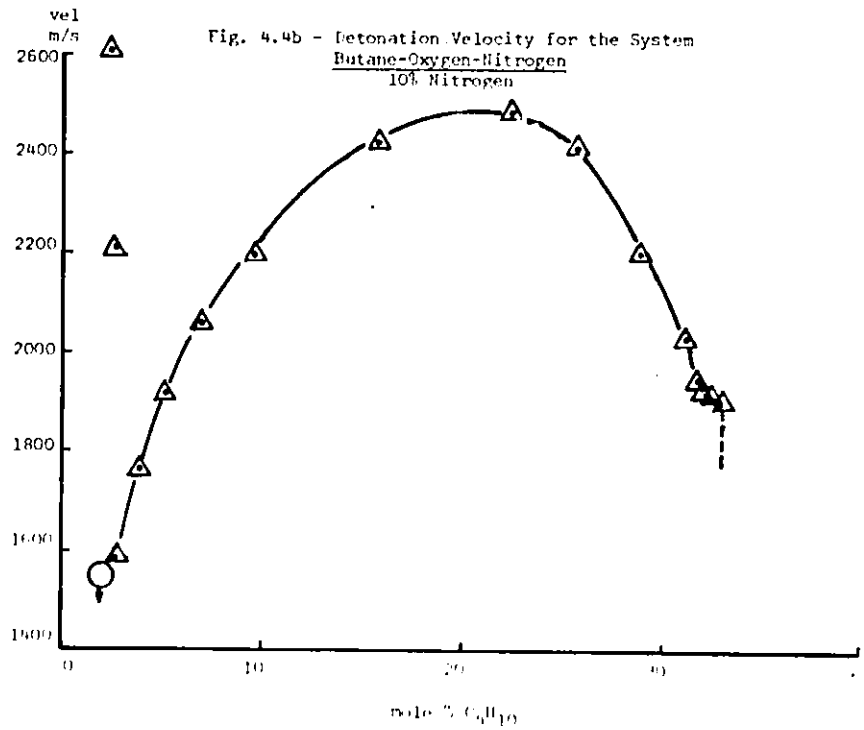


Fig. 4.4b - Detonation Velocity for the System $\frac{\text{Butane-Oxygen-Nitrogen}}{10\% \text{ Nitrogen}}$

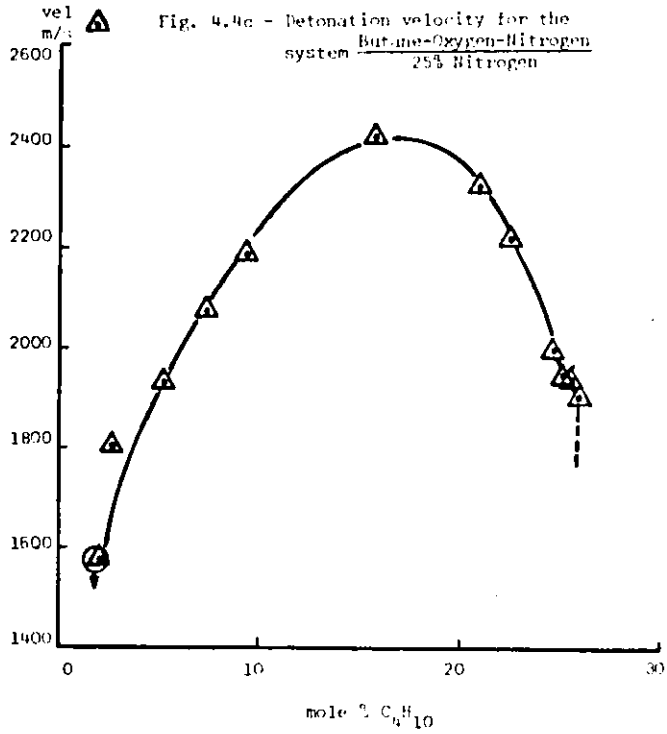


Fig. 4.4c - Detonation velocity for the system Butane-Oxygen-Nitrogen 25% Nitrogen

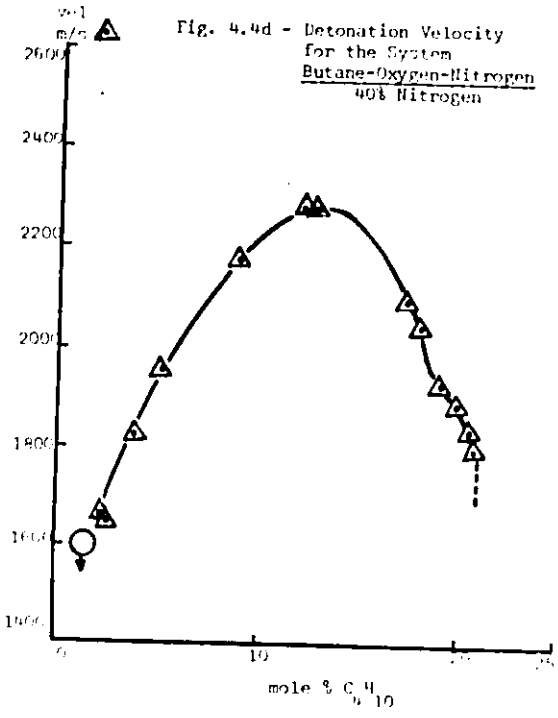


Fig. 4.4d - Detonation Velocity for the System Butane-Oxygen-Nitrogen 40% Nitrogen

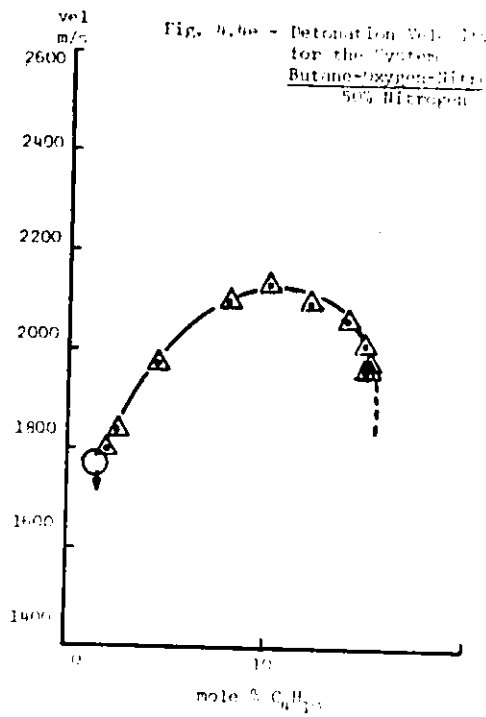


Fig. 4.4e - Detonation Vel[illegible] for the System Butane-Oxygen-Nitrogen 50% Nitrogen

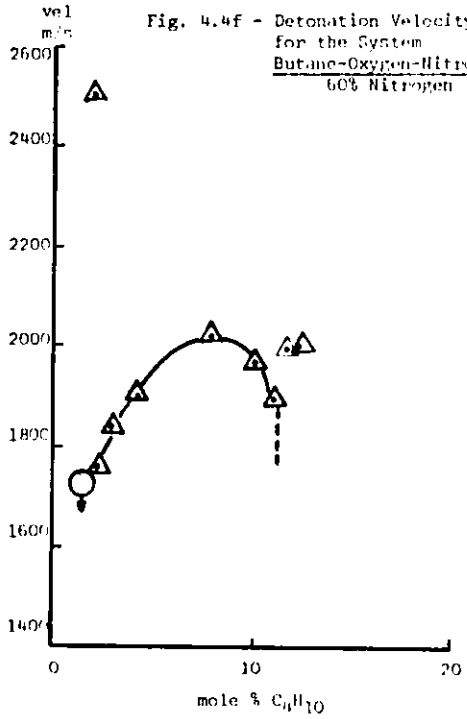


Fig. 4.4f - Detonation Velocity for the System Butane-Oxygen-Nitrogen 60% Nitrogen

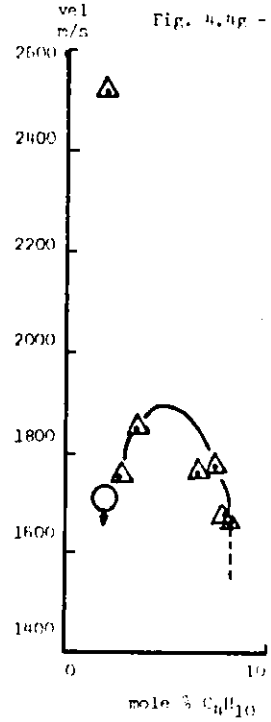


Fig. 4.4g - Detonation Velocity for the System Butane-Oxygen-Nitrogen 70% Nitrogen

CHAPTER FIVE

EVALUATION OF RESULTS

5.1 Triangular Diagrams of Detonation Limits in Ternary Systems

The evaluation of experimental results follows the initial aims of this work, as explained earlier, which can be summarised as follows. Propagation of detonation wave is basically governed by hydrodynamics and thermodynamics. Hydrodynamic principles alone do not predict any existence or location of limits of detonability. Thermodynamically, we will first focus attention on the physico-chemical properties of explosive medias and then, on two critical temperature rises involved in detonation, namely reaction zone temperature and shock front temperature.

The detonability regimes for the systems studied can be shown in ternary composition diagrams. For this purpose, the limits for each system have been plotted using triangular coordinates. Table 5.1.1 shows the choice of limit compositions for different systems used in drawing these ternary diagrams. Data for the system methane, oxygen and nitrogen have been taken from Taylor-Lewis's work (1977). Figures 5.1.1 to 5.1.4 show the limits of detonability of the ternary mixtures Ch_4-O_2-N_2, C_2H_6-O_2-N_2, C_3H_8-O_2-N_2 and C_4H_{10}-O_2-N_2. The air line in each system has been plotted.

5.2 Homologous Correlation of Composition Limits

Michels (1967) assumed similarity of reaction mechanisms in detonation of mixtures of homologously related hydrocarbons with oxygen which give maximum energy output for that mixture. Normalisation of experimental

TABLE 5.1.1

(Fuel-lean, fuel-rich) detonation limit compositions for systems of oxygen and nitrogen with methane, ethane, n-propane and n-butane

	Compositions in mole %									
N_2	0	10	15	20	25	40	50	60	70	75
CH_4*	(8.2, 56.5)	(8, 51)	-	(8, 44.5)	-	(9, 30.5)	(9, 23)	(9, 16)	(9, 11)	-
C_2H_6	(3.5, 52.5)	(3.3, 45.3)	-	(3, 39.2)	-	(3, 28.3)	(3, 22)	(3, 17.1)	-	(3.5, 9)
C_3H_8	(2.2, 43)	-	(2.5, (36.4)	-	(2.3, 32.3)	(2.3, 23)	(2.2, 16.5)	(2.5, 12.5)	(2.5, 9.2)	(2.9, 6)**
C_4H_{10}	(2.15, 38.9)	(2, 33)	-	-	1.7, 26.1)	(1.9, 20.8)	(1.95, 15.2)	(1.9, 11.5)	(2.1, 8.3)	(2.4, 5.4)

* Taylor-Lewis (1977)

** Nitrogen content is 77%

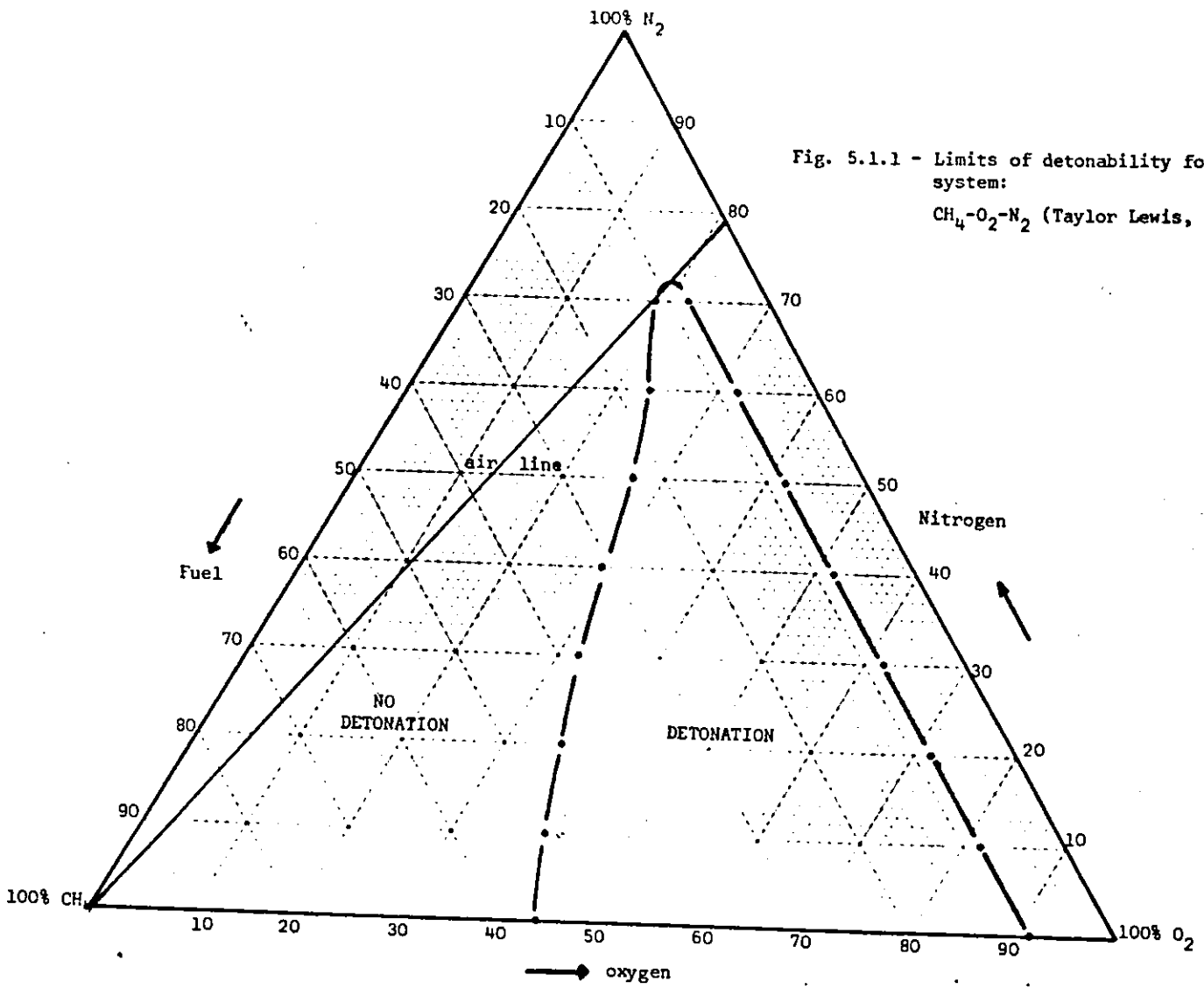


Fig. 5.1.1 - Limits of detonability for the system:
CH_4-O_2-N_2 (Taylor Lewis, 1977)

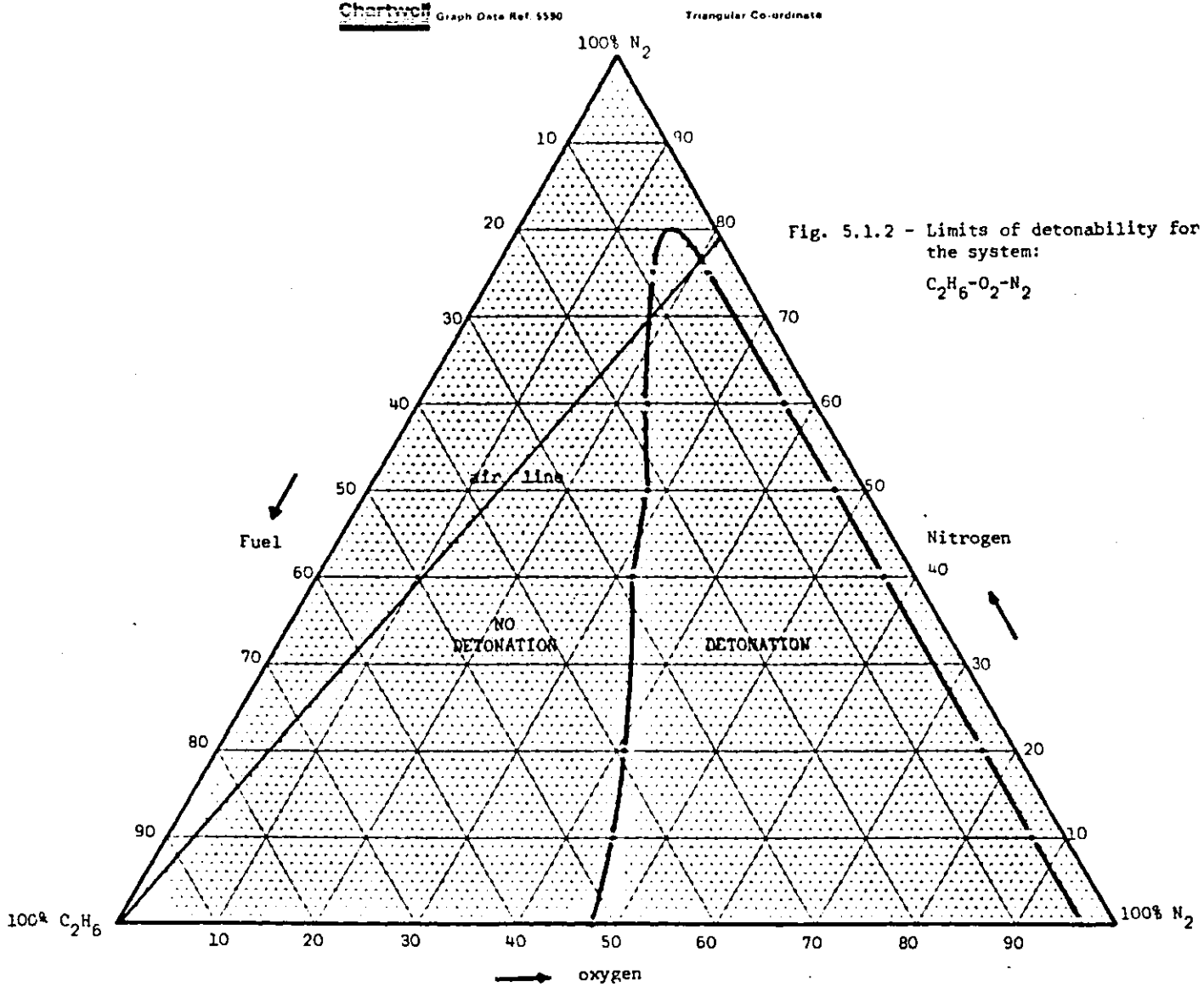


Fig. 5.1.2 - Limits of detonability for the system:

C_2H_6-O_2-N_2

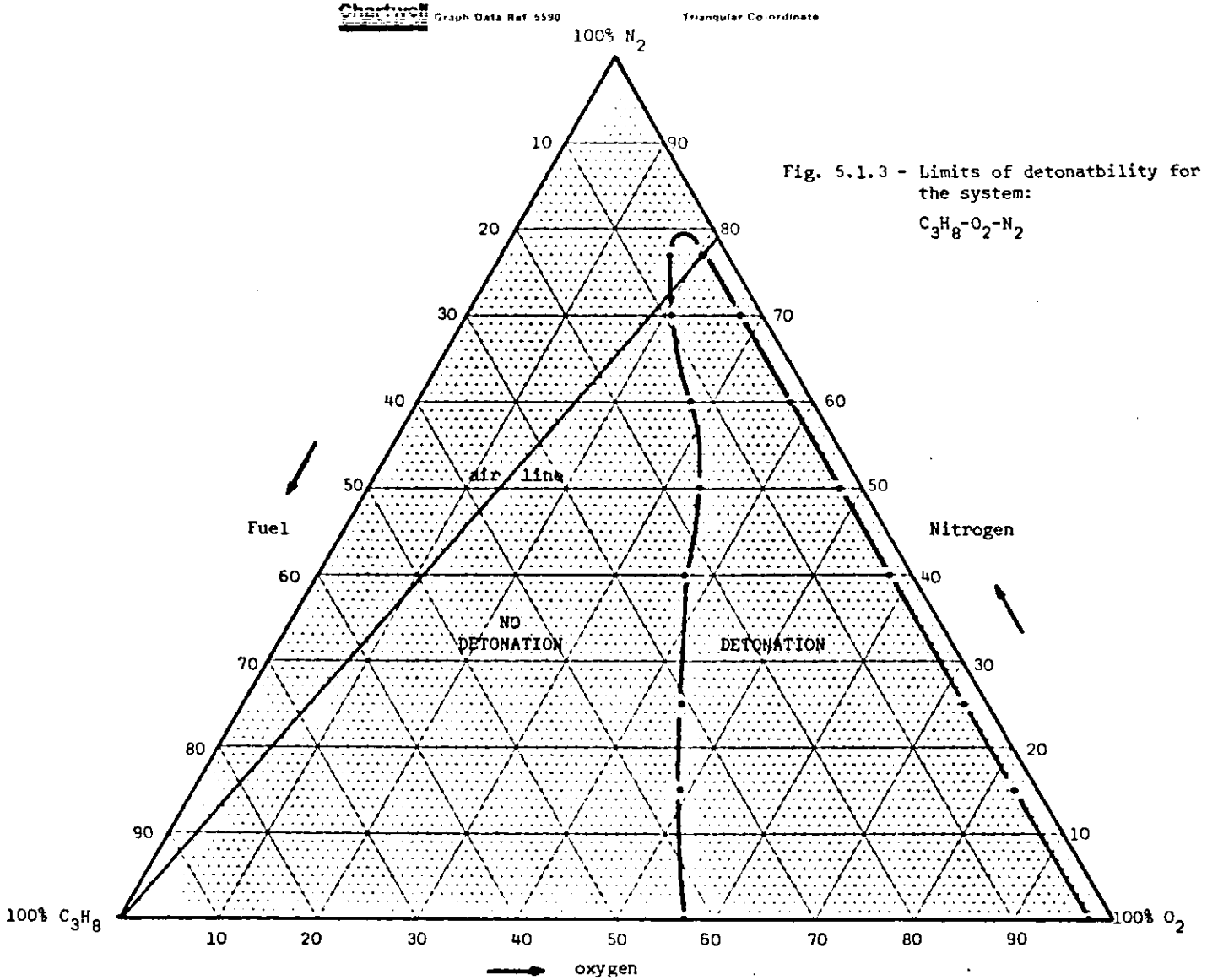


Fig. 5.1.3 - Limits of detonatbility for the system:

C_3H_8-O_2-N_2

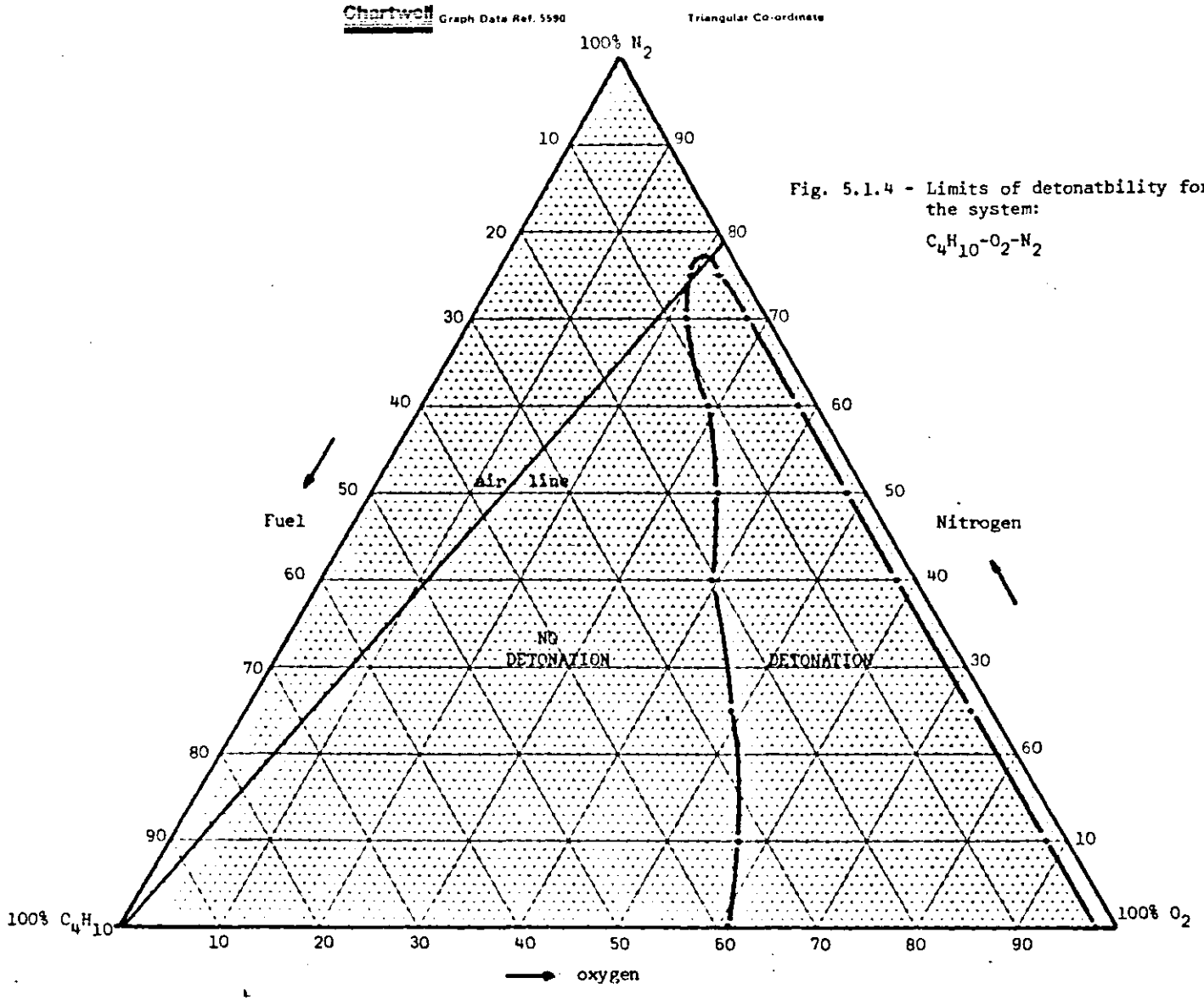


Fig. 5.1.4 - Limits of detonatbility for the system:

C_4H_{10}-O_2-N_2

results on this basis resulted in the construction of a master curve, relating relative Mach-product values ($\gamma M^2/\gamma M^2 max.$) as a function of (original mixture composition)/(compositions at $\gamma M^2 max.$) for different binary systems. This justified the assumption of similarity, and the agreement extended to almost the complete range of the detonation regime. The success of the correlation of experimental results based on the assumed similarity in mechanism was extended further to similarities existing in the unburned mixtures of fuel molecules and oxygen. As explained earlier, the normal saturated aliphatic hydrocarbons (C_nH_{2n+2}) can be treated as ($nCH_2 + H_2$). The new representation of relative Mach-product values vs. a mixture composition expressed on a fuel-homology basis, for different hydrocarbon-oxygen systems gave a most satisfactory agreement for almost the entire composition range of detonation, including C-J conditions, initial mixture compositions, final states, and composition limits.

In detonations of ternary systems studied in this work, attempts to apply once again the principle of homology correlation to the entire range of detonation properties will not be made. Instead, the homologous similarity of fuel molecules will be used only to correlate the different boundaries of detonability regimes established experimentally. The object of this is to define a generalised detonability regime in a triangular coordinate system, for different hydrocarbon fuels, oxygen and nitrogen - with the original molar compositions now expressed on the basis of fuel homology. Tables 5.2.1 and 5.2.2 show the detonation limits and corresponding homology values for, respectively, fuel-lean and fuel-rich limits.

Figure 5.2.1 shows the master detonability boundary for the systems of oxygen and nitrogen with corresponding fuels - based on homology correlation. The agreement, in general, is very satisfactory for the

TABLE 5.2.1

Detonation limits and corresponding homology composition values for fuel-lean mixtures

	mole %		homology % Homology Values	
Fuel	% N_2	% Fuel	% Fuel	% N_2
CH_4	0	8.2	15	0
C_2H_6	0	3.5	9.8	0
C_3H_8	0	2.2	8.3	0
C_4H_{10}	0	2.1	9.7	0
CH_4	10	8	14.8	9.3
C_2H_6	10	3.3	9.3	9.4
C_3H_8	10	2.5	9.3	9.3
C_4H_{10}	10	2	9.3	9.3
CH_4	20	8	14.8	18.5
C_2H_6	20	3	8.5	18.8
C_3H_8	20	2.4	8.9	18.6
C_4H_{10}	20	1.8	8.4	18.7
CH_4	40	9	16.5	36.7
C_2H_6	40	3	8.5	37.7
C_3H_8	40	2.3	8.6	37.4
C_4H_{10}	40	1.9	8.8	37.1
CH_4	50	9	16.5	45.9
C_2H_6	50	3	8.5	47.1
C_3H_8	50	2.2	8.3	46.9
C_4H_{10}	50	1.9	8.8	46.5
CH_4	60	9	16.5	55
C_2H_6	60	3	8.5	56.6
C_3H_8	60	2.5	9.3	55.8
C_4H_{10}	60	1.9	8.8	55.8
CH_4	70	9	16.5	64.2
C_2H_6	70	3.2	9.1	65.7
C_3H_8	70	2.5	9.3	65.1
C_4H_{10}	70	2.1	9.6	64.6
CH_4	75	-	-	-
C_2H_6	75	3.5	9.8	70
C_3H_8	75	2.8	10.3	69.2
C_4H_{10}	75	2.4	10.9	68.4

TABLE 5.2.2

Detonation limits and corresponding homology composition values for fuel-rich mixtures

mole %			homology % Homology Values	
Fuel	% N_2	% Fuel	% Fuel	% N_2
CH_4	0	56.5	72	0
C_2H_6	0	52.5	76.8	0
C_3H_8	0	43	75.1	0
C_4H_{10}	0	38.9	76	0
CH_4	10	51	67.5	6.6
C_2H_6	10	45.3	71.3	5.2
C_3H_8	10	38.8	71.7	4.6
C_4H_{10}	10	33	71.1	4.3
CH_4	20	44.5	61.6	13.8
C_2H_6	20	39.2	66	11.2
C_3H_8	20	33.5	66.8	10
C_4H_{10}	20	28.1	66.1	9.4
CH_4	40	30.5	46.7	30.7
C_2H_6	40	28.3	54.2	25.5
C_3H_8	40	23	54.4	23.6
C_4H_{10}	40	20.8	56.7	21.8
CH_4	50	23	37.4	40.6
C_2H_6	50	22	45.8	34.7
C_3H_8	50	16.5	44.1	33.4
C_4H_{10}	50	15.2	47.2	31
CH_4	60	16	27.6	51.7
C_2H_6	60	17.1	38.2	44.7
C_3H_8	60	12.5	36.4	43.6
C_4H_{10}	60	11.5	39.3	41
CH_4	70	11	19.8	63
C_2H_6	70	12	29	56.4
C_3H_8	70	9.2	28.8	54.8
C_4H_{10}	70	8.3	31	52.5
CH_4	75	-	-	-
C_2H_6	75	9	22.8	63.5
C_3H_8	75	6.7	22.3	62.5
C_4H_{10}	75	5.4	22.2	61.7

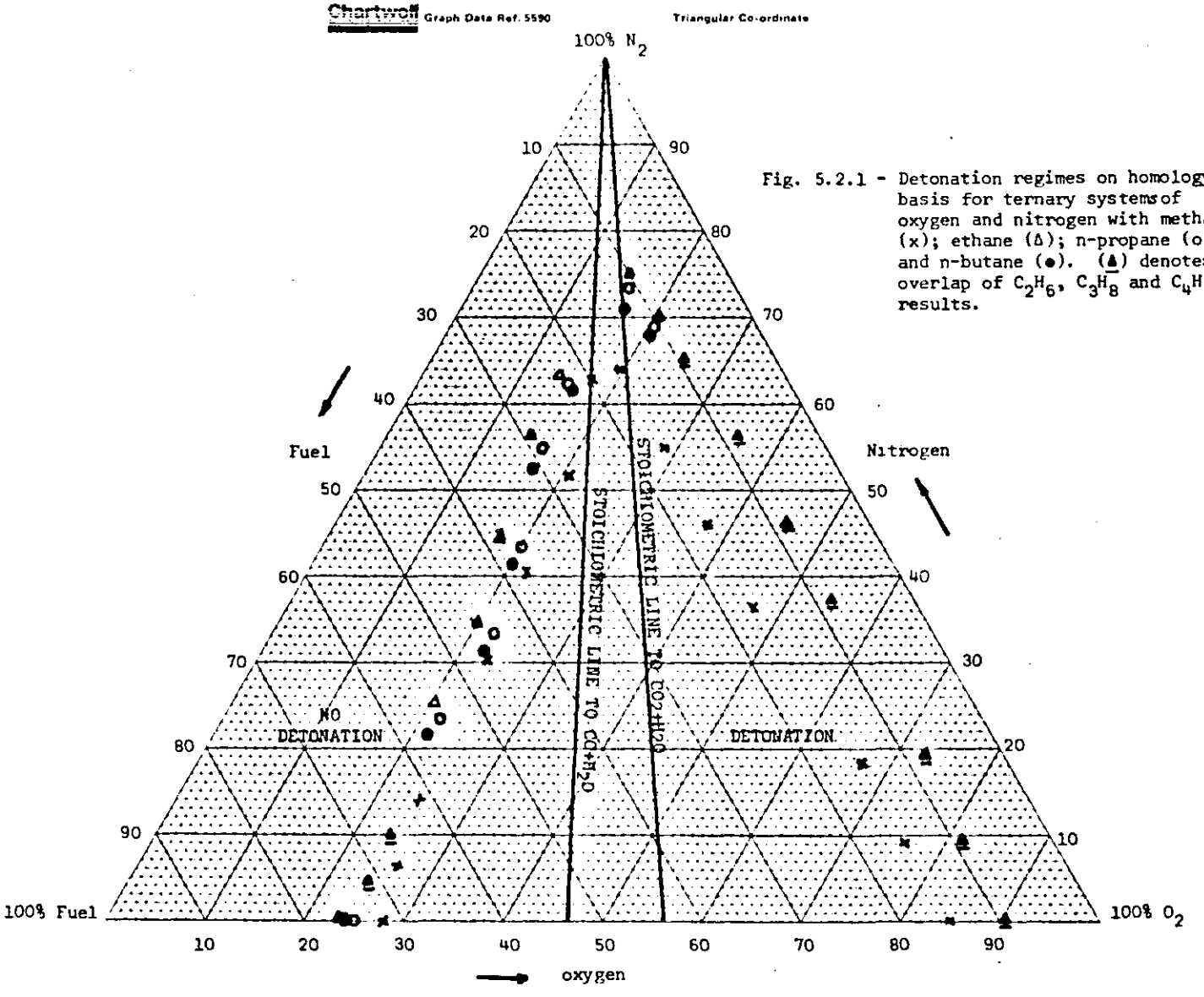


Fig. 5.2.1 - Detonation regimes on homology basis for ternary systems of oxygen and nitrogen with methane (x); ethane (Δ); n-propane (o) and n-butane (•). (▲) denotes overlap of C_2H_6, C_3H_8 and C_4H_{10} results.

system containing ethane, n-propane and n-butane. Mixtures containing methane do not follow the general trend to the same extent. This is not very surprising, as the homology method for binary mixtures of paraffins up to C_5 showed more or less similar correlation deficiencies for methane molecules.

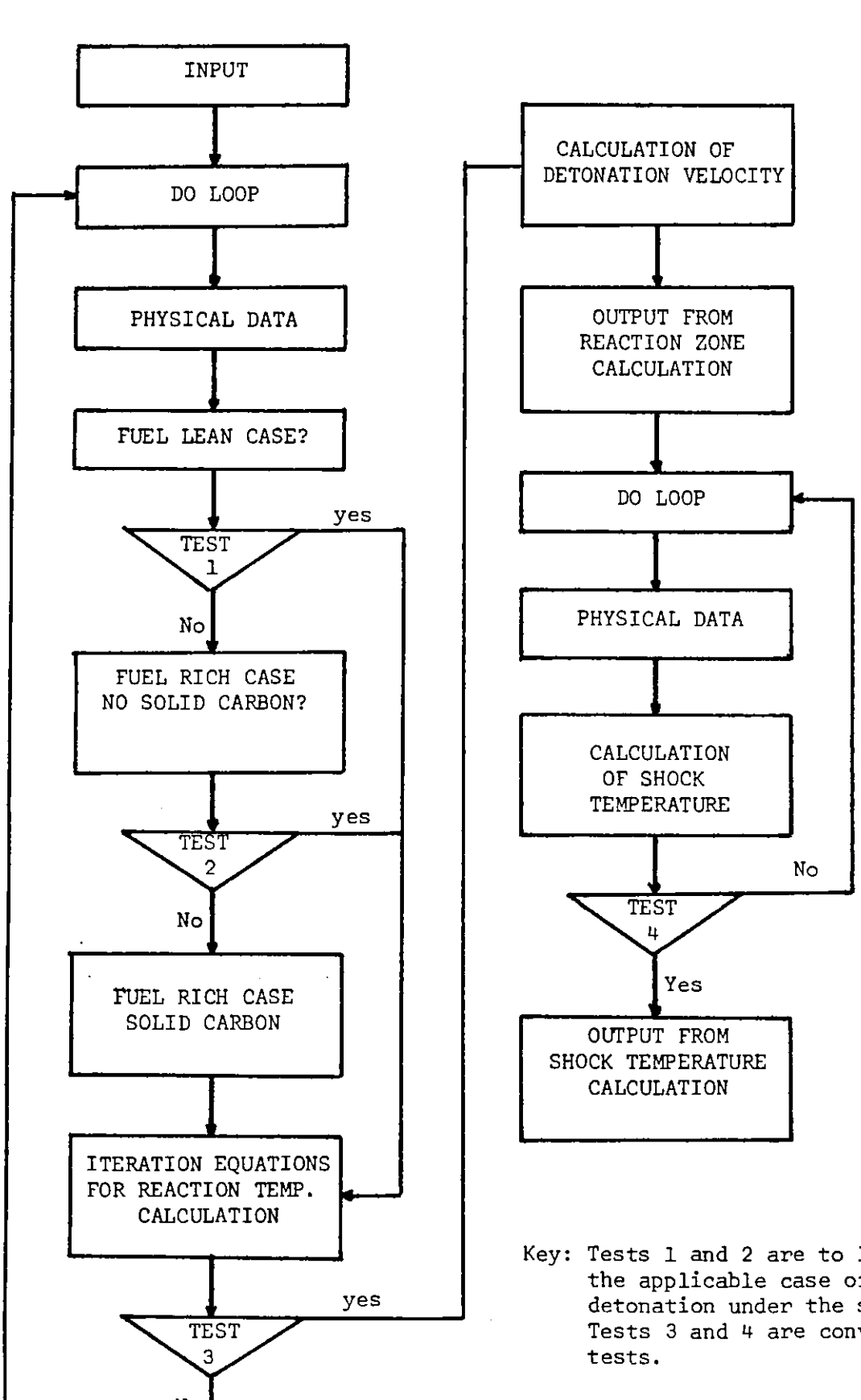
Although the present study was not concerned with correlating the different detonation properties, however, the new presentation extends quite well to comparable situations in steady-state regions of detonation as well. For example, a mixture of 24.5 (homology %) fuel (any one of the three fuels mentioned above), 33 (homology %) nitrogen, and 43.5 (homology %) oxygen would result in a detonation with a characteristic propagation velocity of 2000 metre/sec (± 1%). The classic stoichiometric conversion of different fuels - oxygen and nitrogen mixtures to either carbon dioxide and water vapour or carbon monoxide and water vapour also correlate within an accuracy of about 2 homology % and these homology stoichiometric lines are shown in Fig. 5.2.1 as well.

5.3 Reaction Zone Temperatures and Shock Front Temperatures for Marginal Detonations of Fuel-Oxygen-Nitrogen Mixtures

Simplified procedures, as described in Sections 2.3 and 2.4, were followed to calculate nominal C-J (reaction zone) and shock temperature values. The sequence of operation is as laid down in the diagram of Fig. 5.3.1 and the Fortran programme based on this can be found in Appendix C. This program is used for marginal detonations of saturated aliphatic hydrocarbons C_nH_{2n+2} with oxygen and inert (in this work, nitrogen). Each fuel is indicated by its number of carbon atoms (n).

Tables 5.3a to 5.3d show the values of C-J reaction temperatures and corresponding shock front temperatures for some marginal mixture composition ratios of oxygen and nitrogen with, respectively, methane, ethane, propane and butane.

Fig. 5.3.1 - A block diagram for program DTEMP



Key: Tests 1 and 2 are to locate the applicable case of marginal detonation under the study. Tests 3 and 4 are convergence tests.

TABLE 5.3a - Reaction zone temperatures and shock front temperatures near detonation limits for the system:

CH_4-O_2-N_2

CH_4 mole %	N_2 mole %	$T_{reaction}$ K	T_{shock} K
8.2	0	2706	1380 (1295)
8	40	2726	1413
9	40	2951	1487
10	40	3167	1555
11	40	3374	1617
56.5	0	2688	1532 (1630)
35	40	1904	1231
33	40	2306	1370
31	40	2703	1493
29	40	3099	1605
27	40	3498	1709

TABLE 5.3b - Reaction zone temperatures and shock front temperatures near detonation limits for the system:

C_2H_6-O_2-N_2

C_2H_6 mole %	N_2 mole %	$T_{reaction}$ K	T_{shock} K
3.5	0	2214	1212 (1230)
2.5	40	1807	1074
3	40	2045	1169
4	40	2484	1331
5	40	2881	1467
53	0	1556	1195 (1540)
30	40	1444	1086
29	40	1659	1172
28	40	1873	1252
27	40	2086	1328
26	40	2301	1400

TABLE 5.3c - Reaction zone temperatures and shock front temperatures near detonation limits for the system:

C_3H_8-O_2-N_2

C_3H_8 mole %	N_2 mole %	$T_{reaction}$ K	T_{shock} K
2.25	0	2206	1207 (1200)
2	40	1972	1139
3	40	2588	1366
4	40	3215	1542
5	40	3604	1685
43	0	1784	1287 (1195)
24	40	1655	1175
23	40	1889	1262
22	40	2125	1345
21	40	2364	1424
20	40	2606	1500

TABLE 5.3d - Reaction zone temperatures and shock front temperatures near detonation limits for the system:

C_4H_{10}-O_2-N_2

C_4H_{10} mole %	N_2 mole %	$T_{reaction}$ K	T_{shock} K
2.15	0	2404	1278 (1225)
2	40	2345	1280
3	40	3062	1522
4	40	3676	1705
5	40	4247	1861
38.90	0	1745	1291 (1150)
22	40	1612	1180
21	40	1688	1201
20	40	1764	1221
19	40	2024	1315
18	40	2288	1404

In each case, reaction temperatures and shock temperatures at the limits of detonability for binary mixtures of fuel and oxygen are included as well.

In the tables the values in brackets are shock temperatures calculated by Michels (1967), by a different method and based on experimentally obtained detonation velocities. The agreement is generally quite satisfactory and this, therefore, gives strong support for the use of the simplified assumptions which were made for evaluation of reaction zone temperatures and resultant shock temperatures obtained from theoretically calculated detonation velocities.

5.4 The Constant Temperature Criterion for Prediction of Detonation Limits in Ternary Systems

The next step in the evaluation of results deals with the further investigation of the question, whether estimates of reaction zone temperatures and/or shock front temperatures can themselves be used as a means for predicting detonation limits. The constant temperature criterion is a method of estimating mixture compositions along a fuel-rich or fuel-lean side of a ternary detonation regime which have the same reaction zone/shock front temperature as that of one proven limit mixture along such a side.

For this purpose, variations in temperature (reaction zone and shock front), for a marginal region of detonation of fuel, oxygen, and for an arbitrary selected fixed percentage of inert (N_2) are plotted as a function of fuel compositions in the mixture. First, the temperature rises in a chosen mixture of an experimentally determined composition limit are evaluated. Such temperature rises are taken as the critical values and the corresponding composition is then chosen as a starting point for the fuel-rich side (or fuel-lean side) in a ternary

diagram as appropriate. Compositions of fuel (rich and lean) in one ternary mixture with similar critical temperature rises can thus be obtained from the plots mentioned above. These compositions serve as a second set of points to establish a constant reaction zone temperature or constant shock front temperature line. In a triangular coordinate system, straight lines between these points demonstrate the corresponding constant temperature lines. The validity of these lines for prediction of detonation regime boundaries can be investigated by comparing their trajectory with experimentally obtained detonation regime boundaries.

As briefly pointed out in section 1.6.4, this was first suggested by Taylor-Lewis (1977) in detonation of the CH_4-O_2-N_2 system. He considered two alternative simplified reaction products (similar for both fuel-lean side and fuel-rich side) to provide the necessary energy release values needed for calculations of reaction zone temperature and shock front temperature:

(a) $$CH_4 + 2O_2 \rightarrow CO_2 + 2H_2O$$

(b) $$CH_4 + 1.5O_2 \rightarrow CO + 2H_2O$$

For the fuel-rich side a further reaction was introduced in which unburned fuel was converted endothermically to its elements as

$$CH_4 \rightarrow C_{(graphite)} + 2H_2$$

The study suggested that a constant "shock-temperature" criterion coupled with reaction products (a) provides a reliable basis for prediction of detonation limits in CH_4-O_2-N_2 systems.

In trying to repeat Taylor-Lewis's calculations, it was concluded that part of the work contained errors. As samples of the calculations were not reported, there was no possible way to check details of the

way in which the results were obtained. However, one error in reaction zone temperature calculations, probably taken over from literature (Lewis and von Elhe, 1961, page 524) is the assumption that in case of no dissocation, the number of moles per gram of reactants and products are identical. This is, of course, not true. Also, the formation of carbon dioxide as one of the major products for fuel-rich mixtures seemed very unlikely.

We therefore recalculated his data and subsequently applied the same method to the C_3H_8-O_2-N_2 system. The theoretically obtained constant temperature lines for both systems (CH_4-O_2-N_2 and C_3H_8-O_2-N_2) were compared with experimentally established detonation regimes. This suggested that neither lines of constant shock temperature nor lines of constant reaction zone temperature obtained in this manner can be used to model, with reasonable accuracy, the detonation limit boundaries. Appendix D illustrates the temperature values calculated by the Taylor-Lewis method together with the corresponding constant temperature lines.

In the present study, composition limits for binary mixtures of fuel and oxygen were chosen as the starting points for establishing constant temperature lines. The fuel compositions in ternary mixtures of fuel, oxygen and 40% nitrogen, are shown by dotted lines and arrows in Figs. 5.4a to 5.4d. These figures have been obtained directly from Tables 5.3a to 5.3d and illustrate the variation of marginal reaction zone/shock front temperature vs fuel composition in a ternary mixture.

To illustrate the constant temperature lines in ternary diagrams, two sets of straight lines have been drawn, one set for reaction temperature and another one for shock temperature, respectively for fuel-lean side and fuel-rich side. Each line connects the two points of identical temperature rises initially chosen. These lines terminate at

their intersection with two stoichiometric lines, i.e. for full conversion of reactants to (CO_2 + H_2O) and to (CO + H_2O). These lines are representative for boundaries of marginal regions of, respectively, fuel-lean and fuel-rich sides of the detonation regime. Figures 5.4e to 5.4h show detonability regime boundaries for different systems established on the basis of constant reaction zone/shock front temperature criteria. They closely follow the limit compositions determined experimentally. The agreements for the fuel-lean sides are especially good. This matter will be discussed in the next chapter.

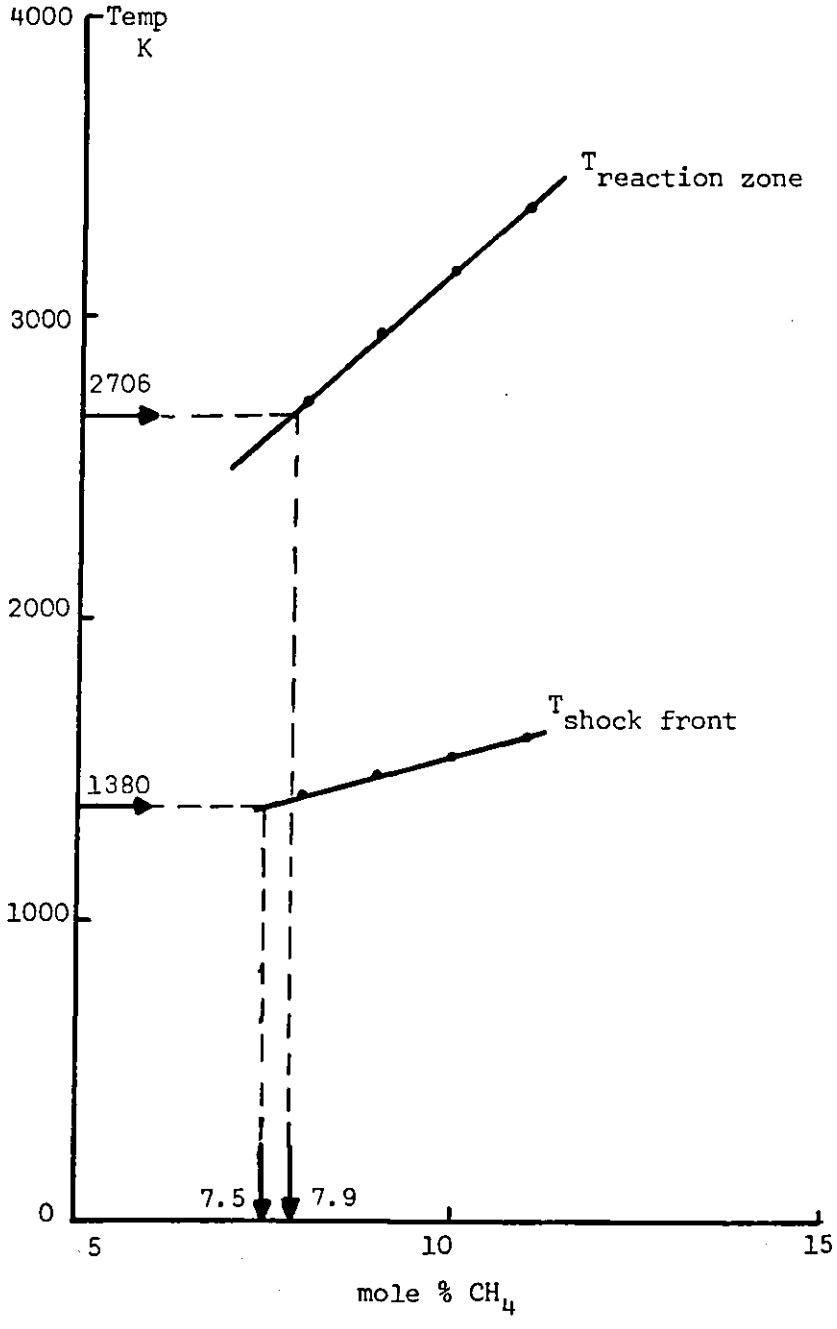


Fig. 5.4.a - Estimate of composition limits to detonation in ternary systems containing nitrogen based on critical temperature values for corresponding binary systems:

"Fuel-lean: CH_4-O_2-40% N_2"

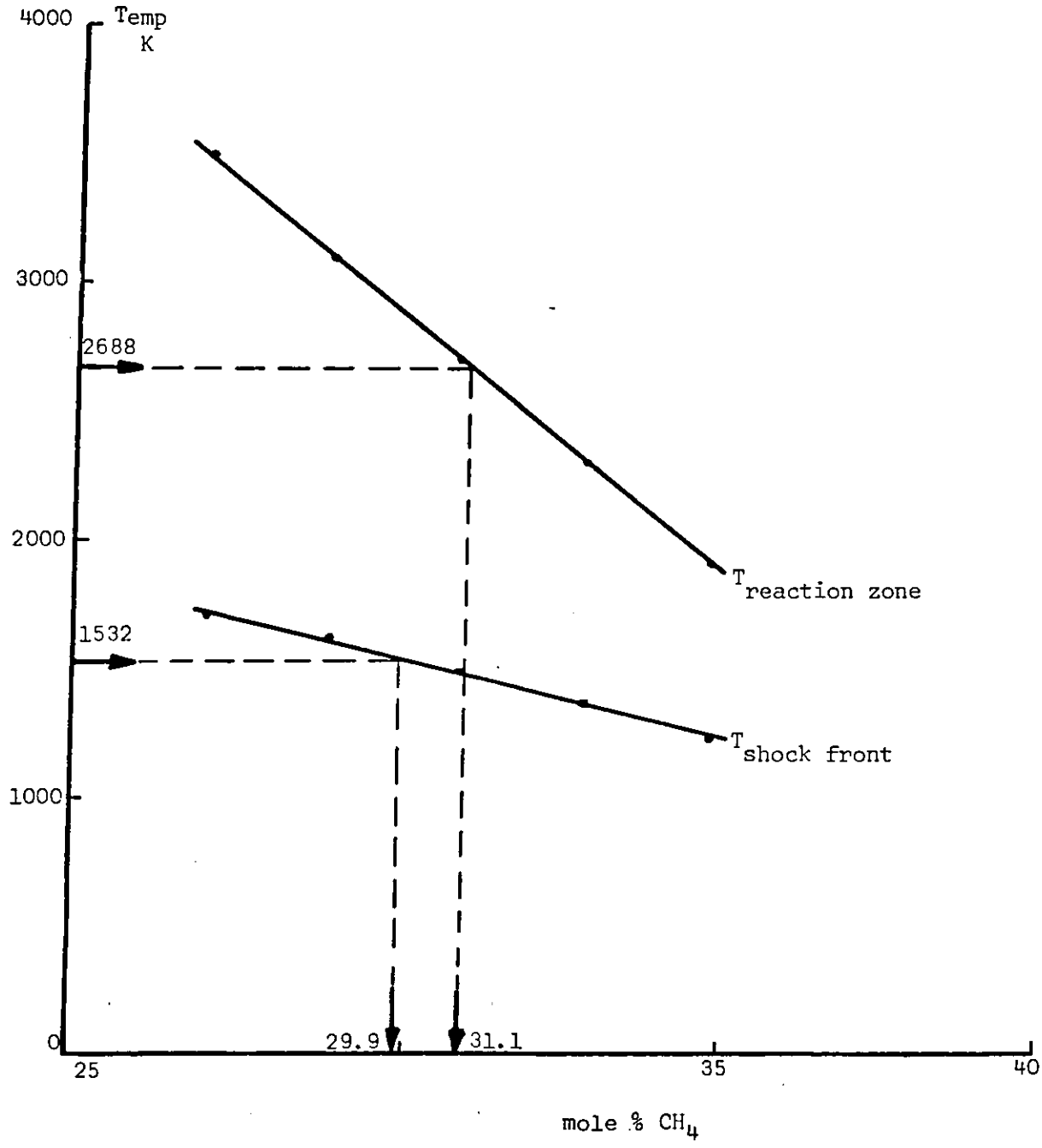


Fig. 5.4.a - Estimate of composition limits to detonation in ternary systems containing nitrogen based on critical temperature values for corresponding binary systems:

"Fuel-rich; CH_4-O_2-40% N_2"

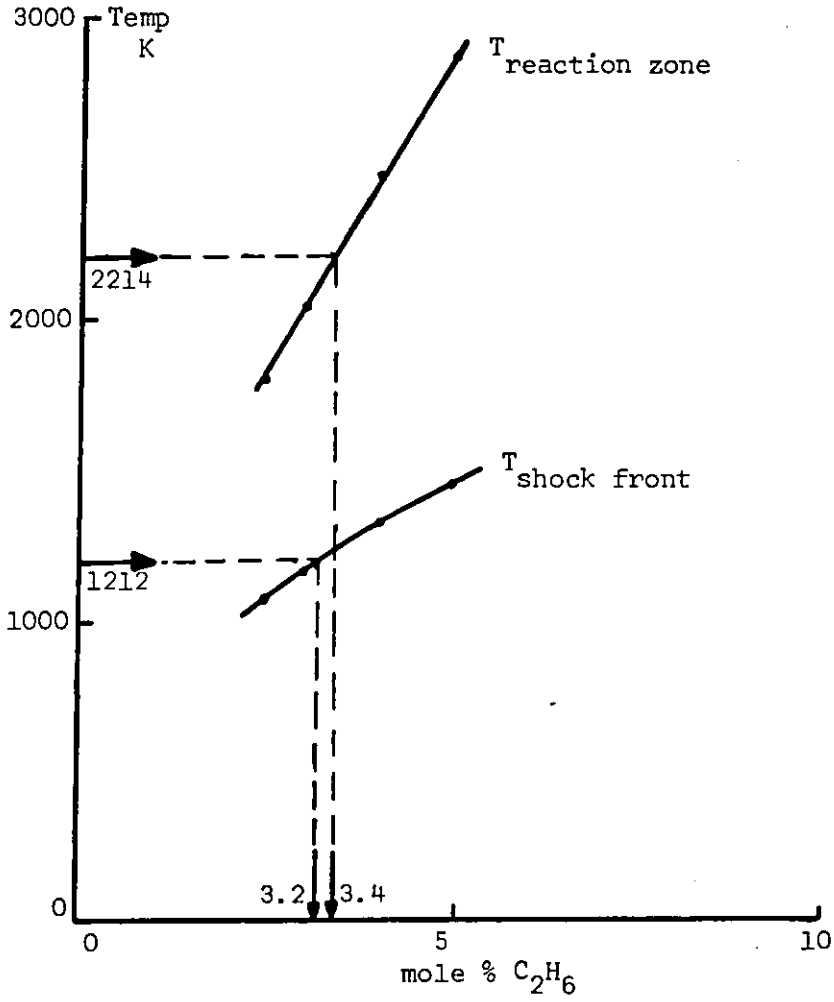


Fig. 5.4.b - Estimate of composition limits to detonation in ternary systems containing nitrogen based on critical temperature values for corresponding binary systems:

"Fuel-lean; C_2H_6-O_2-40% N_2"

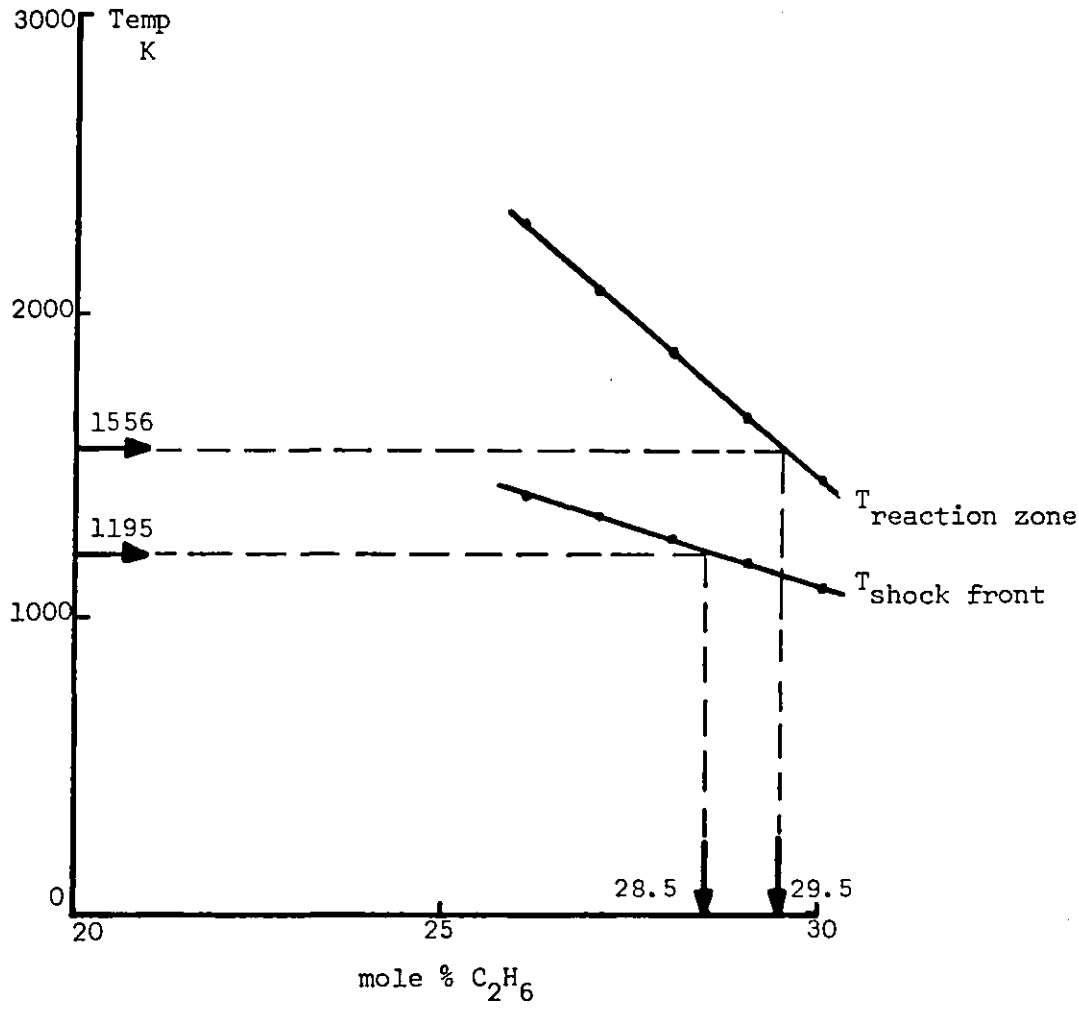


Fig. 5.4.b - Estimate of composition limits to detonation in ternary systems containing nitrogen based on critical temperature values for corresponding systems:

"Fuel-rich; C_2H_6-O_2-40% N_2"

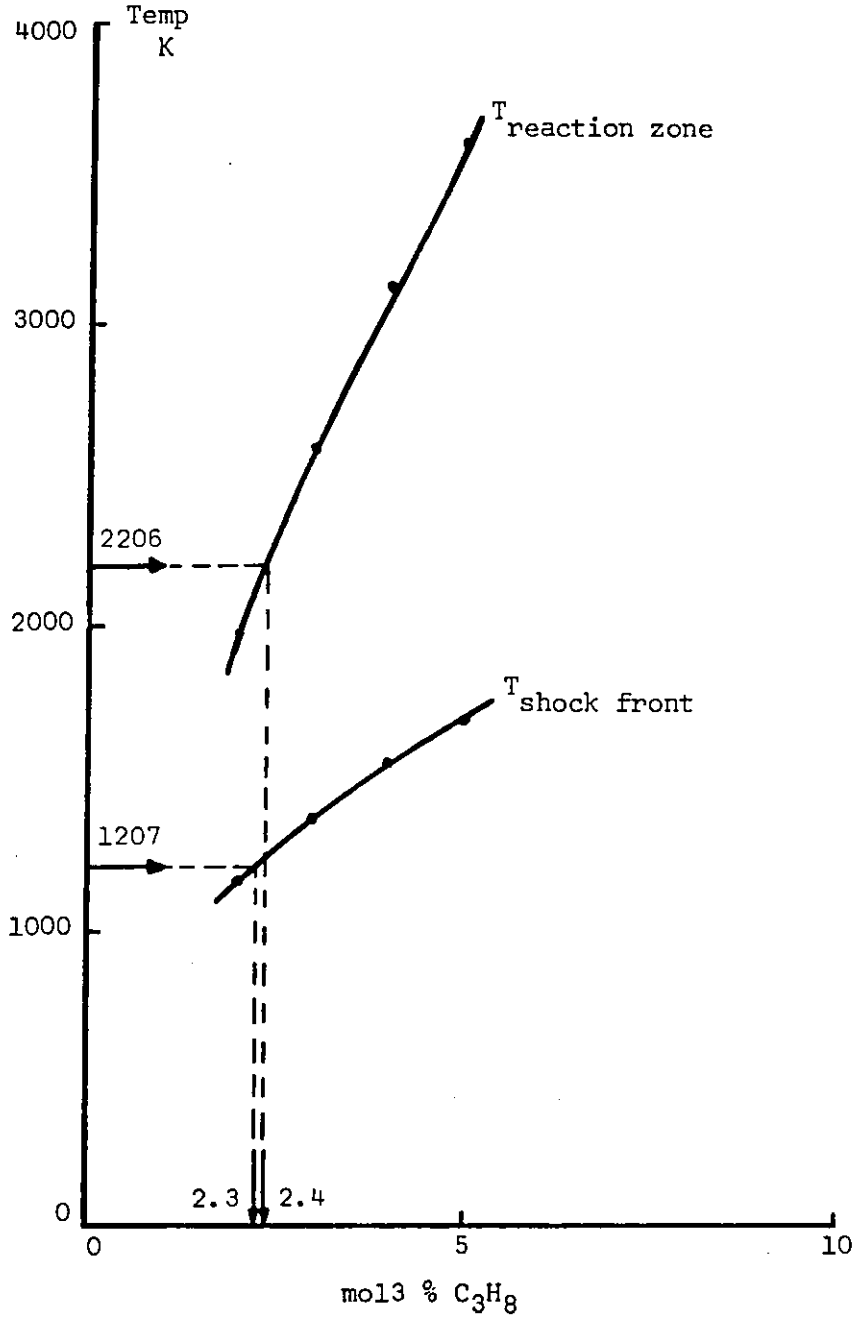


Fig. 5.4.c - Estimate of composition limits to detonation in ternary systems containing nitrogen based on critical temperature values for corresponding binary systems:

"Fuel-lean; C_3H_8-O_2-40% N_2"

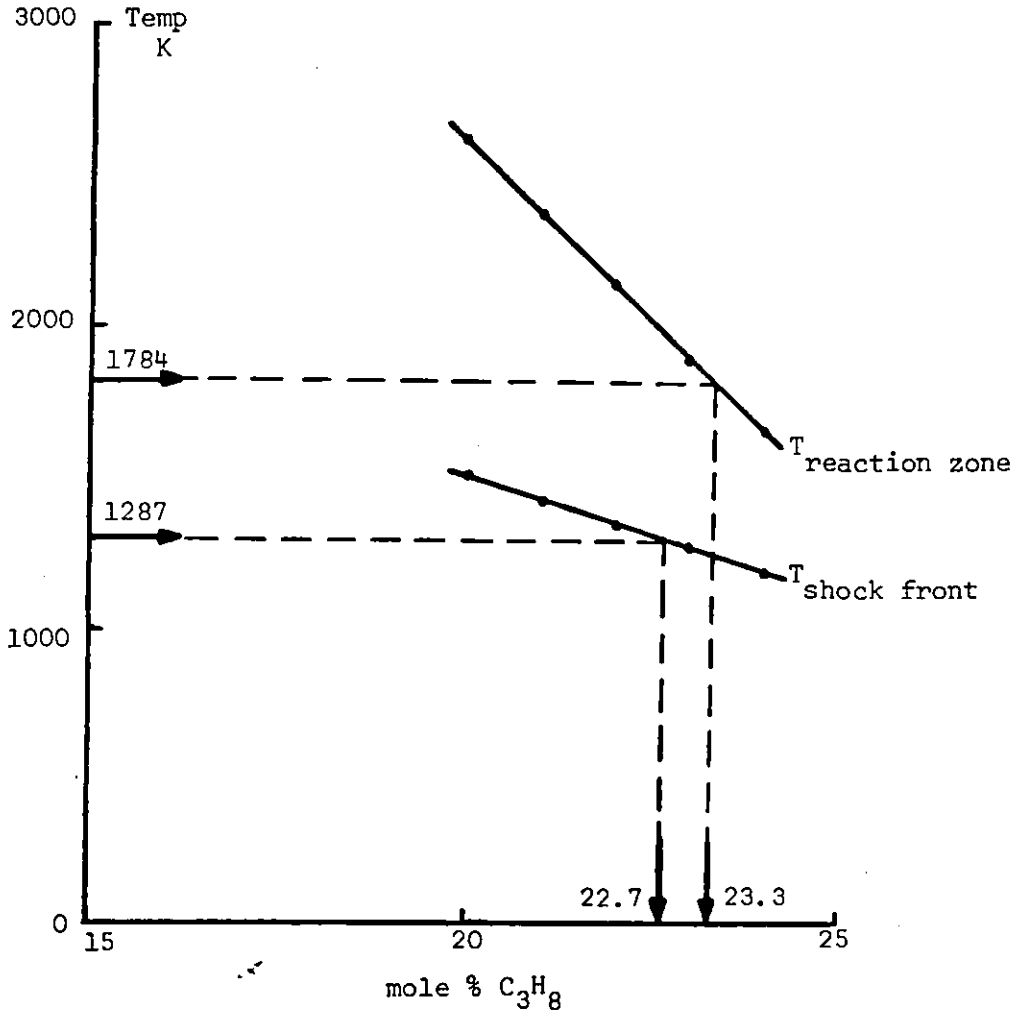


Fig. 5.4.c - Estimate of composition limits to detonation in ternary systems containing nitrogen based on critical temperature values for corresponding binary systems:

"Fuel-rich; C_3H_8-O_2-40% N_2"

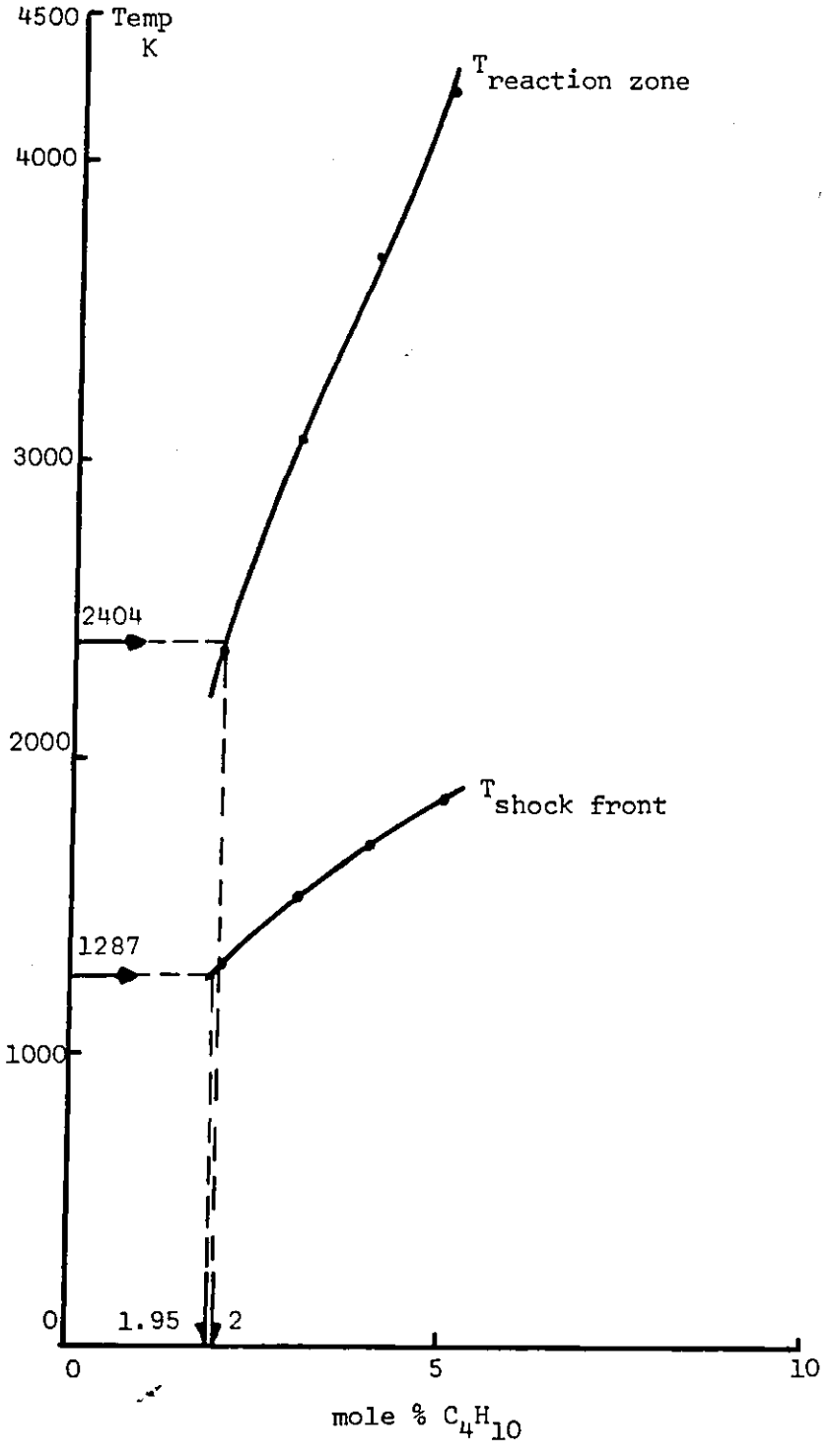


Fig. 5.4.d - Estimate of composition limits to detonation in ternary systems containing nitrogen based on critical temperature values for corresponding binary systems:

"Fuel-lean; C_4H_{10}-O_2-40% N_2"

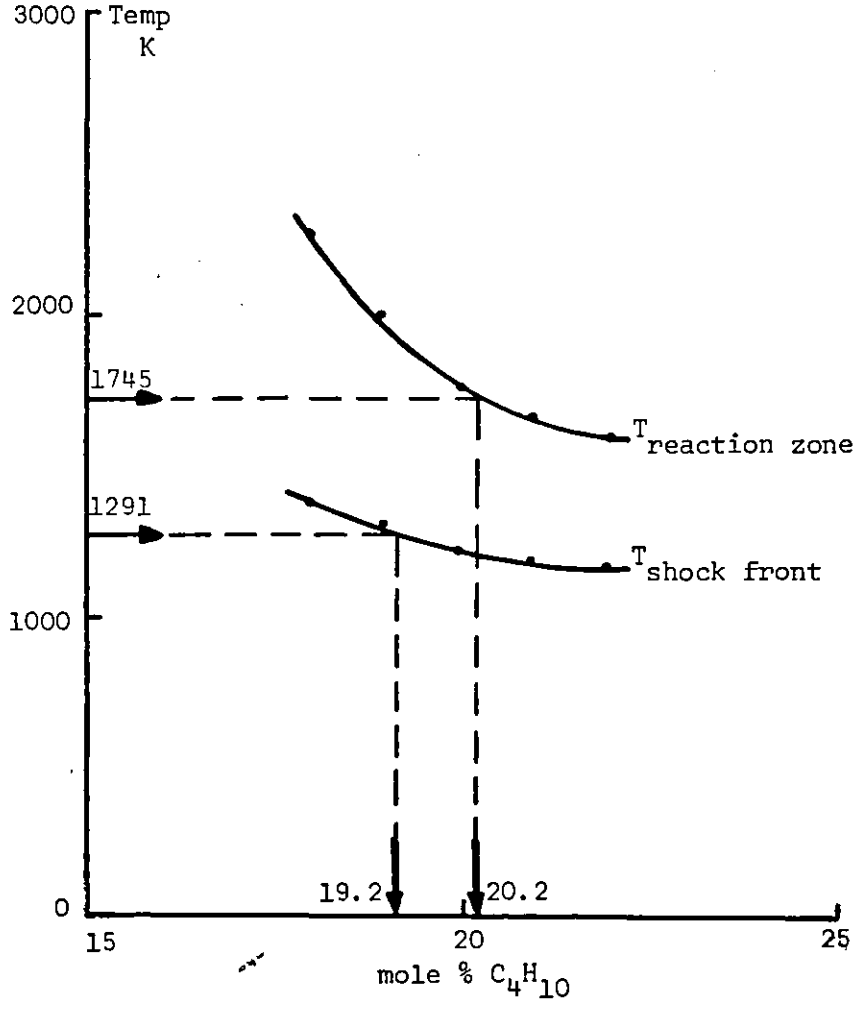
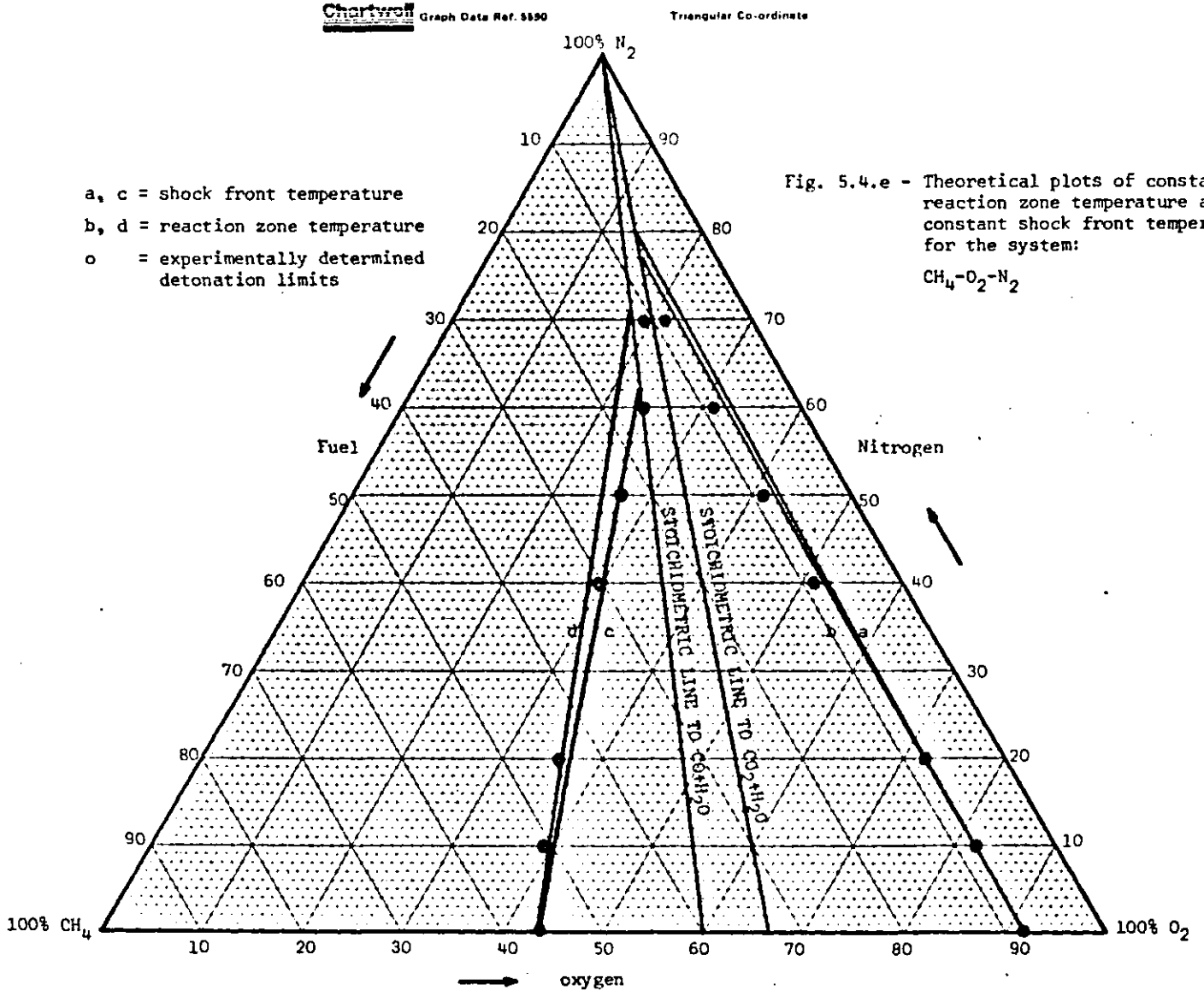


Fig. 5.4.d - Estimate of composition limits to detonation in ternary systems containing nitrogen based on critical temperature values for corresponding binary systems:

"Fuel-rich; C_4H_{10}-O_2-40% N_2"



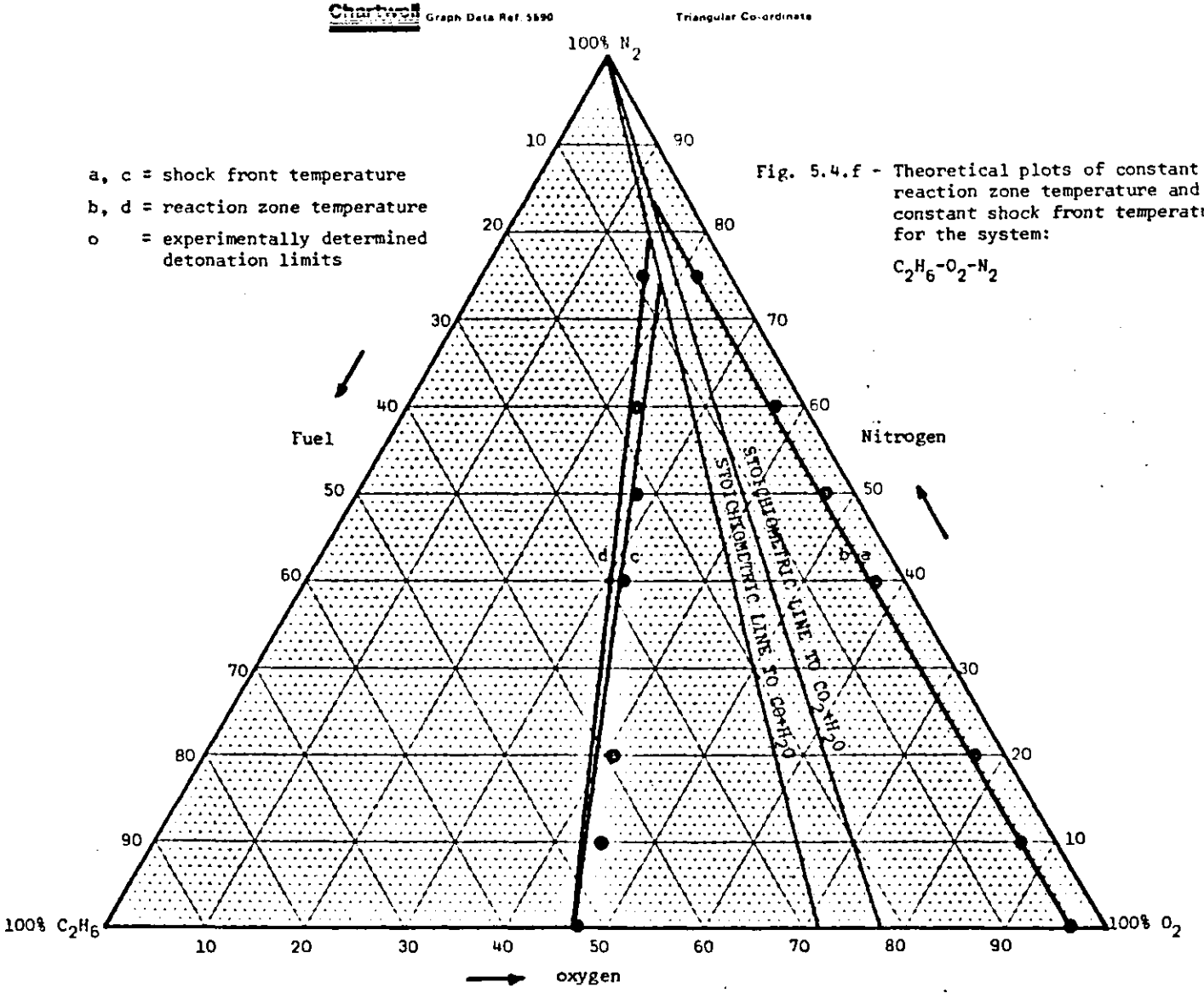
a, c = shock front temperature

b, d = reaction zone temperature

o = experimentally determined detonation limits

Fig. 5.4.e - Theoretical plots of constant reaction zone temperature and constant shock front temperature for the system:

CH_4-O_2-N_2



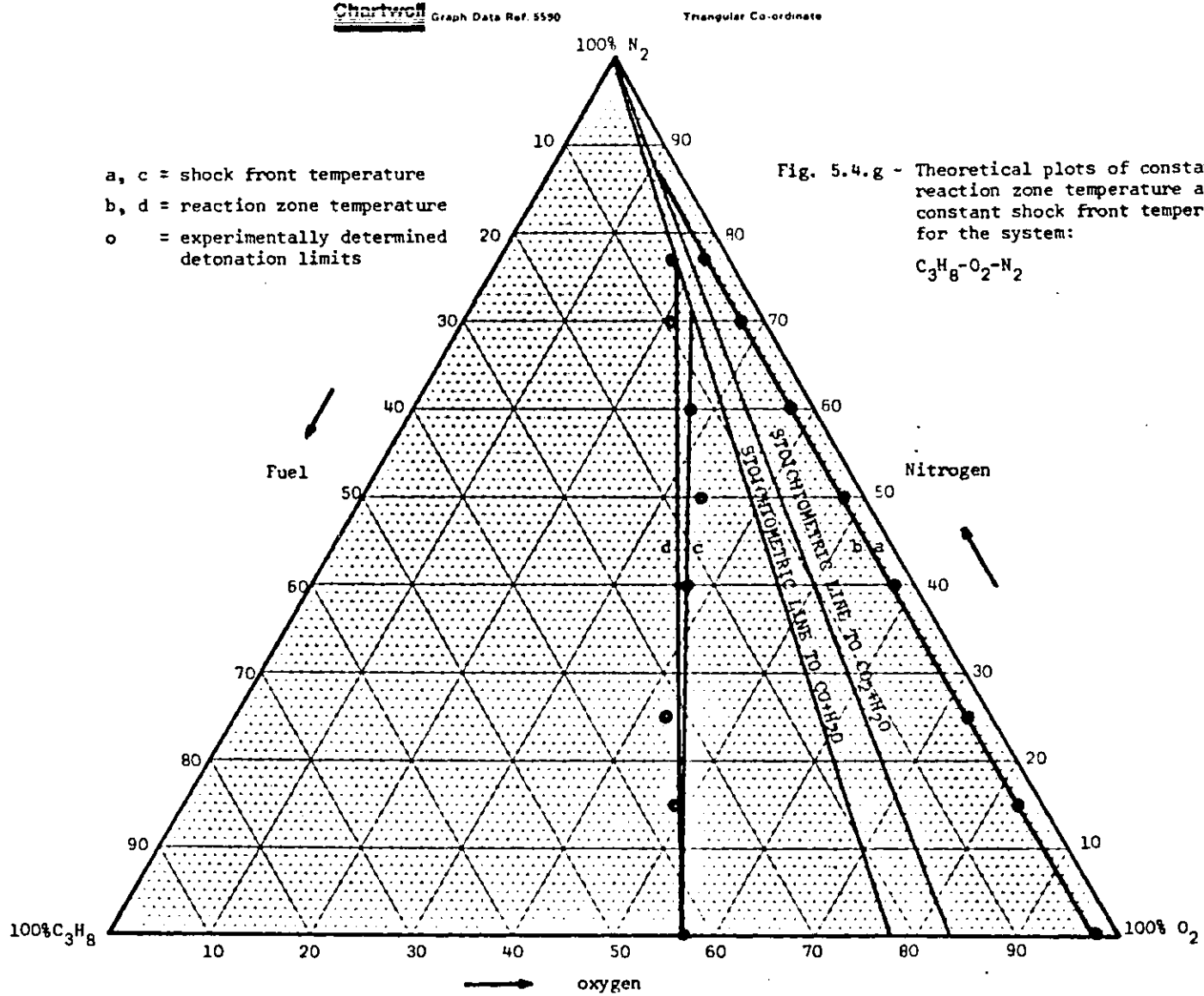
a, c = shock front temperature

b, d = reaction zone temperature

o = experimentally determined detonation limits

Fig. 5.4.f - Theoretical plots of constant reaction zone temperature and constant shock front temperature for the system:

C_2H_6-O_2-N_2



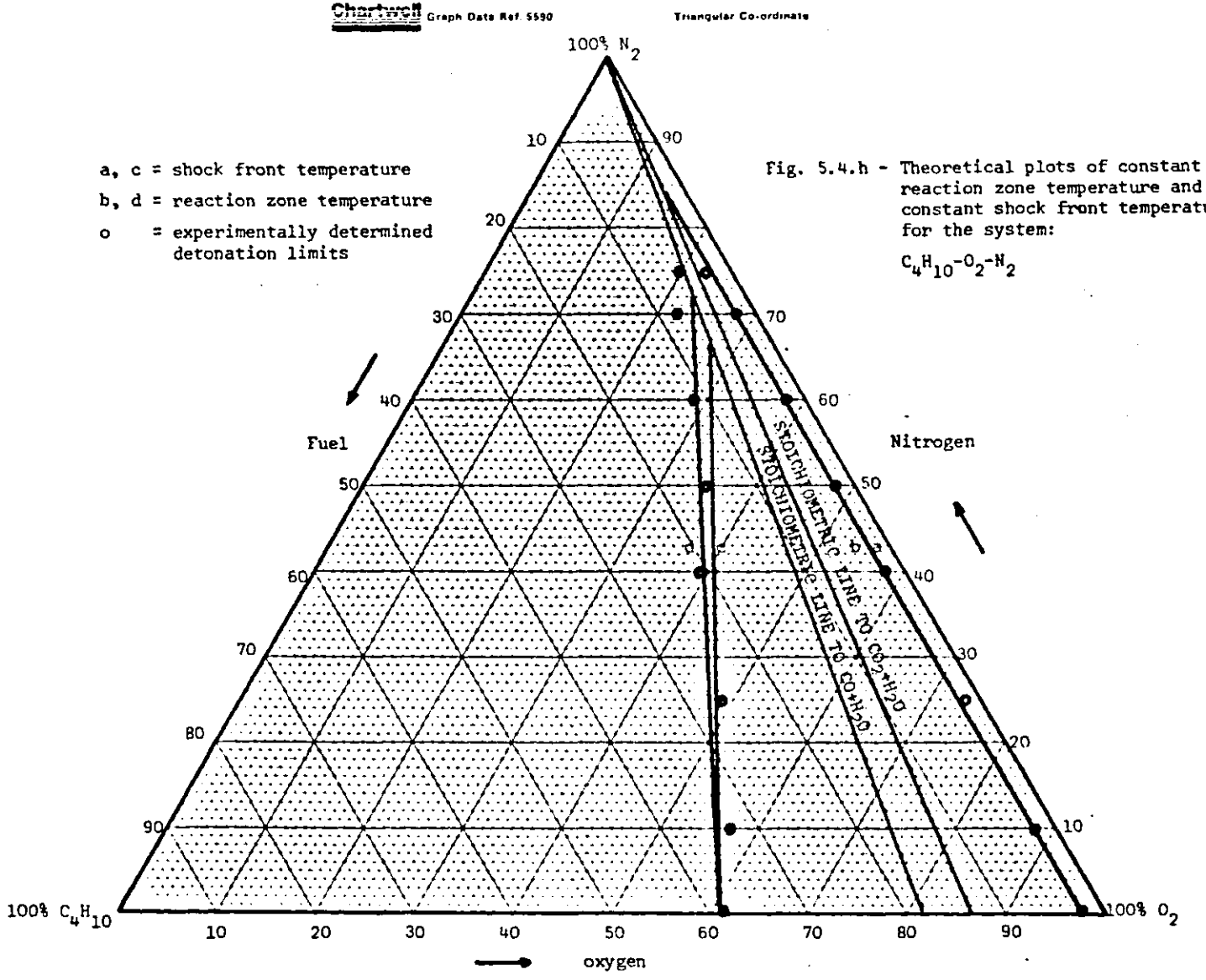
a, c = shock front temperature

b, d = reaction zone temperature

o = experimentally determined detonation limits

Fig. 5.4.g - Theoretical plots of constant reaction zone temperature and constant shock front temperature for the system:

C_3H_8-O_2-N_2



a, c = shock front temperature

b, d = reaction zone temperature

o = experimentally determined detonation limits

Fig. 5.4.h - Theoretical plots of constant reaction zone temperature and constant shock front temperature for the system:

C_4H_{10}-O_2-N_2

CHAPTER 6

DISCUSSION

The simple reaction products from marginal detonation introduced in Chapter 2, were selected as a replacement for the actual hot gaseous mixtures existing at the C-J condition to allow for calculation of nominal temperature rises in the detonation wave. The favoured chemical reactions for marginal detonation of hydrocarbons and oxygen were taken as pyrolysis of fuel molecules and a process of oxidation. This was in agreement with several shock-tube studies (e.g. J. Bradley, 1962) of reactions of paraffinic hydrocarbons. In comparison with computed (C-J) equilibrium compositions for the binary systems of propane and hexane with oxygen (Michels, 1967, Thesis, p. 227-8), this approach suggests carbon dioxide and water vapour as the dominant reaction products in fuel-lean detonations, and carbon monoxide as the major reaction product from marginal detonation towards the fuel-rich side. As pointed out earlier, the relative agreement of shock temperatures calculated on the basis of the above considerations and those obtained by Michels in a quite different way, gives some justification to this method. For further examination of the extent of validity of assumptions upon which the theoretical calculations were based, a comparison between the velocities calculated by C-J theory from the energy released in the simplified reactions and those mean velocities determined experimentally is necessary. Table 6.1 lists both velocities. Here, as in comparisons by other researchers (e.g. Lewis and Frauf, 1930), the measured values are mostly somewhat lower than the predicted values. The calculated velocities for fuel-lean sides are generally (3-8%) higher than the

TABLE 6.1

Comparison of calculated (in this work) and experimental velocities in marginal detonable mixtures of saturated aliphatic hydrocarbons, oxygen and 40 mole % nitrogen.

Hydrocarbon	Mole % Fuel	Calculated Velocity (metre/sec)	Experimental Velocity (metre/sec)
C_2H_6	4	1627	1570
"	5	1764	1680
"	26	2062	2000
"	27	1991	1900
C_3H_8	4	1837	1720
"	5	1985	1840
"	21	2094	2135
"	22	2017	2030
C_4H_{10}	3	1813	1740
"	4	2000	1830
"	19	1986	1940
"	20	1885	1890

experimental values, while for fuel-rich mixtures, the differences between the two velocities drop to (0.5-4)%. The better agreement between calculated and experimental velocities for fuel-rich sides of detonation regimes may be attributed to the fact that the assumptions of chemical products for fuel-rich mixture compositions are more correct than the assumptions for the fuel-lean side of the detonation regimes. This may be so, because there always exist some CO at C-J compositions of fuel-lean detonations and this has been omitted in this work.

For marginal regions of detonation, however, there exist certain differences between calculated and experimentally determined velocities due to near limit effects, as well as to the presence of inert gas (40% N_2). Although the agreement between the calculated and experimental velocities is not as good as in cases where proper C-J equilibrium calculations are used, it is, nonetheless, acceptable, and this suggests that the calculated shock and reaction temperatures should be within reasonable accuracy as well. It also supports the idea mentioned earlier (Section 1.6) that even for marginal conditions, the propagation velocity of detonation predicted by the C-J theory will closely follow the experimental velocity if the latter is determined over sufficiently long distance, or averaged over many short distances.

Propagation or decay of detonation which was established with reference to the constant temperature criterion and which is shown in the theoretical plots of the last chpater, in the first instance indicates an equal success from the use of either shock or reaction temperatures. This was not expected. Instead, it was anticipated that either constant reaction zone temperature or constant shock front temperature coupled with the simple reaction mechanisms and products would be able to predict the mixture compositions at which detonation fails to propagate. Had this

been the case, then the critical importance could have been highlighted of either of the two temperature rises on limits of detonability, even with the theoretical calculations based on the simple assumptions as mentioned in Section 2.1.

Under the present circumstances, the theoretical plots of the last chapter indicate that both reaction zone temperature and shock front temperature can be used as meaningful tools in prediction of mixture compositions at which propagation fails. From the general consistency found, it was deduced that for saturated aliphatic hydrocarbons, oxygen and nitrogen mixtures, detonation would fail to initiate the chemical reaction in the unburned gas if shock front temperature dropped below a critical minimum value. In case that initiation happened, but the reaction zone temperature dropped below some critical minimum value, the rate of chemical reaction would not be rapid enough to sustain the propagation of the wave as a "detonation" and decay would occur. However, at this stage, no valuable justification can be made on the relative merit of shock front temperature or reaction zone temperature in the determination of compositions at which detonation failure occurs, because there exist deficiencies - arising from simplifying assumptions - which make such comparisons unrealistic. For a real understanding, the values calculated have to be compared with accurate data for shock and reaction temperatures, derived from accurate experimental velocities and theoretical C-J equilibrium data respectively. As little of this is available, such comparisons at the moment are not possible.

However, from Figures 5.4.a to 5.4.d, it is clear that the limiting compositions determined with reference to constancy of either reaction zone temperatures or shock front temperatures do not differ more than .2 mole % for the fuel-lean side, and for the fuel-rich side of detonation,

these differences are about 1 mole % of limiting compositions. This might suggest that the two temperature rises are not independent of each other and practically both of the critical temperature rises should correspond to a unique mixture composition. Ideally, this mixture composition should be the limiting composition for detonation propagation.

As the limiting compositions corresponding to the critical temperature rises of reaction zone and shock front have been determined graphically, the agreement among composition mixtures on the fuel-lean side of the detonation regimes seems excellent. The consistent difference of 1 mole % in detonation limits on the fuel-rich side presumably arises from neglecting the condensation enthalpy contribution to the total effective energy release in reaction zone temperature calculations. The problems of formation of solid products in mixtures of oxygen and some gaseous fuels, especially towards the fuel-rich end of the detonation regime, has been widely investigated by Ubbelohde and Munday (e.g. ibid 1968-9). Certain aspects of the production of such solids are of special importance for marginal detonation, as a substantial fraction of the total enthalpy change due to the chemical reaction may not be available until solid products can be formed. It has been argued by the same scientists that when solid products are ultimately formed, the reaction zone lengthens behind the detonation front because of the long reaction time required for the formation of nuclei, and for the deposition of more solids onto such nuclei. In such cases, there is still more heat to be evolved behind the 'gaseous' C-J plane. These references state that if heats of sublimation are high, this energy release in the late stage must be fed to the detonation front by some means in order to continue the propagation of the detonation wave. They suggest that enthalpy liberation due to formation of solid products may give rise to a secondary detonation

wave amongst the reaction products, which may catch up with the first wave. As soon as it has crossed the 'gaseous' C-J plane, either a new detonation is formed with a very long reaction zone, or a pulsating detonation wave might arise. (This can be noticed by the exceptionally vast fluctuations in mean detonation velocities towards fuel-rich sides of detonation).

For theoretical calculations, however, the exact amount of such an enthalpy liberation by the time-dependent carbon deposition process of the type, $C_{gas} \rightarrow C_2 \rightarrow C_5 \rightarrow C_n \rightarrow C_{graphite} + \Delta H$, can be very uncertain because generally only a fraction of $C_{(gas)}$ might deposit to $C_{(graphite)}$. As a result usually an unknown fraction of such an enthalpy release as mentioned above, can contribute to the hydrodynamic mechanism of detonation propagation. The contribution of condensation energy in theoretical calculations of this work, which are based on simplicity, may have no physical reality because the real chemical reactions are much more complicated than could be assumed in the calculations. Consequently, in calculations of temperature rises for detonation of saturated aliphatic hydrocarbons and oxygen, it was assumed that the enthalpy release during the condensation process, occurs far behind the assumed C-J condition. Such energy contributions were not taken into consideration for theoretical calculations of nominal temperature rises in detonation.

The success of the constant temperature criterion in modelling the detonation regime boundaries for saturated aliphatic hydrocarbons, suggested the use of the same technique in predicting detonation limits in ternary systems of unsaturated hydrocarbons, oxygen and nitrogen.

For this purpose, some miscellaneous detonation runs were made for the system C_2H_4-O_2-N_2, to estimate for these mixtures the detonation regime boundary with higher nitrogen dilution than for the air line. Results were reported in Table 5.5d and Fig. 6.1 shows the corresponding part

of the detonation regime boundary. The intention was to compare this limit curve with a theoretically established detonation regime boundary for the system C_2H_4-O_2-N_2 based on the constant temperature criterion. Temperatures were calculated by modifying the computer program to work for C_nH_{2n} type fuels and the binary limit compositions were taken from Michels, 1967. (C-J) reaction-zone temperatures and shock front temperatures for the least nitrogen diluted mixtures measured on the fuel-lean (76 mole % N_2) and fuel-rich (65 mole % N_2) limit sides were calculated for, respectively, O_2-diluted and CO reaction products. The results are shown in Tables 6.2a and 6.2b.

TABLE 6.2a

(C-J) reaction-zone temperatures and shock front temperatures near fuel-lean side for the system: C_2H_4-O_2-76% N_2

mole % C_2H_4	mole % N_2	$T_{reaction}$ K	T_{shock} K
3.4	0	2089	1166
3	76	2017	1180
4	76	2460	1366
5	76	2865	1550

TABLE 6.2b

(C-J) reaction-zone temperatures and shock front temperatures near fuel-rich side for the system: C_2H_4-O_2-65% N_2

mole % C_2H_4	mole % N_2	$T_{reaction}$ K	T_{shock} K
12	65	3360	1695
15	65	2650	1500
18	65	2080	1320
66.5	0	2987	1911

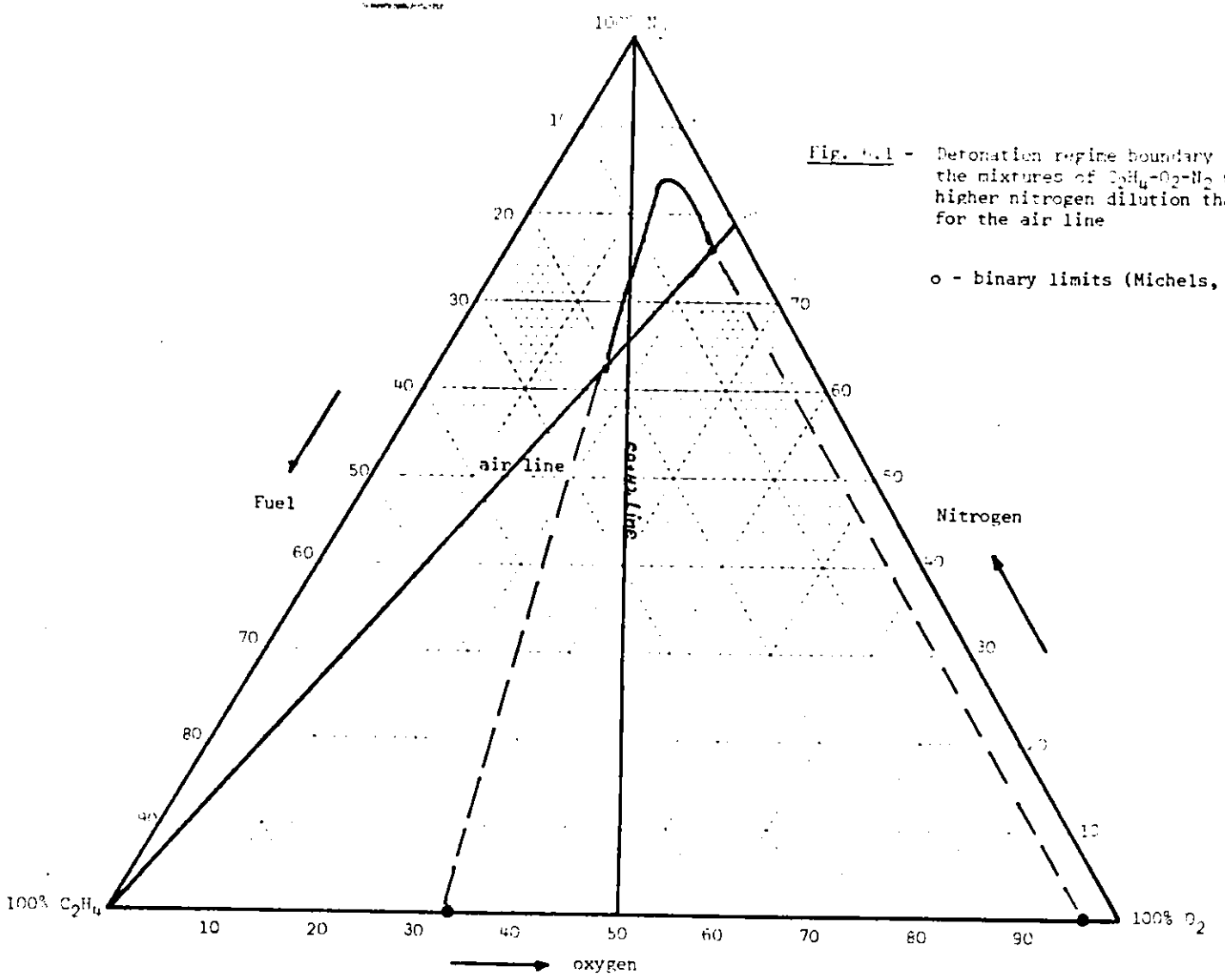


Fig. 4.1 - Detonation regime boundary for the mixtures of C_2H_4-O_2-N_2 with higher nitrogen dilution than for the air line

o - binary limits (Michels, 1967)

Following the procedures outlined in Section 5.4 for detonation of saturated hydrocarbons, the results of Tables 6.2a and 6.2b can be plotted as in Figs. 6.2a and 6.2b. Applications of the constant temperature criterion to estimate the fuel-lean composition limit to detonation in ternary system of C_2H_4-O_2-76% N_2, based on critical temperature values for corresponding binary systems results in a limiting composition of around 3 mole % ethylene which is shown by dotted lines and arrows in Fig. 6.2a. The experimentally-determined fuel-lean composition limit for the system of C_2H_4-O_2-76% N_2 is around 4 mole % of ethylene. Such differences can probably be ascribed to experimental uncertainty (see Table 4.5a) and perhaps to the high dilution of the system by nitrogen, which may begin to affect the proportionality of changes that fuel and oxygen will interact. However, within the accuracy limits it suggests that the criterion is capable of predicting detonation limits for fuel-lean side of the ternary system of C_2H_4-O_2-N_2. On the evidence obtained with the saturated hydrocarbons, there is, furthermore, enough justification to expect a straight-line fuel-lean limit of $\sim$(3-4) mole % ethylene along the O_2-N_2 side of the ternary diagram from 0-80% N_2 (see Fig. 6.1.).

The similar procedure for the fuel-rich limit, however, shows an appreciable difference between estimated and determined limit compositions (see Fig. 6.2b). Thus in difference with the results for saturated hydrocarbons, the criterion obviously does not work for the fuel-rich side of the ethylene system.

Some understanding of the possible reasons why the constant temperature criterion fails for the fuel-rich limit of the ethylene system can be obtained by considering first a wider composition range for calculating reaction zone temperatures following the simplified procedures previously

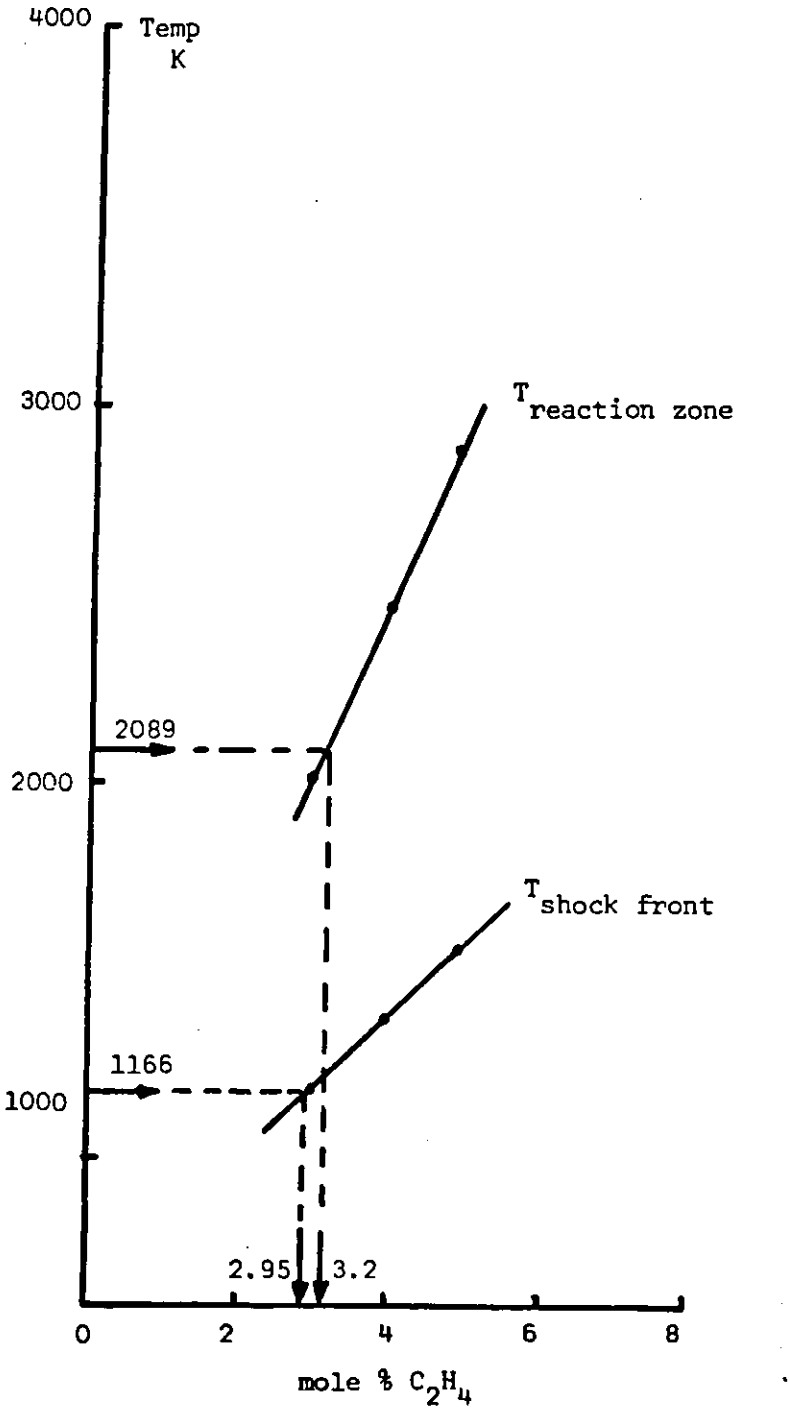


Fig. 6.2a Estimate of composition limits for the fuel-lean detonation in ternary system of C_2H_4-O_2-76% N_2, based on critical temperature values ($T_{reaction}$ and T_{shock}) for corresponding binary systems. "Experimentally determined composition limit is 4 mole % C_2H_4"

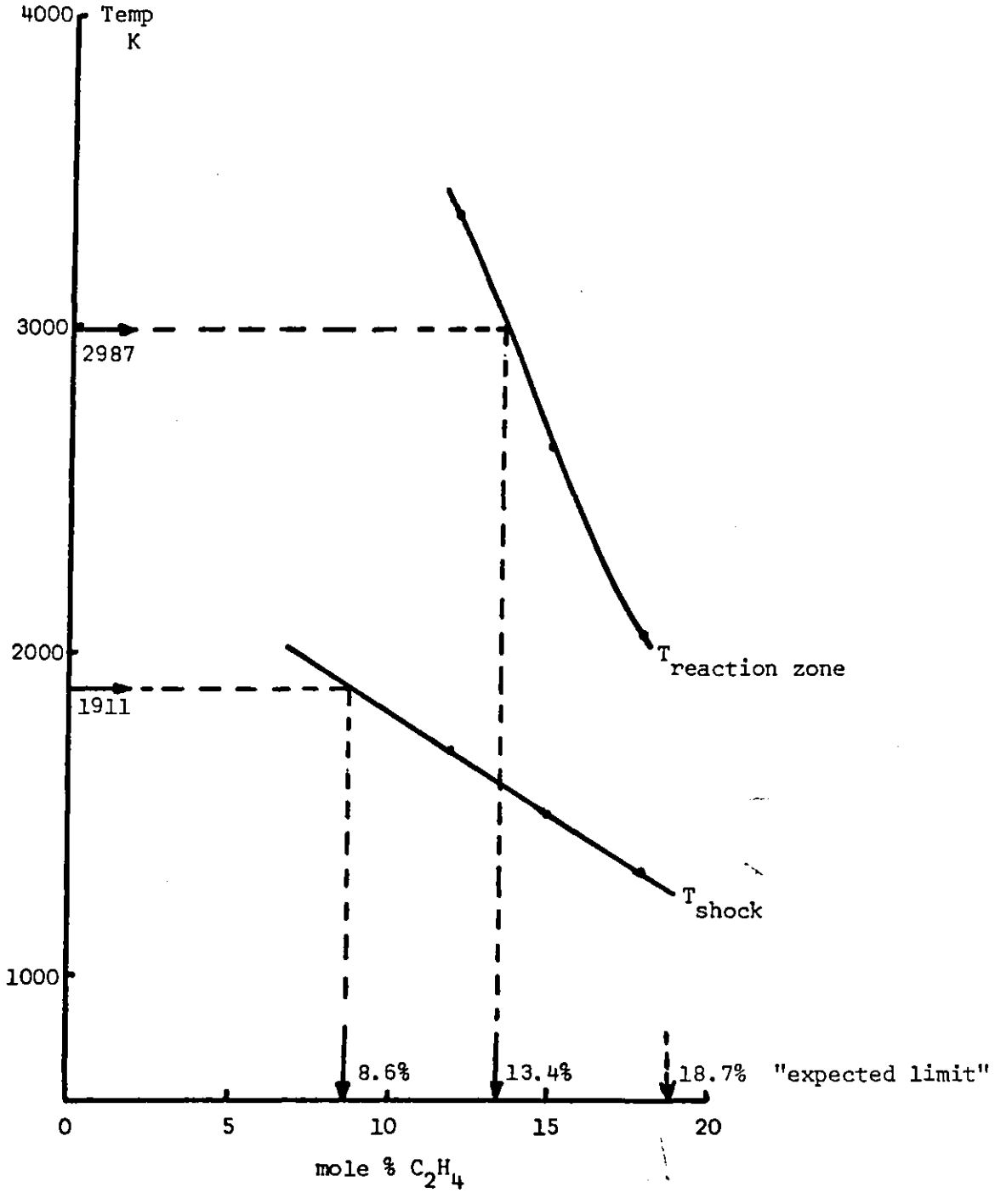


Fig. 6.2b - Estimate of composition limits for the fuel-rich detonation in ternary systems of C_2H_4-O_2-65% N_2, based on critical temperature values ($T_{reaction}$ and T_{shock}) for corresponding binary systems. "Experimentally determined composition limit is 18.7 mole % C_2H_4".

described. This has been done for part of the system C_2H_4-O_2-40% N_2; a series of results are listed in Table 6.3 and also recorded in Fig. 6.3. As can be seen, around the fuel-lean limit, estimated for this system, the variation of the reaction zone temperature is continuous and very steep with respect to even slight changes of fuel concentration in the mixture. This is as expected and corresponds with observations for detonations of paraffinic hydrocarbons, as shown in earlier chapters. Towards the fuel-rich limit, the reaction zone temperature initially also drops steeply as fuel concentration in the mixture is increased. However, when the fuel concentration rises above the amount required for full conversion to (CO + H_2), according to the simple reaction mechanisms used, (i.e. 30 mole % ethylene in the system C_2H_4-O_2-40% N_2) the temperature does no longer change appreciably with increase of fuel concentration (see Fig. 6.3). As can be observed, there is a distinct discontinuity in the curve, where the slope changes abruptly, at 30% C_2H_4.

TABLE 6.3

(C-J) temperature rises for marginal detonations for the system: C_2H_4-O_2-40% N_2

mole % C_2H_4	mole % N_2	$T_{reaction\ zone}$ K
3	40	1965
4	40	2400
5	40	2800
6	40	3172
25	40	3675
30	40	2685
33	40	2587
34	40	2556
35	40	2524
36	40	2491
37	40	2458

It is relatively easy to understand why the discontinuity arises and what the sections of the curve on either side of this point (A) represent. Point A indicates the C-J temperature for a detonation in a mixture which contains just sufficient oxygen to convert only all carbon atoms to carbon monoxide. To the left of A the temperature rises steeply as further oxygen is considered to produce some water. To the right of A the temperature changes little as some carbon remains unoxydised. Although a straight-line estimate of the fuel-rich detonation limit between the experimentally-determined limits of the binary system (67% C_2H_4) and of the ternary system with 65% nitrogen (18.7% C_2H_4) will not be very accurate, the resulting fuel-rich limit prediction for the system with 40% nitrogen will be around 37% C_2H_4 (see Fig. 6.1 and Fig. 6.3). The estimated limit is therefore well inside the range of partial carbon formation.

If similar stoichiometry is applied to the binary and 65% nitrogen-diluted system, the equivalent discontinuity points beyond which carbon formation is assumed, are respectively 50% and 17.5% C_2H_4 while the corresponding experimentally-determined limits are 67 and 18.5% C_2H_4 (see Fig. 6.2b).

It would appear, therefore, that the criterion in its present form does not work well, when carbon formation is likely to occur over a significant part of the detonation regime. Why this should be so is at this stage not well understood. Very likely, some energy contributions to detonation propagation from condensation to solids, such as proposed by e.g. Faraday (1970) or Mader (1979) will have to be included in calculations of simplified "C-J" temperatures for fuel-rich ethylene-containing mixtures. Once an adequate quantitative assessment has been made, it will not be difficult to incorporate these in the computer program.

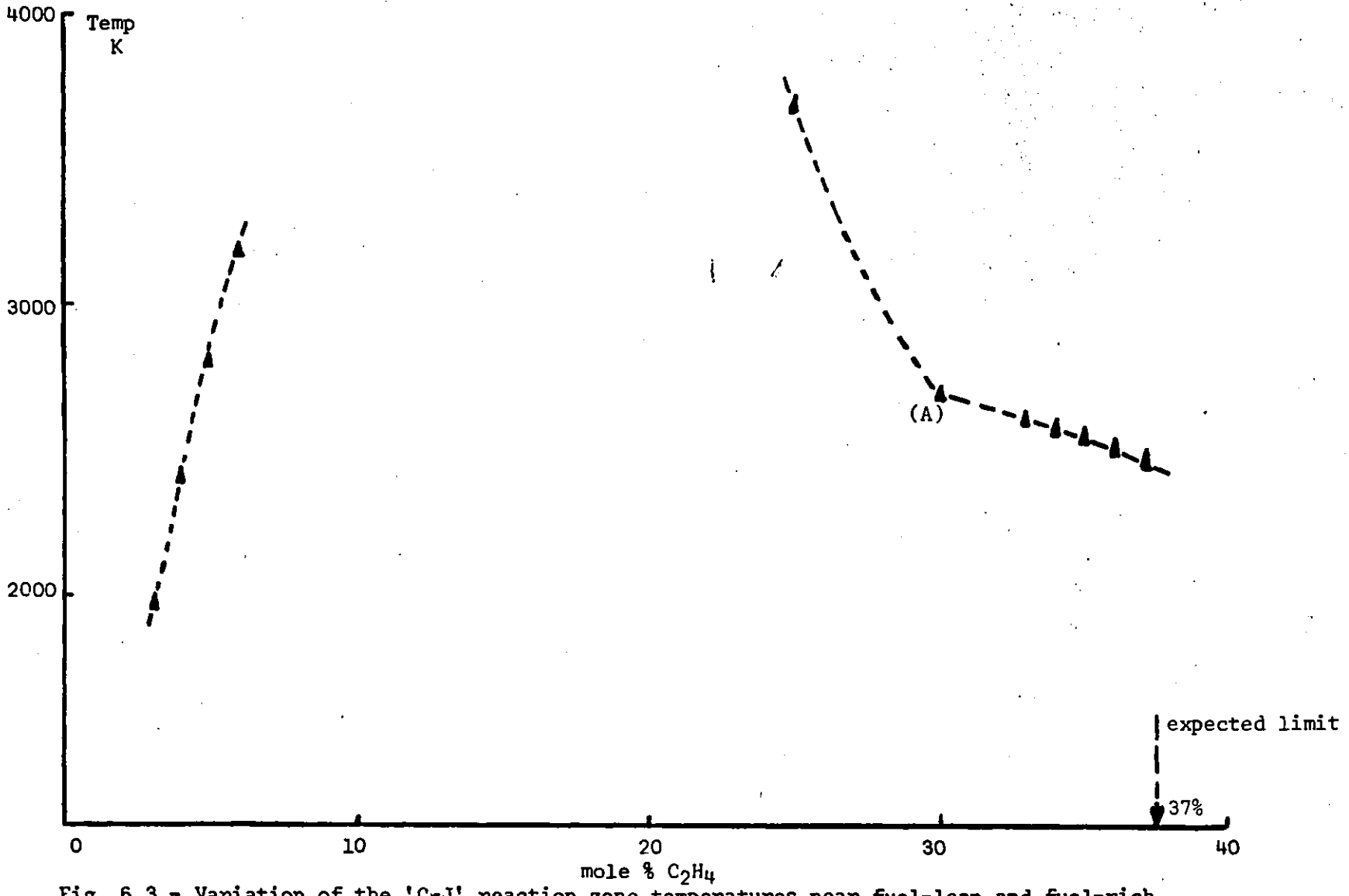


Fig. 6.3 - Variation of the 'C-J' reaction zone temperatures near fuel-lean and fuel-rich detonations of the system: C_2H_4-O_2-40% N_2

The notion that the criterion works well in the "steep-curve" section, left of A and at the oxygen/nitrogen diluted fuel-lean limits, invites a check on the fuel-rich limit of the butane-oxygen-nitrogen system, where experimentally soot products were found. Fig. 5.4d shows the estimate for the fuel-rich limit with 40% N_2. Stoichiometry shows that the equivalent of point A in Fig. 6.3 would occur at 20% C_4H_{10}. As it is, the estimated limit was 20.2% C_4H_{10}, i.e. just inside the carbon-forming range. The suggestion that the curve for $T_{reaction\ zone}$ should have a discontinuity at 20% C_4H_{10} is actually supported by the points on the curve.

As mentioned in the last chapter, the homology representation of detonation limits in ternary systems shows some correlation deficiency for the methane system. In the previous study of binary mixtures (Michels, 1967), comparison with the calculated shock temperatures showed that such deficiency may be attributed to the relatively high energy needed to rupture methane molecules. By comparison, C-C bond energies for higher paraffins up to C_5 are lower and more or less identical. In ternary systems, however, the deficiency of the homology method in correlating methane limits is less significant on the fuel-rich side of the detonation regime. This may be in agreement with the fact that the calculated reaction and shock temperatures in Table 5.3a to 5.3d show a better similarity at fuel-rich limits than fuel-lean limits.

Conclusions and Suggestions for Further Investigation

The main results of a practical nature of the present work suggest that

(a) The limits of detonability for mixtures of some hydrocarbons, oxygen and nitrogen may be correlated within reasonable accuracy by the use of fuel homology methods, such that the hazards of detonation can be evaluated under one master detonability regime expressed on homology % of compounds.

(b) Both reaction zone and shock front temperatures, calculated from simplified reaction mechanisms as linear composition relations passing through two points on either side of the detonation regime, with temperature values similar to those of limits of corresponding binary systems, predict regime boundaries with great accuracy.

(c) The same procedure for a system of unsaturated hydrocarbon fails to predict the detonability limit for fuel-rich side. The latter case emphasises the contribution from enthalpy liberation from at least part of the carbon condensation process, to support the propagation of detonation wave near the fuel-rich end.

To understand why (b) works, the urgent need is to compare these temperatures with values calculated accurately. This may not only throw light on various assumptions made by this work, but also provide an interesting basis for reviewing the homology correlation principle. Research is going on in the Department for C-J equilibrium data calculations. It is also necessary to consider the quantitative contribution of the energy of carbon condensation to the total effective energy release and thus to temperature values in detonations of C_2H_4-O_2-N_2 systems, and to expand the experimental research into C_nH_{2n} type fuels.

REFERENCES

Becker, R., 1922, Zeits. für Physik 8, 321.

Bone, W.A. and Fraser, R.P., 1932, Phil. Trans. Roy. Soc. 230A, 363.

Bone, W.A., Fraser, R.P. and Wheeler, W.H., 1936, Phil. Trans. Roy. Soc. 235A, 29.

Bradley, J.N., 1962, Shock Waves in Chemistry and Physics, Methuen & Co. Ltd.

Bradley, J.N. and Kistiakowsky, G.B., 1961, J. Chem. Phys. 35, 264.

Breton, M.J., 1936, Ann. off. nat. Combustible Liquids 11, 487, Thesis, Faculté des Sciences Université de Nancy.

Brinkley, S. Jr. and Richardson, J., 1953, IVth Symp. (Int.) on Combustion, p. 450, Williams and Wilkins, Baltimore.

Chapman, D.L., 1899, Phil. Mag. 5, 47, 90.

DÖring, W., 1943, Ann. Physik 43, 421.

Faraday, A.G., 1970, PhD Thesis, University of London.

Faraday, A.G., Munday, G. and Ubbelohde, A.R., 1970, Proc. 3rd Conf. on Industrial Carbons and Graphite, Imperial College, London.

Fay, J.A., 1952, J. Chem. Phys. 20, 942; 1953, 4th Symp. (Int.) on Combustion, p. 501, Williams and Wilkins, Baltimore.

Fickett, W. and Davis, W., 1979, Detonation, University of California Press.

Gaydon, A. and Hurle, I., 1963, The shock tube in high-temperature chemical physics, Chapman and Hall.

Green, E.F., Taylor, R.L. and Patterson, W.L. Jr., 1958, J. Phys. Chem. 62, 238.

Jouguet, E., 1905, J. Math., 347.

Kauzmann, W., 1966, Kinetic Theory of Gases, W. Benjamin Inc., New York.

Kirkwood, J.G. and Wood, W.W., 1954, J. Chem. Phys. 22, 1915.

Lewis, B. and Fiauf, J.B., 1930, J. Am. Chem. Soc. 52, 3905.

Lewis, B. and Von Elbe, G., 1961, Combustion, Flame and Explosions of Gases, Academic Press, Inc.

Mader, C.L., 1979, Numerical Modelling of Detonations, University of California Press.

Michels, A. and Boerboom, A., 1953, Bull. Soc. Chim. Belg. 62, 119 (comm. "van der Waals Fund. 134).

Michels, H.J., 1967, PhD Thesis, University of London.

Michels, H.J., Munday, G. and Ubbelohde, A.R., 1970, Proc. Roy. Soc. A319, 461.

Miles, J.E.P., Munday, G. and Ubbelohde, A.R., 1962, Proc. Roy. Soc. A269, 165; 1966, ibid. A291, 167.

Munday, G., Ubbelohde, A.R. and Wood, I.F., 1968a, Proc. Roy. Soc. A306, 171.

Munday, G., Ubbelohde, A.R. and Wood, I.F., 1968b, Proc. Roy. Soc. A306, 159.

Munday, G, Ubbelohde, A.R. and Wood, I.F., 1968c, Proc. Roy. Soc. A306, 179.

Neumann, J. von, 1942, O.S.R.D. Report No. 549.

Schüller, W., 1954, Dissertation, Darmstadt.

Skinner, G.B. and Ruehrwein, R.A., 1959, J. Phys. Chem. 63, 1736.

Strehlow, R.A., 1964, Phys. of Fluids, 7, 908.

Strehlow, R.A. and Fernandes, F.D., 1965, Combustion and Flame 9, 109.

Strehlow, R.A., Liaugminas, R., Watson, R.H. and Eyman, J.R., 1967, 11th Symp. (Int.) on Combustion, p. 683, Combustion Institute, Pittsburgh.

Taylor-Lewis, D., 1977, MSc Thesis, University of London.

Ubbelohde, A.R. and Munday, G., 1969, 12th Symp. (Int.) on Combustion, p. 809, Combustion Institute, Pittsburgh.

Wagner, H., 1961, Fundamental data obtained from shock tube experiments, (ed. A. Ferri), Pergamon Press.

Way, R.E., 1971, PhD Thesis, University of London.

White, D.R., 1961, Phys. of Fluids 4, 465.

White, J.K., 1961, Shock Tubes, Methuen and Co. Ltd.

Zeldovich, Y.B., 1940, J.E.T.P. (USSR), 10, 542, Translation: NACA TM-1261 (1950).

APPENDIX A1

The equations for calculation of reaction zone temperatures

U_1 and U_2 may be eliminated from equation (1.5) by the use of equations (1.7) and (1.8), and by application of the following differential equation for isentropic compression in the burned gas,

$$\frac{dP_2}{dV_2} = -\frac{\gamma_2 P_2}{\gamma_2}$$

equation (1.5) reduces to the equation:

$$\frac{V_1}{V_2}\gamma_2 + \frac{P_1}{P_2} = \gamma_2 + 1 \qquad \text{(A.1.1)}$$

Replacing $\frac{P_1}{P_2}$ in the equation above by $\frac{n_1 T_1 V_1}{n_2 T_2 V_2}$, from the equation of state, (A.1.1) leads to the first equation which was used for calculation of reaction zone temperatures as follows

$$\frac{V_1^2}{V_2^2} - \frac{\gamma_2+1}{\gamma_2} \cdot \frac{V_1}{V_2} + \frac{n_1}{n_2} \cdot \frac{T_1}{T_2\gamma_2} = 0 \qquad \text{(A.1.2)}$$

The second equation needed may be obtained by the use of perfect gas law in the equation (1.10);

$$\overline{C}_v(T_2 - T_1) - \Delta E_c - \frac{R}{2}\left(\frac{V_1}{V_2} - 1\right)\left(n_2 T_2 + n_1 T_1 \frac{V_2}{V_1}\right) = 0 \qquad \text{(A.1.3)}$$

as given in section (2.3) of the main text.

APPENDIX A2

The equation for the calculation of detonation velocities

From equation (A.1.1) and equation (1.7), it follows that:

$$U_1 = V_1\sqrt{\frac{\gamma_2 P_2}{V_2}} \qquad (A.2.1)$$

With the equation of state for a perfect gas, equation (A.2.1) can be reduced to

$$U_1 = \frac{V_1}{V_2}\sqrt{n_2\,\gamma_2\,RT_2} \qquad (A.2.2)$$

APPENDIX A3

Calculations of physical data

The values for the ratio of specific heats γ_2 for the burned gas are calculated as

$$\gamma_2 = \Sigma\, Cp_i \cdot n_i / \Sigma\, Cv_i \cdot n_i$$

in which: Cp_i = specific heat at constant pressure of each component

Cv_i = specific heat at constant volume of each component

n_i = mole fraction of each component

Power series in the temperature were developed for calculations of specific heats. Individual data needed for development of these power series were taken from A.P.I. project 44. The coefficients of the power series for different compounds are shown in Table A.3.1.

TABLE A.3.1

Coefficients for the equation of the heat capacity

$$Cp = a + bT + CT^2$$

	a	b	c	Temp range (deg K)
N_2	6.67	$1.35 * 10^{-3}$	$-2.02 * 10^{-7}$	1000 - 4000
O_2	7.5	$9.14 * 10^{-4}$	$-7.7 * 10^{-8}$	1000 - 4000
H_2	5.93	$1.456 * 10^{-3}$	$-1.657 * 10^{-7}$	1000 - 4000
CO_2	10.987	$2.33 * 10^{-3}$	$-3.216 * 10^{-7}$	1000 - 4000
CO	6.857	$1.266 * 10^{-3}$	$-1.897 * 10^{-7}$	1000 - 4000
H_2O	6.757	$3.61 * 10^{-3}$	$-5.053 * 10^{-7}$	1000 - 4000

C_v values for each component are obtained from the perfect gas law:

$C_v = C_p - R.$

Average specific heat ($\overline{C}_v$) values needed for reaction temperature calculation are calculated from the relations

$$\overline{C}_{v,i} = \frac{1}{T_2 - T_1} \int_{T_1=298\ K}^{T_2} C_{v,i}\, dT$$

$$\overline{C}_v = \Sigma\, \overline{C}_{v,i} \cdot n_i$$

ΔE_c is calculated as the algebaric sum of the formation energy of one gram of products and the atomization energy of one gram of fuel mixture.

APPENDIX B1

The equations for the calculation of shock front temperatures for polytropic gases

Conservation equations (1.4), (1.5) and (1.6) with the term $\Delta E_c = 0$ in equation (1.6), are valid for the passage of unit mass of gas through unit area of shock front. From the equation of state for perfect gases and relations $C_p - C_v = R$, $\gamma = \frac{C_p}{C_v}$, equation (1.9) reduces to

$$H = \left(\frac{\gamma}{\gamma-1}\right) PV \qquad \text{(B.1.1)}$$

Substitution of equation (B.1.1) into equation (1.6) gives for an ideal polytropic gas:

$$\left(\frac{\gamma}{\gamma-1}\right)P_1V_1 + \tfrac{1}{2}U_1^2 = \left(\frac{\gamma}{\gamma-1}\right)P_2V_2 + \tfrac{1}{2}U_2^2 \qquad \text{(B.1.2)}$$

The above equation, after substituting for U_1 and U_2 from equations (1.4) and (1.5), can be rearranged as follows:

$$\frac{P_2}{P_1} = \frac{1 - \left(\frac{\gamma-1}{\gamma+1}\right)\frac{V_2}{V_1}}{\frac{V_2}{V_1} - \frac{\gamma-1}{\gamma+1}} \qquad \text{(B.1.3)}$$

$$\frac{V_2}{V_1} = \frac{\left(\frac{\gamma-1}{\gamma+1}\right)\frac{P_2}{P_1} + 1}{\frac{\gamma-1}{\gamma+1} + \frac{P_2}{P_1}} \qquad \text{(B.1.4)}$$

Combination of equation (1.4) and (1.5), also leads to

$$\frac{P_2}{P_1} = 1 + \frac{U_1^2}{P_1V_1}\left(1 - \frac{V_2}{V_1}\right) \qquad \text{(B.1.5)}$$

It is convenient now to introduce the concept of the detonation Mach number M, where

$$M = \frac{U_1}{C_o} = \frac{\text{velocity of detonation}}{\text{velocity of sound}} \quad ; \quad C_o = \sqrt{\gamma P_1 V_1}$$

Use of these relations in equation (B.1.5) leads to

$$\frac{P_2}{P_1} = 1 + \gamma M^2 (1 - \frac{V_2}{V_1}) \qquad \text{(B.1.6)}$$

Let $\mu = \frac{\gamma-1}{\gamma+1}$, then combination of equation (B.1.6) and (B.1.4) results:

$$\frac{P_2}{P_1} = M^2(1 + \mu) - \mu \qquad \text{(B.1.7)}$$

If $M^2(1+\mu)-\mu = y$, then substitution of (B.1.7) in (B.1.4) gives:

$$\frac{V_1}{V_2} = \frac{\mu + y}{1 + \mu y} \qquad \text{(B.1.8)}$$

Use of the equations (B.1.7) and (B.1.8) with the equation of state of a perfect gas leads to the temperature rise ratio:

$$\frac{T_1}{T_o} = y \frac{1 + \mu y}{\mu + y} \qquad \text{(B.1.9)}$$

APPENDIX B1.A

The equations for the calculation of shock front temperatures for non-polytropic gases

For non-polytropic gases, the specific heat is dependent on the temperature due to the fact that at higher temperatures, degrees of freedom which were not exited at low temperatures begin to take up energy and thus the effective specific heat increases. By assuming the validity of the perfect gas law can still hold, it becomes possible to calculate a mean specific heat for a particular temperature range (initial temperature - shock front temperature) from the relations

$$\overline{C}_{p,i} = \frac{1}{T_1 - T_o} \int_{T_o}^{T_1} C_{p,i} \, dT$$

$$\overline{C}_p = \Sigma \, \overline{C}_{p,i}, \, n_i$$

Using these relations, a mean value for γ (or μ) over the mentioned temperature range can be determined as follows:

$$\bar{\gamma} = \frac{\bar{C}_p}{\bar{C}_v} = \frac{\bar{C}_p}{\bar{C}_p - R}$$

so that the temperature relation takes the form

$$\frac{T_1}{T_o} = y\,\frac{1 + \mu y}{\mu + y} \quad \text{where} \quad \mu = \frac{\bar{\gamma} - 1}{\bar{\gamma} + 1}$$

as given in section (2.4) of the main text.

APPENDIX B2

Calculations of physical data

The Mach number may be calculated from the equation

$$M^2 = \frac{U_1^2}{C_o^2} = \frac{m_1 . U_1^2}{R\, T_o\, \gamma_1}$$

in which: U_1 = detonation velocity (metre/sec)

m_1 = mean molecular weight of reactants (gram/mole)

T_o = initial temperature = 298 K

γ_1 = specific heat ratio of reactants at 298 K

Similar power series in the temperature were developed for calculations of specific hat values (C_p). Individual data for developing these power series were taken from A.P.I. Project 44. Table B.2.1 shows the coefficients for the evaluation of C_p values for different compounds.

TABLE B2.1

Coefficients for the equation of the heat capacity

$$C_p = a + bT + cT^2$$

	a	b	c	Temp range (deg K)
CH_4	3.526	1.84×10^{-2}	-4.455×10^{-6}	1000 - 1600
C_2H_6	2.328	3.74×10^{-2}	-1.057×10^{-5}	1000 - 1600
C_3H_8	2.39	5.58×10^{-2}	-1.64×10^{-5}	1000 - 1600
C_4H_{10}	3.878	7.14×10^{-2}	-2.109×10^{-5}	1000 - 1600
O_2	6.187	3.04×10^{-3}	-8.931×10^{-7}	1000 - 1600
N_2	6.546	1.43×10^{-3}	-1.6116×10^{-7}	1000 - 1600

APPENDIX C

Following is the listing of FORTRAN program developed for computation of reaction zone temperatures and shock front temperatures for the marginal detonation of saturated aliphatic hydrocarbons with oxygen and nitrogen.

```
      PROGRAM DTEMP(INPUT,OUTPUT,TAPE5=INPUT,TAPE6=OUTPUT)
      REAL MO2,MN2,MCO,MCO2,MH2O,MCH,MC,MTOT,N,N1,N2
      REAL MH2,MY,M
      READ(5,*) YCH,YN2,N,T2,MCH,HCH,CPCH
      YO2=1-YCH-YN2
      IMAX=50
      WRITE(6,25) YN2
C     ENTHALPIES OF FORMATION AT 298K
      WRITE(6,150) YCH,YO2,YN2
      HCO2=-94050
      HCO=-26420
      HH2O=-57800
      HC=0.
C     MOLECULAR WEIGHTS
      MO2=32.
      MN2=28.
      MH2O=18.
      MCO=28.
      MCO2=44.
      MH2=2.01
      MC=12.
      TEST=0.
      DO 1 I=1,IMAX
C     CALCULATION OF CP AND CV VALUES
      CPO2=7.5+9.14E-4*T2-7.7E-8*T2*T2
      CPN2=6.67+1.35E-3*T2-2.02E-7*T2*T2
      CPH2=5.93+1.456E-3*T2-1.657E-7*T2*T2
      CPCO2=10.987+2.33E-3*T2-3.216E-7*T2*T2
      CPCO=6.857+1.266E-3*T2-1.897E-7*T2*T2
      CPH2O=6.757+3.61E-3*T2-5.053E-7*T2*T2
      R=1.987
      CVN2=CPN2-R
      CVO2=CPO2-R
      CVCO=CPCO-R
      CVCO2=CPCO2-R
      CVH2=CPH2-R
      CVH2O=CPH2O-R
C     CALCULATION OF EQUATION PARAMETERS
      X=YO2/YCH
      HR=HCH
      EC=N*CVCO2+(N+1)*HH2O-HR
      MTOT=X+.5*(N+1)+YN2/YCH
      XCO2=N/MTOT
      XH2O=(N+1)/MTOT
```

```
      XO2=(X-(3*N+1)/2.)/MTOT
      XCO=0.
      XH2=0.
      AC=0.
      XN2=YN2/(MTOT*YCH)
      N1=1/(YCH*MCH+YO2*MO2+YN2*MN2)
      N2=1/(XCO2*MCO2+XH2O*MH2O+XO2*MO2+XN2*MN2)
      BETA=N+2.
      IF(X.GT.BETA) GOTO 10
      EC=N*HCO+(2*X-N)*HH2O-HR
      MTOT=2*N+1+YN2/YCH
      XCO2=0.
      XN2=YN2/(MTOT*YCH)
      XH2O=(2*X-N)/MTOT
      XO2=0.
      XCO=N/MTOT
      XH2=(2*(N-X)+1)/MTOT
      AC=0.
      N2=1/(XN2*MN2+XO2*MO2+XCO*MCO+XH2*MH2+XH2O*MH2O)
      BETA1=.5*N+.01
      IF(X.GT.BETA1) GOTO 10
      EC=2.*X*HCO+(N-2*X)*HC-HR
      MTOT=2*N+1+YN2/YCH
      XCO2=0.
      XO2=0.
      XN2=YN2/(YCH*MTOT)
      XCO=2*X/MTOT
      XH2=(N+1)/MTOT
      XH2O=0.
      AC=(N-2*X)/MTOT
      N2=1/(XH2*MH2+XN2*MN2+XCO*MCO+AC*MC)
      IF(X.LT.BETA1) GOTO 10
      STOP
C TRANSFORMING THE ENERGY RELEASE TO GRAM/FUEL MIXTURE
   10 ECA=-EC*YCH*N1
C CALCULATION OF REMAINING EQUATION PARAMETERS
      G1=YO2*7.017+YN2*6.961+YCH*CPCH
      CVCH=CPCH-R
      G1=G1/(YO2*5.01+YN2*4.97+YCH*CVCH)
      G2=XO2*CPO2+XN2*CPN2+XH2*CPH2+XCO*CPCO+XCO2*CPCO2+XH2O*CPH2O
      G2=G2+3*AC
      G2=G2/(XO2*CVO2+XN2*CVN2+XH2*CVH2+XCO*CVCO+XCO2*CVCO2+XH2O*CVH2O+6*A
      TSAVE=T2
      IF(T2.GT.4000)  T2=4000
      T1=298
      OXY=5.513*(T2-T1)+4.57E-4*(T2*T2-T1*T1)
      OXY=OXY-2.566E-8*(T2*T2*T2-T1*T1*T1)
      OXY=OXY*XO2
      NIT=4.683*(T2-T1)+.675E-3*(T2*T2-T1*T1)
      NIT=NIT-.6733E-7*(T2*T2*T2-T1*T1*T1)
      NIT=NIT*XN2
      HYD=3.943*(T2-T1)+.728E-3*(T2*T2-T1*T1)
      HYD=HYD-.5523E-7*(T2*T2*T2-T1*T1*T1)
      HYD=HYD*XH2
      CDIO=9.9*(T2-T1)+1.165E-3*(T2*T2-T1*T1)
      CDIO=CDIO-1.072E-7*(T2*T2*T2-T1*T1*T1)
      CDIO=CDIO*XCO2
      CMON=4.87*(T2-T1)+.633E-3*(T2*T2-T1*T1)
      CMON=CMON-.8323E-7*(T2*T2*T2-T1*T1*T1)
      CMON=CMON*XCO
      WATR=4.77*(T2-T1)+1.805E-3*(T2*T2-T1*T1)
      WATR=WATR-1.884E-7*(T2*T2*T2-T1*T1*T1)
      WATR=WATR*XH2O
      Q=OXY+NIT+HYD+CDIO+CMON+WATR+AC*6.
      AVPCV=Q*M2/(T2-T1)
      T2=TSAVE
```

```
C ITERATION EQUATIONS
A=(G2+1)/(2*G2)
VRATIO=A+SQRT(A*A-.298*M1/(M2*T2*G2))
A=(AVRCV+R/2.*(1-VRATIO)*M2)
T2=1/A*((AVRCV+R/2.*(1-1/VRATIO)*M1)*298+ECA)
RAP=ABS(T2-TEST)
IF(RAP.LT.0.001) GOTO 20
TEST=T2
1 CONTINUE
C SHOCK TEMPERATURES
20 WRITE(6,26)
WRITE(6,114) XO2,XN2,XH2,XH2O,XCO,XCO2
WRITE(6,110) G1,G2
WRITE(6,111) AVRCV
WRITE(6,112) ECA
WRITE(6,113) VRATIO
WRITE(6,101) T2
TEST=0.
D=VRATIO*(G2*T2*8314*M2)**.5
M=D*D*(MCH*YCH+MN2*YN2+MO2*YO2)/(8314.*298*G1)
T1=298

T0=1000
DO 2 J=1,IMAX
C CAL.OF AV.SPECIFIC HEATS OVER T1-TSHOCK RANGE
IF(M.EQ.1) GO TO 60
IF(M.EQ.2) GO TO 62
IF(M.EQ.3) GO TO 64
IF(M.EQ.4) GO TO 66
60 CPAV=3.526*(T0-T1)+.0092*(T0*T0-T1*T1)-1.485E-6*(T0*T0*T0-T1*T1*T1
CPAV=CPAV/(T0-T1)
GO TO 68
62 CPAV=2.523*(T0-T1)+.0187*(T0*T0-T1*T1)-.3524E-5*(T0*T0*T0-T1*T1*T1
CPAV=CPAV/(T0-T1)
GO TO 68
64 CPAV=2.390*(T0-T1)+.0279*(T0*T0-T1*T1)-.5466E-5*(T0*T0*T0-T1*T1*T1
CPAV=CPAV/(T0-T1)
GO TO 68
66 CPAV=3.878*(T0-T1)+.0357*(T0*T0-T1*T1)-.7033E-5*(T0*T0*T0-T1*T1*T1
CPAV=CPAV/(T0-T1)
68 CPO2=6.187*(T0-T1)+1.52E-3*(T0*T0-T1*T1)-2.977E-7*(T0*T0*T0-T1*T1*
CPO2=CPO2/(T0-T1)
CPN2=3.546*(T0-T1)+.715E-3*(T0*T0-T1*T1)-.5372E-7*(T0*T0*T0-T1*T1*T1)
CPN2=CPN2/(T0-T1)
AVCP=YCH*CPAV+YO2*CPO2+YN2*CPN2
AVCV=AVCP-R
```

```
      G=AVCP/AVCV
      MY=(G-1.)/(G+1.)
      Y=(M*(MY+1)-MY)
      TSHOCK=298*(1+MY*Y)/(MY+Y)
      TSHOCK=TSHOCK*Y
      TEST=ABS(T0-TSHOCK)
      IF(TEST.LT.0.001) GOTO 50
      T0=TSHOCK
    2 CONTINUE
   50 WRITE(6,102) TSHOCK
      WRITE(6,103) D
  101 FORMAT(1X,' REACTION ZONE TEMPERATURE        ',F10.3,' K')
  102 FORMAT(1X,' SHOCK TEMPERATURE                ',F10.3,' K')
  103 FORMAT(1X,' DETONATION VELOCITY              ',F10.3,' M/S')
  110 FORMAT(1X,'SPECIFIC HEAT RATIOS G1 AND G2 RESP.  ',2F10.5)
  111 FORMAT(1X,'AVERAGE CV-VALUE      ',F10.5,' CAL./GRAM')
   25 FORMAT(1X,'CALCULATION FOR THE          SYSTEM',F8.4,'   N2')
   26 FORMAT(1X,'MOLAR FRACTIONS IN OUTPUT ORDER O2,N2,H2,H2O,CO,CO2')
  112 FORMAT(1X,'ENERGY RELEASE/GRAM OF FUEL MIXTURE   ',F10.3,' CAL/GR.'
  113 FORMAT(1X,'VOLUME RATIO           ',F10.5,)
  114 FORMAT(1X,'MOLARFRACTIONS  ',  6F6.4)
  150 FORMAT(1X,'REACTANT COMPOSITION CH, O2, N2 ',3F6.4)
      STOP
      END
```

APPENDIX D

Table D.1 shows a comparison of C-J reaction and shock temperatures calculated in this work and by Taylor-Lewis (1977). The results are for marginal detonation of CH_4-O_2-N_2 mixtures. It is assumed that the reaction products are (CO_2 + H_2O), for both fuel-lean and fuel-rich mixtures.

TABLE D.1 - Reaction temperatures and shock temperatures near detonation limits for the system: CH_4-O_2-N_2. "CO_2 is the primary product"

		T. Lewis		This Work	
mole % CH_4	mole % N_2	$T_{reaction_K}$	T_{shock_K}	$T_{reaction_K}$	T_{shock_K}
8.5	0	2888	1527	2720	1433
5	35	2087	1233	2008	1140
7.5	35	2763	1492	2616	1396
10	35	3042	1813	3125	1597
30	30	4256	1907	4295	2229
35	30	3649	1465	3630	2107
40	30	3053	1283	2995	1908
56.5	0	2999	1322	3475	2278

Table D.2 shows reaction and shock temperatures near detonation limits for the system: C_3H_8-O_2-N_2 with the same reaction products for the methane system. Application of constant temperature criterion as outlined in Section 5.4 for fuel-rich side of these two systems results in Figs. D.1 and D.2 with corresponding constant temperature plots, shown in Figs. D.3 and D.4. The failure of theoretical plots to follow the experimentally determined limits towards the fuel-rich end

of the detonation regime in both systems, as mentioned earlier, led to the introduction of new reaction products as explained in Chapter 2 of the main text.

TABLE D.2

Reaction temperatures and shock temperatures near detonation limits for the system: C_3H_8-O_2-N_2
"CO_2 is the primary product"

mole % C_3H_8	mole % N_2	$T_{reaction}$ °K	T_{shock} °K
2.45	0	2230	1237
2	40	2005	1142
2.5	40	2320	1277
3.5	40	2855	1495
5	40	3540	1764
43	0	2810	2200
18	40	3720	2097
20	40	3095	1914
23	40	2685	1800

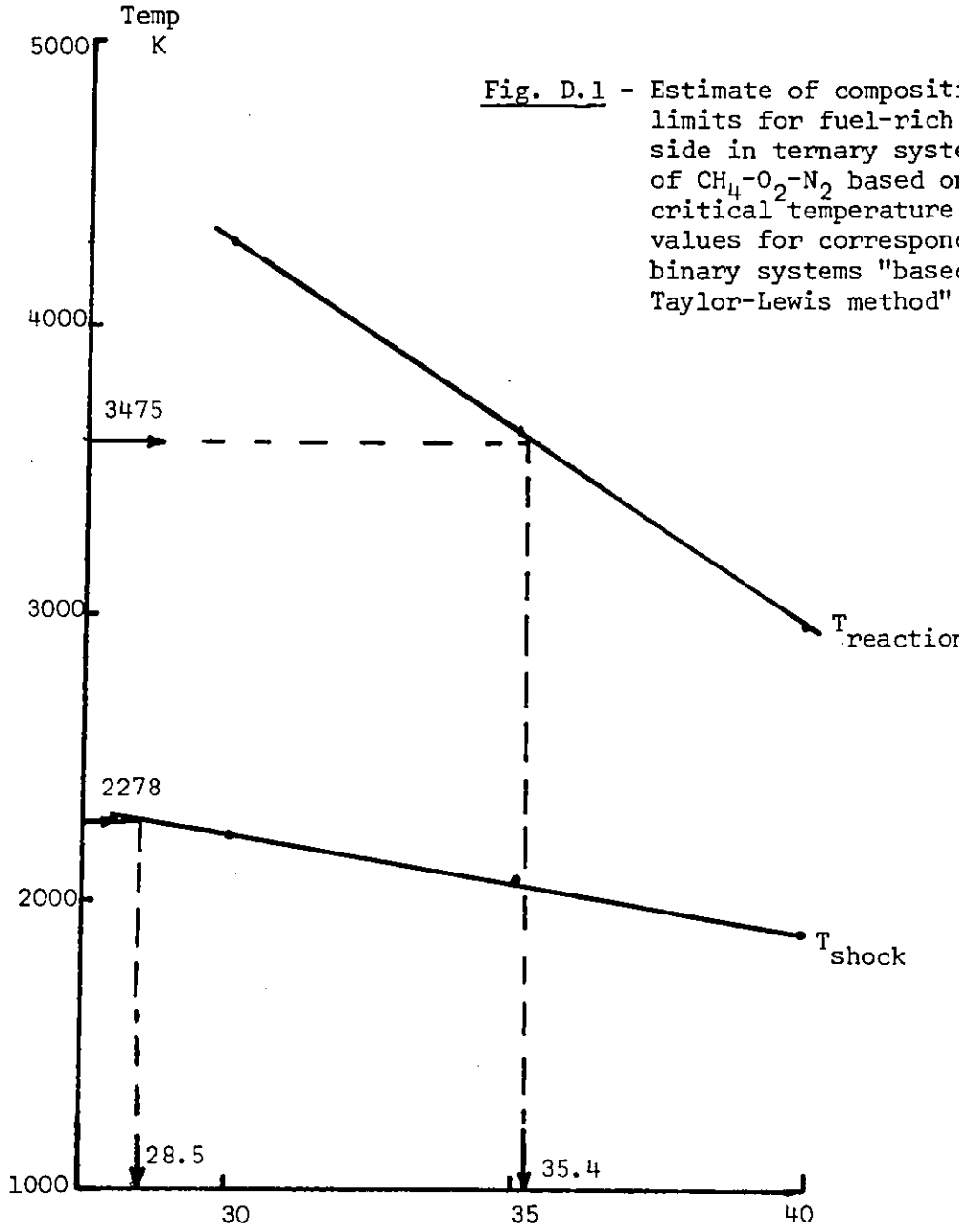
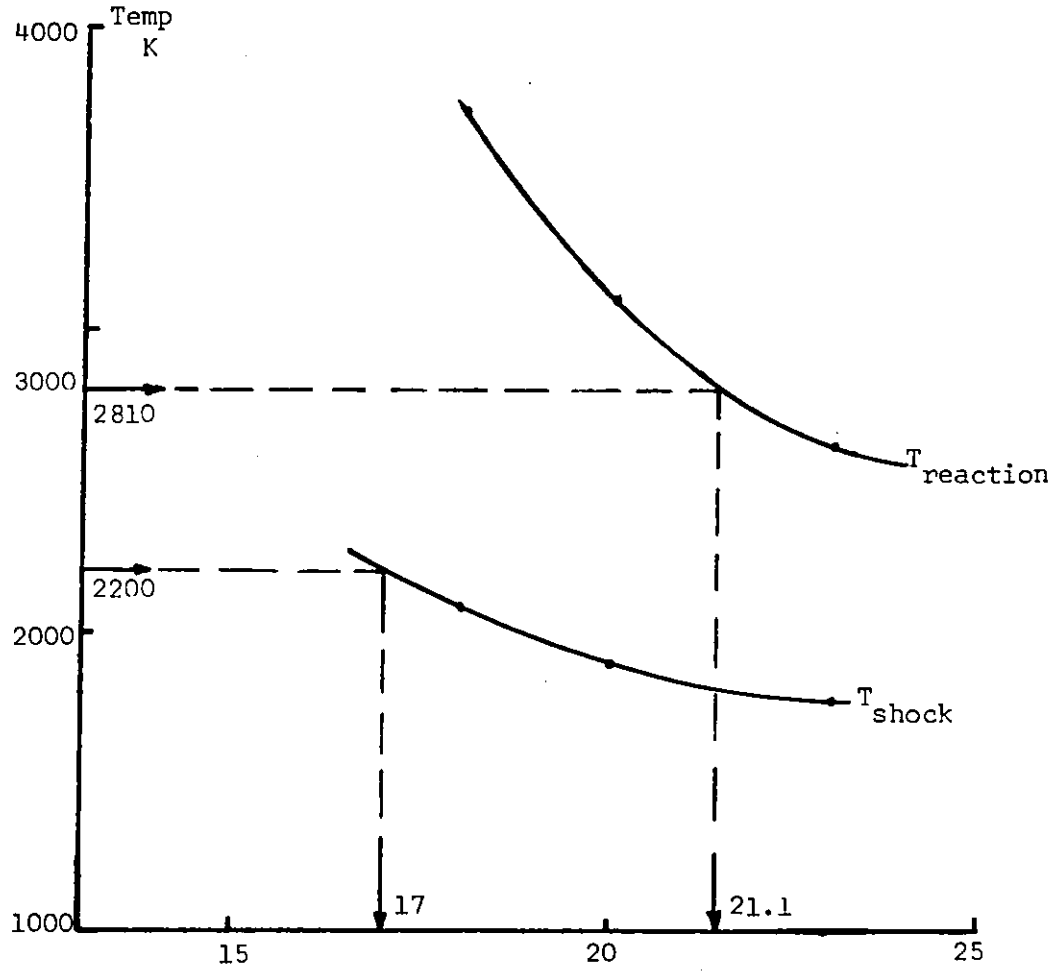


Fig. D.1 - Estimate of composition limits for fuel-rich side in ternary systems of CH_4-O_2-N_2 based on critical temperature values for corresponding binary systems "based on Taylor-Lewis method"

Fig. D.2 - Estimate of composition limits for fuel-rich side in ternary systems of C_3H_8-O_2-N_2 based on critical temperature values for corresponding binary systems "based on Taylor-Lewis method"



a - shock temperature

b - reaction temperature

o - experimentally determined detonation limits

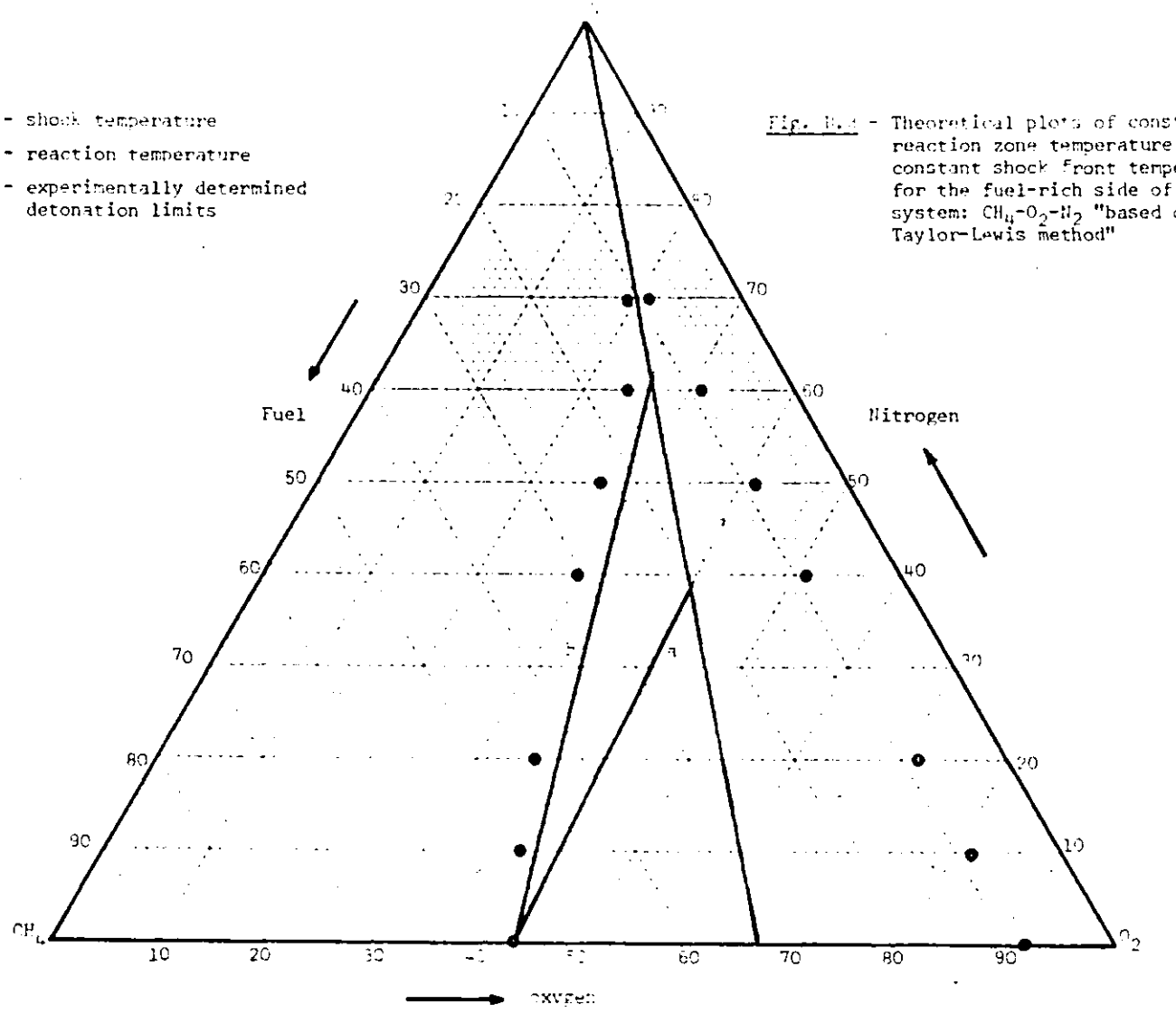


Fig. B.4 - Theoretical plots of constant reaction zone temperature and constant shock front temperature for the fuel-rich side of the system: CH_4-O_2-N_2 "based on Taylor-Lewis method"

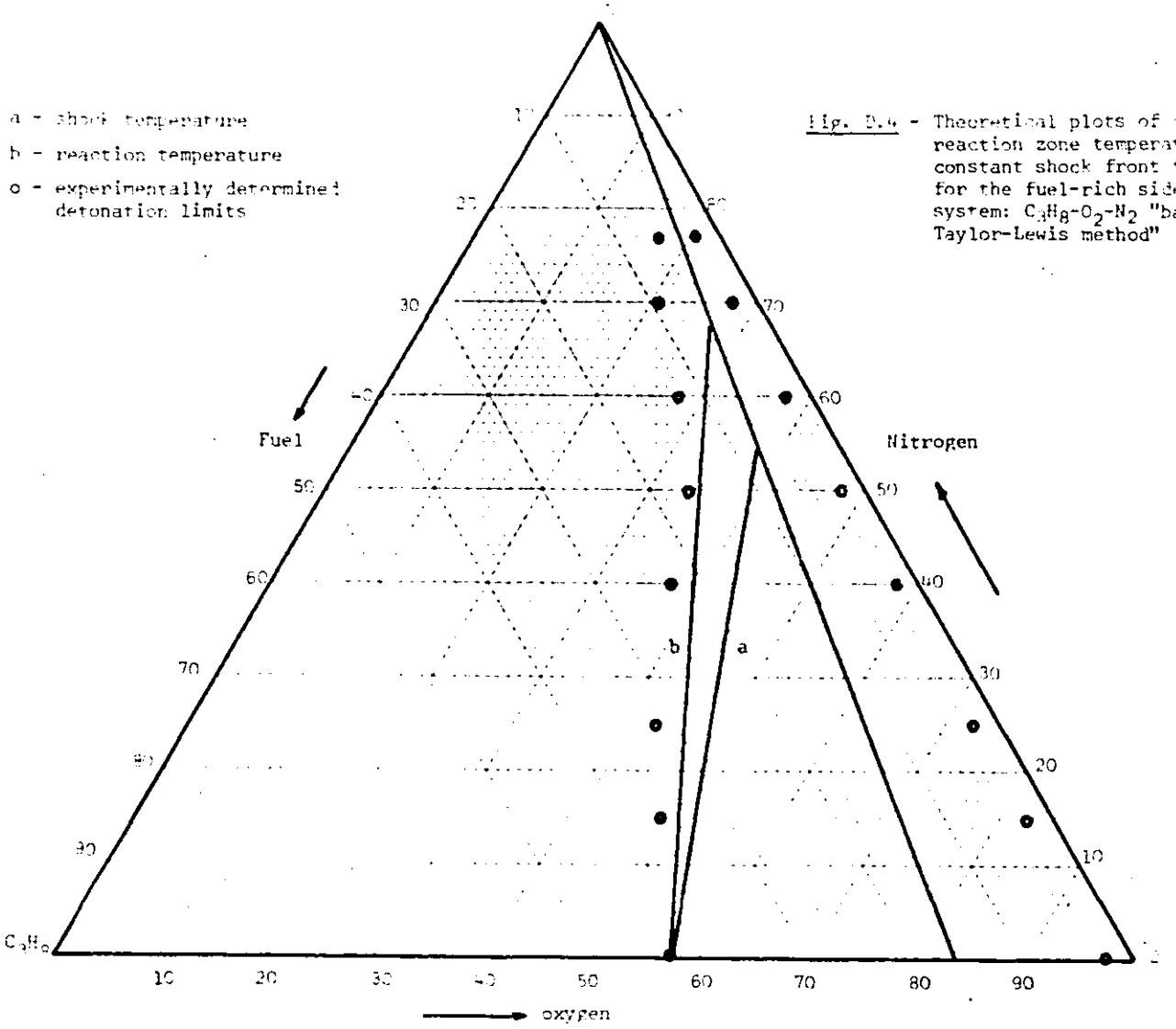


Fig. D.4 - Theoretical plots of constant reaction zone temperature and constant shock front temperature for the fuel-rich side of the system: C_3H_8-O_2-N_2 "based on Taylor-Lewis method"